KATHOLIEKE UNIVERSITEIT
LEUVEN

Faculteit
Ingenieurswetenschappen

Mathematical modelling of calcium influence on the activity of osteogenic cells

Aurélie Carlier

Thesis voorgedragen tot het behalen van de graad van Master in de ingenieurswetenschappen: biomedische technologie, optie biomechanica en biomaterialen

Promotoren:

Prof. dr. ir. H. Van Oosterwyck
Prof. dr. ir. L. Geris

Academiejaar 2009 – 2010

Master in de ingenieurswetenschappen: biomedische technologie

KATHOLIEKE UNIVERSITEIT
LEUVEN

Faculteit
Ingenieurswetenschappen

Mathematical modelling of calcium influence on the activity of osteogenic cells

Aurélie Carlier

Thesis voorgedragen tot het behalen van de graad van Master in de ingenieurswetenschappen: biomedische technologie, optie biomechanica en biomaterialen

Promotoren:
Prof. dr. ir. H. Van Oosterwyck
Prof. dr. ir. L. Geris

Assessoren:
Prof. dr. ir. J. Vander Sloten
dr. ir. J. Schrooten

Begeleiders:
dr. ir. T. Theys
Prof. dr. ir. L. Geris

Academiejaar 2009 – 2010

Preface

A model should be as simple as possible. But no simpler.
Albert Einstein

As Albert Einstein stated, a model should be as simple as possible. But this does not imply that the whole process of developing this (mathematical) framework is simple, on the contrary, it is a challenge. This Master's thesis, as well as the 5 years of education that proceeded it, allowed me to acquire technological knowledge and understanding in the multidisciplinary background of biomedical engineering. It allowed me to develop a systematic, critical and scientific approach and to refine my research skills. But most of all, this thesis gave me the possibility to be creative in the thing that I'm passionate about: research.

Research, however, is not a solo activity. It is done with a group of enthusiastic scientists that are always willing to help and advise. Professor Geris has guided me throughout the whole year, and these vivid meetings have only increased my interest in research in the tissue engineering field. I cannot think of a better assistant. A bit later on the journey, dr. Theys also became my assistant. She gladly guided me through some Matlab troubles and provided new insights to the problem we were trying to solve. Dr. Moesen has helped me enormously with the chapter on design of experiments. With his expertise, we successfully explored a new method of sensitivity analysis. He always pushed me to further improve my work. I would also like to thank my promotor, professor Van Oosterwyck, for his expert opinion and contribution to this Master's thesis.

Besides the aforementioned group of researchers, there are also other people that have supported me throughout the year. Véronique, thank you for critically reading my text. My friends, and especially Lieselotte, Hannelore and my sister Laurence, who listened endlessly to my stories and always make me laugh. Finally, I would like to show my gratitude to my parents for all the opportunities they have given me.

To everybody, thanks!

Aurélie Carlier

Contents

Abstract

Bone formation is a very complex physiological process, involving the participation of many different cell types and regulated by countless biochemical and mechanical factors. In this Master's thesis a bioregulatory model of the effect of calcium phosphate biomaterials and Ca^{2+} on the activity of osteogenic cells was developed and implemented. The mathematical framework consists of six differential equations that describe the temporal evolution of the osteogenic cells, the collagen and mineral matrix and several biochemical factors. The predicted amount of bone formation corresponds to the amount measured experimentally under similar conditions. Moreover, the model is able to qualitatively predict some impaired bone formation conditions. Various strategies to compensate for insufficient cell seeding densities were designed. The most influential parameters of the model were determined using a sensitivity analysis by design of experiments. This work compared three different methods and the results clearly indicated the strengths and shortcomings of every method. In the last part of this Master's thesis, the calcium model was extended to spatial coordinates. In summary, this work illustrates the potential of mathematical models in further unraveling the complex biological process of bone formation and designing more efficient calcium phosphate scaffolds and therapies.

Samenvatting

titel: *Wiskundige modellering van de invloed van calcium op de activiteit van osteogene cellen*

Botvorming is een zeer complex fysiologisch proces, waar verschillende celtypes, groeifactoren en weefsels bij betrokken zijn. Deze masterproef beschrijft de ontwikkeling en implementatie van een wiskundig model dat de invloed van calcium en calciumfosfaten op de activiteit van osteogene cellen simuleert. Dit wiskundig kader bestaat uit zes differentiaalvergelijkingen die de temporele evolutie van de verschillende celsoorten, weefsels en biochemische factoren weergeven. De resultaten van het calcium model komen goed overeen met experimentele data. Het model voorspelt verder ook kwalitatief enkele verstoorde botvormingscondities en reikt mogelijke behandelingsstrategieën aan. De belangrijkste modelparameters werden geïdentificeerd aan de hand van een sensitiviteitsanalyse op basis van de experimentele ontwerpmethode, waarbij er drie verschillende methodes vergeleken werden. In het laatste hoofdstuk werd het bestaande model uitgebreid met twee ruimtelijke dimensies. Dit werk illustreert de kracht van wiskundige modellen bij het ontrafelen van complexe, biologische processen zoals botvorming. Bovendien laten zij toe om *in silico* efficiëntere draagstructuren en therapieën te ontwerpen.

List of Figures

List of Tables

List of Abbreviations and Symbols

1D	one-dimensional
2D	two-dimensional
3D	three-dimensional
∇	$\frac{\partial i}{\partial x} + \frac{\partial j}{\partial y} + \frac{\partial k}{\partial z}$
ALP	alkaline phosphatase
Ca^{2+}	calcium ion
CaP	calcium phosphate
dde	delay differential equations
DNA	desoxyribonucleic acid
DOE	design of experiments
ECM	extracellular matrix
ER	endoplasmic reticulum
HA	hydroxyapatite
hPDC	human periosteum derived stem cell
LH	latin hypercube
LHD	latin hypercube design
LHS	latin hypercube sampling
ME	main effect
MSC	mesenchymal stem cell
OAT	one-at-a-time
PTH	parathyroid hormone
RNA	ribonucleic acid
SS	sum of squares
SSE	error sum of squares
TS	total sensitivity

Glossary

alkaline phosphatase (ALP): is often considered to be an early biochemical marker of differentiation towards osteoblasts. 9

ANOVA: an acronym for "**an**alysis **o**f **va**riance", a statistical technique that separates the variation in an experiment into categories relating to the causes of the variation. 40

appositional ossification: formation of new bone on existing bone. 5

bone lining cell: inactive osteoblasts that cover the available bone surface. 3

bone marrow: soft tissue filling the cavities of bones, source of stem cells. 3, 5, 9, 20, 26, 48, 54

bone morphogenetic protein (BMP): a member of a family of proteins that promote bone formation and regeneration. 23

chemotaxis: the directional movement of cells or organisms towards or away from a chemical stimulus. 7, 9, 10

chondrocyte: cartilage cell, produces and maintains the cartilaginous matrix. 25

collagen: the major protein (comprising over half of that in mammals) of the white fibers of connective tissue, cartilage, and bone. 1, 3, 9, 11, 13, 14, 16–19, 25, 26, 37, 46, 51, 54, 55

cortical bone: the compact bone of the shaft of a bone that surrounds the marrow cavity. 4

cytosol: the fluid component of the cytoplasm without the organelles. 8, 14, 17

design of experiments (DOE): is a statistical technique that allows you to run the minimum number of experiments to optimise your product or process. It involves determining the best experiments to run to fit a particular mathematical model. 28

differentiation: biological process by which a less specialised cell develops or matures into a cell with distinct form and function. 3–9, 12, 13, 15, 16, 18, 19, 21, 25, 26, 37, 38, 41, 42, 44, 52

ectopic: occurring at an abnormal location, e.g bone formation outside the area in which it is normally expected to occur. 5, 6, 10, 16, 19, 20, 23

endochondral ossification: ossification that occurs in and replaces cartilage. 4

endoplasmic reticulum (ER): a membrane network within the cytoplasm of cells involved in the synthesis, modification, and transport of cellular materials. 25

extracellular matrix: an insoluble protein scaffold on which cells reside. The extracellular matrix provides structure, attachment sites and signals through cell surface receptors. 6, 13, 18, 38, 51

factor: in the context of DOE this is a variable over which you have direct control in an experiment (e.g time, temperature, and pressure). 28–33, 35, 38–42, 44, 46–49

fibroblast: a cell from which connective tissue develops. 25

growth factor: a protein that promotes cell proliferation and differentiation when it binds to specific receptors on the cell surface. 1, 5, 11, 12, 14, 16–19, 21, 23, 25, 26, 37, 41, 42, 51–55, 58, 60

haematopoietic stem cell: cells that reside in the bone marrow and have the ability to give rise to all the different mature blood cell types. 4, 9

histomorphometry: the quantitative study of the microscopic organisation and structure of a tissue (e.g. bone) especially by computer-assisted analysis of images formed by a microscope. 22

homeostasis: the tendency of a physiological system to maintain internal stability, owing to the coordinated response of its parts to any situation or stimulus tending to disturb its normal condition or function. 25, 26

hydroxyapatite: a naturally occurring mineral form of calcium apatite with the formula $Ca_5(PO_4)_3OH$, a large percentage of bone is made up of a modified form of the inorganic mineral hydroxyapatite. 3, 5, 6, 13, 14, 25, 41, 46

interaction: is a joint effect of factors. A common example is drug interaction, where two medicines taken together produce an effect that neither could produce by itself. 27–32, 35, 38, 40, 41, 44, 46–50, 59

intramembranous ossification: ossification that occurs in and replaces connective tissue. 4, 25

lamellar bone: mature bone in which the collagen fibers are in an orderly layered arrangement, called “lamellae”. 4

level: in the context of DOE this is the value to which a factor should be set in an experiment (e.g 6 h is a level for time). 28–30, 32, 33, 38, 39, 41, 44, 46

main effect: the main effect for a factor is the effect on a response due to that factor only. 27, 29–31, 35, 40, 41, 46

mechanotransduction: refers to the many mechanisms by which cells convert a mechanical stimulus into chemical activity. 3

mesenchymal stem cell (MSC): multipotent stem cells that can differentiate into a variety of cell types like osteoblasts, fibroblasts and chondrocytes. 1, 3, 5–7, 9, 11, 12, 14–21, 23, 25, 37, 38, 42, 46, 48, 51, 52, 54–56, 63

mesenchyme: the part of the embryonic tissue that consists of loosely packed, unspecialised cells from which connective tissue, bone, cartilage, and the circulatory and lymphatic systems develop. 4

mitochondrion: spherical or rod-shaped organelles, are referred to as the "powerhouse" of the cell since they act as the site for the production of high-energy compounds, which are the vital energy source for several cellular processes. 6

non-union: permanent failure of healing following the fracture of a bone. 1, 3, 5, 59

osteoblast: a mononuclear cell that forms bone. Osteoblasts produce osteoid and are responsible for the mineralisation of the osteoid matrix. 1, 3, 4, 6–9, 11–18, 20, 21, 23, 25, 37, 38, 41, 42, 46, 48, 51, 52, 54, 63

osteocalcin: a protein found in the extracellular matrix of bone and dentin and involved in regulating mineralisation in the bones and teeth. 3, 9

osteoclast: a large multinuclear cell associated with absorption and removal of bone. 3, 4, 9, 25

osteoconductivity: facilitation of cell and nutrient infiltration through the 3D porous structure. 5

osteocyte: a mature osteoblast that has become embedded in the bone matrix. 3, 13

osteogenicity: supply of bone-forming cells by the bone marrow. 5

osteoid: the initial, organic matrix laid down by the osteoblasts, later it will be calcified. 4, 5, 19

osteoinduction: initiation of the differentiation of mesenchymal stem cells towards the osteogenic lineage. 3, 6

osteopontin: a protein that is abundant in bone mineral matrix and accelerates bone regeneration and remodelling. 3

osteoprogenitor: a stem cell that differentiates into an osteoblast, also called preosteoblast. 18, 25

pericyte: a slender cell that wraps around capillaries or other small blood vessels. 6

periosteum: a dense membrane covering the surface of bones (except at their extremities) and serving as an attachment for tendons and muscles. 4

phagocytosis: the process of engulfing microorganisms, other cells, and foreign particles by specific cells. 6

proliferation: increase in cell number by division. 4, 7–9, 12, 13, 15, 25, 26, 37, 42, 44, 46, 48, 52, 63

receptor: a molecular structure within a cell or on the surface characterised by selective binding of a specific substance and a specific physiologic effect that accompanies the binding. 7, 14, 52

scaffold: an artificial structure capable of supporting three-dimensional tissue formation. iv, 5, 6, 16, 19–26, 48, 55, 56, 58–60

trabecular bone: bone composed of thin intersecting trabeculae resulting in a porous structure. Trabecular bone is usually found at the ends of long bones. It also also referred to as "spongy" and "cancellous" bone. 4

woven bone: primitive bone with coarse collagen bundles arranged in a disorderly fashion and replaced subsequently by lamellar bone. 4

Chapter 1

Introduction

The need for bone tissue regeneration is continuously increasing due to the improvement of the quality of life and the increase in life expectancy. In the United States alone approximately 6 million fractures occur yearly, of which 5-10 % result in a delayed union or in a non-union. An extrapolation of these numbers to the Indian population results in 240 million fractures a year, of which 12 million non-unions [Bhandari and Jain, 2009].

Bone tissue engineering aims at finding a better solution for the healing of large bone defects and non-unions. This interdisciplinary research field applies principles of engineering and life sciences to create an *in vivo* micro-environment that promotes local bone repair or regeneration [Habibovic and de Groot, 2007; Eyckmans et al., 2010]. Bone formation is a very complex physiological process, involving the participation of many different cell types and regulated by countless biochemical and mechanical factors. Therefore, mathematical models can make a significant contribution in further unravelling the interactions between the different influential factors. Thus, *in silico* experimentation seeks to explain and understand the underlying principles of the biological phenomenon. Moreover, mathematical models can be used to design and test possible experimental and therapeutic strategies *in silico* before they are tested *in vitro* or *in vivo*. These experimental results will, in turn, guide further model building.

This Master's thesis describes the development and implementation of a bioregulatory model of calcium. The presented mathematical framework is inspired by the bioregulatory model of bone regeneration during fracture healing by Geris et al. [2008] and simulates the effect of calcium and calcium phosphate (CaP) on the activity of osteogenic cells as a temporal variation of six variables: calcium concentration (Ca), mesenchymal stem cell (MSC) density (c_m), osteoblast density (c_b), mineral matrix density (b), collagen matrix density (m) and a generic osteogenic growth factor concentration (g_b). Chapter 2 explains the basic notions of bone biology. After this general description, the influence of calcium on cellular differentiation, proliferation and migration is treated in more detail. The following chapter covers the proposed calcium model. Firstly, the mathematical framework and implementation are discussed. Secondly, some results on normal and impaired bone formation are provided. A thorough discussion of the calcium model concludes the chapter. Chapter 4 describes the sensitivity analysis that was performed on the calcium model. This chapter starts with an overview of different methods that can be used for a sensitivity analysis. In this Master's thesis three methods have been explored : a latin hypercube, a fractional factorial and a uniform design. The results of the sensitivity analysis clearly

indicate the strengths and shortcomings of every method. Chapter 5 presents a spatial extension of the calcium model. The mathematical framework focusses primarily on the migration of the different cells and biochemical factors. The last chapter summarises the most important conclusions of this Master's thesis and gives suggestions for further development of the (extended) calcium model, as well as possible *in vitro* or *in vivo* experiments.

Chapter 2

The biology of bone formation

2.1 Introduction

Due to its scarless regeneration capacity, bone is a unique biological tissue. To find better solutions for the healing of large bone defects and non-unions, it is important to understand the fundamental process of bone formation.

This chapter starts with a brief description of bone biology, explaining the basic notions of bone composition, bone structure and the modelling activities of bone (section 2.2). Subsequently, section 2.3 discusses some of the mechanisms of osteoinduction proposed in literature. Finally, the influence of Ca^{2+} on cellular activities will be described in section 2.4.

2.2 Bone biology

2.2.1 Bone composition

Bone is a very complex connective tissue, composed of three different phases: an organic phase, an anorganic phase and water [Geris et al., 2008]. Collagen is the main constituent of the organic phase, providing tensile strength and flexibility to the bone tissue. The organic phase contains, besides collagen, also osteocalcin and osteopontin. The inorganic phase mainly consists of hydroxyapatite. The compression strength and stiffness of the bone is provided by these bioapatite crystals.

Osteoclasts, osteoblasts, osteocytes and bone lining cells are four important cell types found in bone. The polynuclear osteoclasts play a key role in bone resorption. Osteoblasts are mononuclear bone forming cells that arise from the differentiation of MSCs. The third bone cell type, the osteocyte, is a differentiated osteoblast and is the mechanosensor of the bone. The osteocytes sense the mechanical load on the bone tissue and transduce it into specific chemical stimuli. From this point of view the osteocytes are an essential part of mechanotransduction. The last type of bone cells are the bone lining cells. These cells are also former osteoblasts like osteocytes, but they are not buried in newly formed bone matrix. Instead, they become quiescent, elongated cells that are flattened against the bone surface when they are no longer engaged in bone matrix production. Figure 2.1 presents a schematic overview of the different cell types.

The bone marrow is a major source of osteogenic cells. It contains the precursors of

osteoclasts (haematopoietic stem cells) and osteoblasts (bone stromal cells). Aside from the bone marrow, the periosteum is another very important source of osteogenic cells (i.e. human periosteal derived cells, hPDC's) [Hall, 1990]. The periosteum defines the boundary between bone and overlying soft tissue and is derived from the mesenchyme [Hall, 1992].

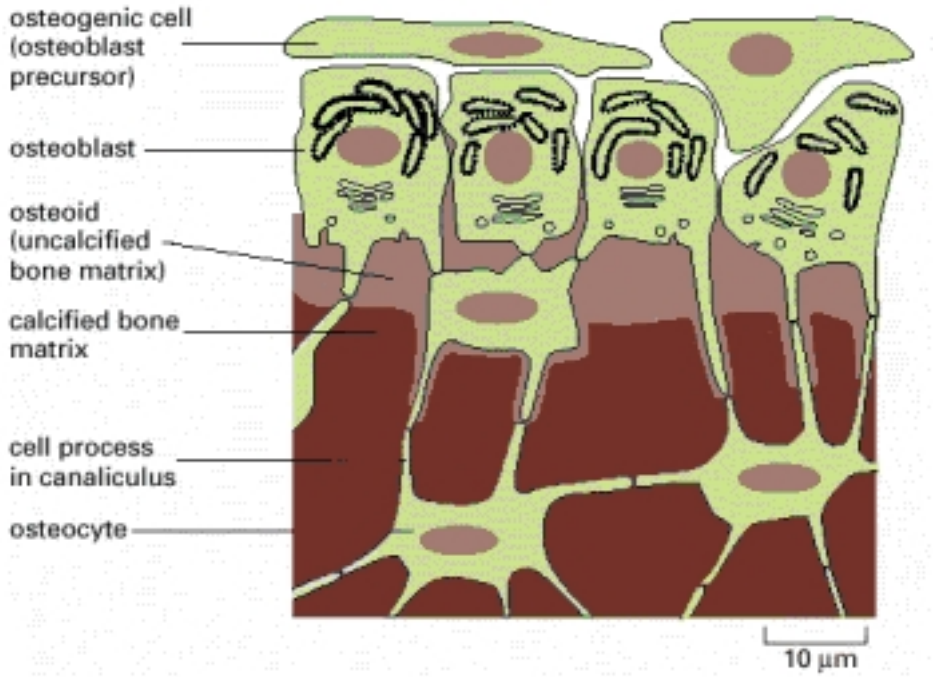

Figure 2.1: Deposition of bone matrix by osteoblasts [Alberts et al., 2007].

2.2.2 Bone structure

Bone is characterised by different structures on the macroscopic and microscopic level. Macroscopically one distinguishes cortical bone and trabecular bone. The first is a very compact, well-vascularised and mineralised tissue, found at the outer surface of bone [Hall, 1990]. The latter consists of different "trabeculae", which results in a porous structure. Nerve tissue, as well as blood vessels and other tissues, are found in the open spaces between the "trabeculae". On the microscopic level lamellar and woven bone can be found. Lamellar bone is formed slowly, but is strongly organised in parallel "lamellae". Woven bone, on the other hand, is formed more quickly but is characterised by a less organised structure.

2.2.3 Bone formation

Bone formation is a multistep process, which starts with the proliferation of the precursor cells and differentiation into active osteoblasts. In the second step active osteoblasts deposit osteoid on a support. Depending on the supporting tissue, different osteogenic processes are distinguished. In intramembranous ossification, the support for bone deposition is provided by connective tissue. Endochondral ossification, which is characterised by the formation of osteoid on cartilage, represents the second category of ossification processes. The last

type of osteogenic processes is appositional ossification, in which case previously formed bone tissue acts as a support for osteoid deposition [Geris et al., 2008]. The last step of osteogenesis is the calcification of the bone matrix. In this mineralisation process insoluble calcium phosphate salts are first deposited in the osteoid. Subsequently, these salts are replaced by more stable hydroxyapatite crystals. The formation of bone is schematically shown in figure 2.1.

In cases of impaired healing of bone fractures or even non-unions, biomaterials can help to induce bone formation. The next section discusses the influence of CaP biomaterials on bone formation in more detail.

2.3 Influence of calcium phosphate granules on bone formation

Tissue engineering aims to develop biological substitutes that restore, maintain or improve tissue function. Two main strategies have been developed to regenerate bone tissue: the use of biomaterials to induce bone formation chemically and the construction of hybrid implants composed of a biomaterial scaffold seeded with osteogenic cells [Habibovic and de Groot, 2007; Langer and Vacanti, 1993]. The following terms are often used to characterise the biological performance of biomaterials [Habibovic and de Groot, 2007]:

- osteogenicity: supply of osteogenic (bone-forming) cells by the bone marrow
- osteoinductivity: initiation of the differentiation of MSCs towards the osteogenic lineage
- osteoconductivity: facilitation of cell and nutrient infiltration through the 3D porous structure

Delayed and non-unions are characterised by an *in vivo* micro-environment that fails to support bone repair or tissue regeneration. Hence, the micro-environment found at a non-union can be considered as an ectopic site [Eyckmans et al., 2010]. Consequently, the tissue engineering constructs should display osteoinductive properties. Calcium phosphate (CaP) bioceramics are then interesting candidates, because of their biocompatibility, bioactivity and osteoinductive characteristics. It has been clearly shown that calcium phosphates induce bone formation, but the exact mechanism is still largely unknown [Eyckmans et al., 2010; Yuan et al., 2007, 2006; Chang et al., 2000; Hanawa et al., 1997; Barrère et al., 2003; Ripamonti, 1996]. There are, however, several different mechanisms proposed in literature to explain the influence of calcium phosphate particles on bone formation as observed in many experiments.

It has been stated that a high local concentration of growth factors and proteins can be achieved by adsorption on the biomaterial substrate, thereby creating a favourable micro-environment for bone formation [Yuan et al., 2006; Liu et al., 2008; Ripamonti, 1996]. Another explanation for the osteoinductive properties of CaP biomaterials is given by the surface topography, since it influences the osteoblastic guidance and attachment and can cause the asymmetrical division of MSCs [Barrère et al., 2006, 2003]. Barrère et al. [2003] also suggest that the surface charge of the substrate can play a key role by triggering cell differentiation. Furthermore, negative charges distributed on the surface of the biomaterial can be an obstacle for cell-material adhesion, because the cell surface is negatively charged [Zhou et al., 2007; Shelton et al., 1988]. The bioapatite layer, formed *in vivo*, might also be

recognised by MSCs [Habibovic and de Groot, 2007]. A low oxygen tension in the central region of the biomaterial, which triggers the pericytes of microvessels to differentiate in osteoblasts, is another mechanism proposed in literature [Barrère et al., 2003].

However, the release of calcium and phosphate ions by dissolution, is believed to be the main origin of the bioactivity of calcium phosphate biomaterials [Habibovic and de Groot, 2007; Barrère et al., 2006; Chang et al., 2000; Barrère et al., 2003]. The dissolution properties of calcium phosphate biomaterials are influenced by the exposed surface area, the composition and the pH. Pioletti et al. [2000] showed that small calcium phosphate particles (< 10 μm) can induce phagocytosis. This process could then, in turn, produce an accumulation of Ca^{2+} in the mitochondria, which can cause lysis of the mitochondria and cell death. Phagocytosis also alters the pH of the surrounding body fluids. This pH-change subsequently alters the dissolution properties of the calcium phosphate particles.

The size of the particles is not only critical because it can induce phagocytosis, it also determines the reactivity of the particles. The smaller the particles, the larger the exposed surface to the environment and the faster the biomaterial will dissolve. The dissolution rate will increase, simply because larger quantities of exchange can take place [Barrère et al., 2006].

The composition of the calcium phosphate biomaterials is another important characteristic that determines the dissolution properties. A change in the calcium to phosphate ratio means a change in phase composition, which directly affects the ionic exchange mechanisms [Barrère et al., 2006].

Experimental evidence clearly indicates the key role of calcium and phosphate ions in osteoinduction. Yuan et al. [2006] observe more bone formation in scaffolds made up of biphasic calcium phosphate than of hydroxyapatite, the latter having a lower dissolution rate. The effect of calcium ion implantation in titanium on bone formation was investigated by Hanawa et al. [1997]. They found a larger amount of new bone on the Ca^{2+}-treated side than on the untreated side. Eyckmans et al. [2010] noticed that the CaP granule remnants in a decalcified scaffold serve as anchoring points for cell attachment (see figure 2.2). Titorencu et al. [2007] report that osteoblasts respond to changes in Ca^{2+} concentration in the bone micro-environment. Moreover, differentiation of MSCs towards osteoblasts is accompanied by the expression of Ca^{2+} binding-proteins and the incorporation of Ca^{2+} into the extracellular matrix [Titorencu et al., 2007]. It also appears that osteoblasts sense and respond to the extracellular Ca^{2+} concentration independently of systemic calciotropic factors in a concentration-dependent manner [Dvorak et al., 2004]. Bootman et al. [1996] report that the extracellular calcium concentration could control the frequency of the intracellular calcium spiking, which encodes specific cellular information according to Sun et al. [2007].

It appears that the primary condition to induce ectopic bone formation is a critical level of free, extracellular Ca^{2+}. Therefore, this Master's thesis will focus on the effect of Ca^{2+} on the activity of osteogenic cells and bone formation.

2.4 Influence of calcium ions on cellular activity

As stated above, the release of Ca^{2+} by the dissolution of calcium phosphate biomaterials constitutes the principal mechanism of osteoinduction. In this section the effect of Ca^{2+} on cellular activity will be more elaborated.

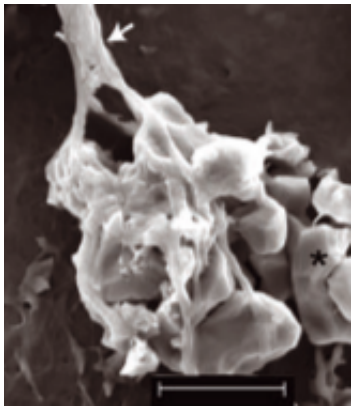

Figure 2.2: Scanning electron microscope image of a remnant granule serving as an anchoring point for cell attachment (the white arrow indicates a cell attaching to the mineral remnants, the asterisk indicates a CaP granule, magnification 5000 x, scale bar = 5 μm) [Eyckmans et al., 2010].

Experiments show that the influence of Ca^{2+} differs from cell type to cell type [Barrère et al., 2006]. This section will look primarily at MSCs and osteoblasts, since these osteogenic cells will play a key role in the mathematical model which is presented in chapter 3. Notice that the extracellular calcium ion can be bound to proteins (e.g. albumin). In this complexed form the ion cannot influence cellular behaviour like differentiation and proliferation. The term "calcium ion" refers, in the remaining part of this document, to the active, free ion.

In general, extracellular Ca^{2+} plays a role in regulating proliferation, differentiation and migration via the activation of calcium sensing receptors (CaSR) and/or by increasing the influx of Ca^{2+} [Zayzafoon, 2006]. The CaSR may act as a (gradient) sensor, triggering chemotaxis of motile cells to critical micro-environments and transducing the Ca^{2+} signal to intracellular signalling pathways regulating cell function [Breitwieser, 2008].

Although the mechanism of Ca^{2+} sensing remains unclear, it has been discovered that osteoblasts express a similar calcium sensing receptor as the parathyroid cells. The calcium sensor in the parathyroid and kidney is a G-protein coupled receptor with seven transmembrane domains that detects the extracellular calcium concentration (see figure 2.3). Studies suggest that the calcium sensing receptor in osteoblasts is functionally similar to but molecularly distinct from the calcium sensing receptor present in the parathyroid and the kidney [Zayzafoon, 2006; Dvorak et al., 2004]. However, more studies are necessary to characterise the complete function of the calcium sensing receptor in osteoblasts, as well as its role in osteoblast differentiation, proliferation and migration.

2.4.1 Influence of Ca^{2+} concentration on proliferation

Mesenchymal stem cells

Dvorak et al. [2004] report an increase of proliferation of MSCs in a concentration dependent manner. The experiments of Liu et al. [2009] show that, when the Ca^{2+} concentration is lower than 1.8 mM, a decrease of Ca^{2+} concentration significantly inhibits the proliferation of MSCs. When the Ca^{2+} concentration is higher than 1.8 mM, the cellular proliferation

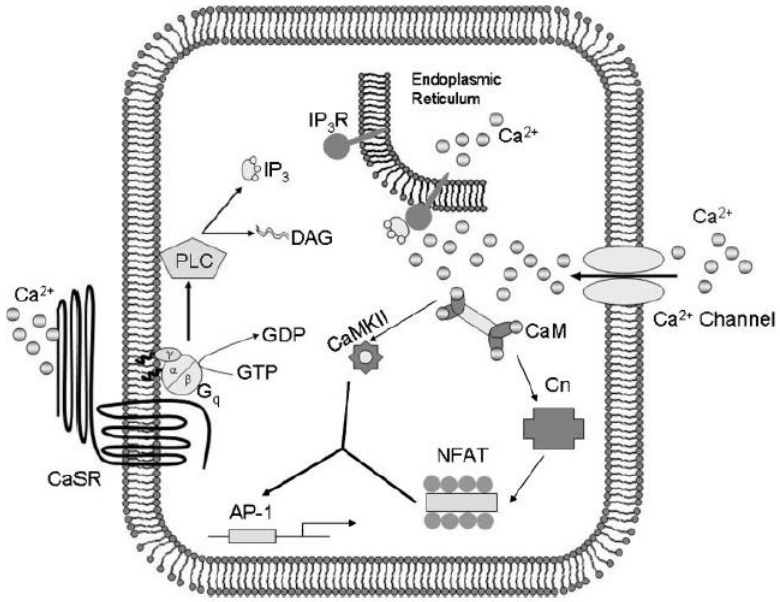

Figure 2.3: Different signaling pathways to regulate the gene expression in osteoblasts. The extracellular calcium concentration is sensed by the calcium sensing receptor (CaSR, left) [Zayzafoon, 2006].

does not change with varying Ca^{2+} concentrations [Liu et al., 2009]. By contrast, the influence of Ca^{2+} on proliferation follows a Gaussian distribution according to unpublished data of Yoke Chin Chai [Lab for Skeletal Development and Joint Disorders, K.U. Leuven, Belgium].

Osteoblasts

Osteoblasts sense and respond to the extracellular Ca^{2+} concentration independently of systemic calciotropic factors in a concentration dependent manner [Dvorak et al., 2004]. As a consequence, local fluctuations in Ca^{2+} can regulate osteoblast activity. Zayzafoon [2006] reports the importance of calcium channels in osteoblast proliferation. He suggests that an increase in the intracellular Ca^{2+} concentration activates the Ca^{2+} signalling pathways that are dedicated to induce proliferation. Maeno et al. [2005] studied the effects of Ca^{2+} on osteoblast proliferation and found a Gaussian dependency on calcium concentration. 5 mM Ca^{2+} was associated with maximum proliferation for both a monolayer and a 3D culture. They suggest a concentration range of 0-6 mM Ca^{2+}, which is slightly lower than that suitable for differentiation.

2.4.2 Influence of Ca^{2+} concentration on differentiation

Mesenchymal stem cells

The intracellular Ca^{2+} oscillation is a complex process that reflects the transfer of Ca^{2+} into and from the extracellular space, cytosol, intracellular stores and the buffering due to the binding to proteins. Cells recognise these oscillations through intricate mechanisms to decode the information that is embedded in the Ca^{2+} dynamics [Sun et al., 2007]. Bootman

et al. [1996] report that the extracellular calcium concentration can control the frequency of the intracellular calcium spiking. A lower extracellular calcium concentration leads to a lower intracellular calcium spiking frequency [Bootman et al., 1996]. Sun et al. [2007] demonstrate that the calcium spiking frequency is closely related to the differentiation potential of MSCs. They show that, in response to osteoinductive factors, the Ca^{2+} spikes decrease to a level similar to the one found in osteoblasts. Therefore, in order to influence the differentiation, a similar spiking pattern to the one of osteoblasts must be established in MSCs. According to Bootman et al. [1996] this can be achieved by altering the extracellular calcium concentration. Quantitative results were unfortunately not available. However, qualitatively one can state that an optimal extracellular calcium concentration, altering the intracellular spiking pattern of the MSCs so that it resembles the one of osteoblasts, leads to the differentiation of MSCs towards osteoblasts.

Dvorak et al. [2004] report that elevations of Ca^{2+} promote the differentiation of MSCs. They indicate a narrow optimal range (1.2 - 1.8 mM Ca^{2+}). The results of Sun et al. [2007] show that a depletion of extracellular Ca^{2+} interferes with the proper differentiation of MSCs. This suggests a critical role for Ca^{2+} influx. Liu et al. [2009] found that different biochemical markers for differentiation (e.g. ALP, collagen I and osteocalcin) reach a maximal concentration at 1.8 mM, which corresponds well with the results of Dvorak et al. [2004]. Liu et al. [2009] found a Gaussian dependency of differentiation on calcium concentration.

Osteoblasts

Maeno et al. [2005] studied the effects of Ca^{2+} on osteoblast differentiation and found a Gaussian dependency on the calcium concentration. 8 mM Ca^{2+} was associated with maximum differentiation for a monolayer. They suggest a concentration range of 6-8 mM Ca^{2+}, which is slightly higher than that suitable for proliferation.

Biologically, the regulation of osteoblastic proliferation and differentiation by extracellular Ca^{2+} can be considered as a coupling factor between osteoclasts and osteoblasts [Duncan et al., 1998]. At bone erosion sites the Ca^{2+} concentrations exceed physiological concentrations, which may stimulate osteoblast proliferation and differentiation, leading to bone formation.

2.4.3 Influence of Ca^{2+} on cellular migration

Extracellular Ca^{2+} gradients are present in a number of distinct micro-environments and can represent potent chemical signals for cell migration (chemotaxis) and directed growth (see figure 2.4) [Lobovkina et al., 2010]. Moreover, Ca^{2+} is an important homing signal that brings together different cell types required for the initiation of a multicellular process like bone remodelling or wound repair [Breitwieser, 2008]. Many experimental studies have investigated the chemotactic response of monocytes [Olszak et al., 2000], osteoblasts [Godwin and Soltoff, 1997], breast cancer cells [Saidak et al., 2009], haematopoietic stem cells [Adams et al., 2006] and bone marrow progenitor cells [Aguirre et al., 2010] to Ca^{2+}. They report a dose-dependent relationship, with a maximal effect achieved at concentrations ranging from 3-10 mM Ca^{2+} [Aguirre et al., 2010].

The regulation of migration by extracellular Ca^{2+} is biologically a coupling factor between osteoclasts and osteoblasts. High Ca^{2+} concentrations have been shown to

stimulate preosteoblast chemotaxis to the site of bone resorption, and their maturation into cells that produce new bone [Dvorak and Riccardi, 2004].

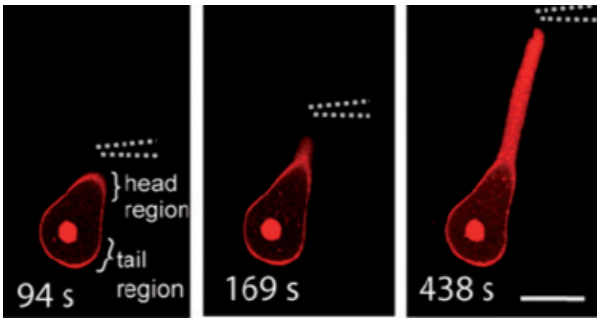

Figure 2.4: Confocal fluorescence microscopy images showing protrusive growth in surface-adhered flat lipid vesicles caused by a Ca^{2+} gradient (scale bar is 10 μm, the pipette, indicated by the dashed lines, forms the Ca^{2+} source) [Lobovkina et al., 2010].

2.5 Conclusion

This chapter explained the basic notions of bone composition, bone structure and the modelling activities of bone. In some cases of impaired healing of bone fractures or even non-unions, biomaterials can help to induce bone formation. Some of the mechanisms proposed in literature to explain the osteoinductive properties of CaP biomaterials were treated in more detail. From this discussion, it appeared that the primary condition to induce ectopic bone formation is a critical level of free, extracellular Ca^{2+}. The experimental evidence of the influence of Ca^{2+} on cell proliferation, differentiation and migration was also investigated in this chapter.

Chapter 3

Calcium model

3.1 Introduction

Improvements in computer capacity now enable computer simulations, in a dynamic sense, as opposed to the earlier computer analyses, which predicted only a steady state configuration [van der Meulen and Huiskes, 2002]. As a consequence of this technological revolution, there has been an enormous increase in the use of mathematical models in biology and medicine. These mathematical models can propose and test possible biological mechanisms, contributing to the unravelling of the complex nature of biological systems. Moreover, they can be used to design and test possible experimental strategies *in silico* before they are tested *in vitro* or *in vivo*.

This chapter describes the mathematical model that simulates the effect of Ca^{2+} and calcium phosphates on cellular activity as function of time. The proposed model is a 1D model since time is the only dimension. An extension of this model, including a spatial dependency, is given in chapter 5. Section 3.2 describes the functional forms and equations of the proposed mathematical model. The derivation of the different parameter values is explained in section 3.3. Section 3.4 provides information on the different simulation details. A sensitivity analysis was performed to identify the most influential parameters, which is discussed more in depth in chapter 4. The results of the calcium model are described in section 3.5. Section 3.6 thoroughly discusses the results and simplifications of the mathematical model. Finally, the last section summarises the most important conclusions of this chapter.

3.2 Mathematical framework

The presented mathematical calcium model is inspired by the bioregulatory model of Geris et al. [2008]. It consists of six partial differential equations and describes the effect of calcium phosphates on the activity of osteogenic cells as a temporal variation of six variables: calcium concentration (Ca), MSC density (c_m), osteoblast density (c_b), mineral matrix density (b), collagen matrix density (m) and a generic osteogenic growth factor concentration (g_b). The sum of the mineral matrix and the collagen matrix represents the total bone density. The following sections describe the individual reaction terms. A schematical overview of the model is presented in figure 3.1.

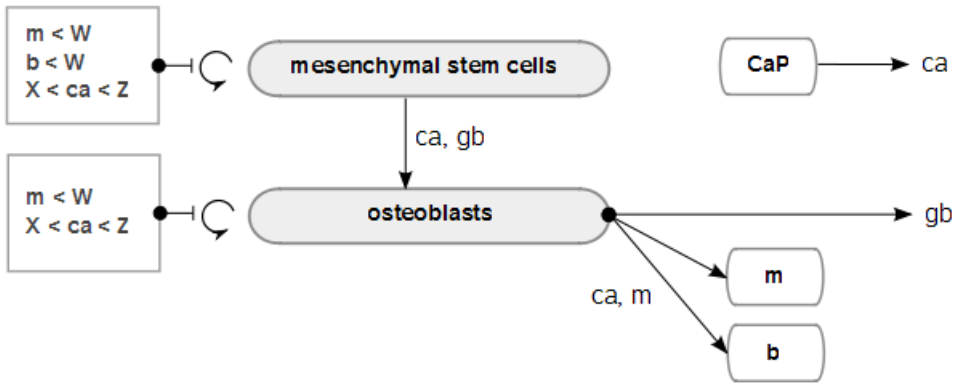

Figure 3.1: Schematic overview of the calcium model. W = maximum tissue density for proliferation, X = minimum calcium concentration for proliferation, Z = maximum calcium concentration for proliferation. The participation of a variable in a subprocess is indicated by showing the name of that variable next to the arrow representing that subprocess, e.g. calcium interferes with differentiation and bone formation.

Mesenchymal stem cells

The proliferation of MSCs is modelled by a logistic growth function where the proliferation rate (A_m) depends on the surrounding matrix density (m) and calcium concentration (Ca) [Olsen et al., 1997; Weinberg and Bell, 1985; Yoshizato et al., 1985]. The calcium dependency of the proliferation follows a Gaussian distribution (last two factors in equation (3.1)).

$$A_m = \frac{A_{m0}.m}{K_m^2 + m^2}.\frac{a_{cm}}{c_{cm}}.exp\left(-\frac{1}{2}.\left(\frac{Ca - b_{cm}}{c_{cm}}\right)^2\right) \tag{3.1}$$

The derivation of the constants in equation (3.1) and all the following equations is discussed in section 3.3.

The differentiation of MSCs towards osteoblasts is mediated by a generic osteogenic growth factor (g_b). A minimal chemical concentration is included in the computational model by defining a sixth order polynomial function. For high chemical concentrations a saturation effect was modelled to take place [Bailón-Plaza and van der Meulen, 2001]. According to Liu et al. [2009] the calcium dependency of the differentiation follows a Gaussian distribution (last two factors in equation (3.2)).

$$F_1 = \frac{Y_{11}.g_b^6}{H_{11}^6 + g_b^6}.F_{11}.exp\left(-\frac{1}{2}.(Ca - F_{12})^2\right) \tag{3.2}$$

Upon production of mineral matrix, MSCs gradually become entrapped. When the stem cell is surrounded by the bone matrix, it will differentiate or die (apoptosis), the latter being modelled by a decay term:

$$d_{cm}.b.c_m \tag{3.3}$$

Osteoblasts

The proliferation of osteoblasts is modelled by a logistic growth function where the proliferation rate (A_b) depends on the surrounding matrix density (m) and calcium concentration (Ca) [Olsen et al., 1997; Weinberg and Bell, 1985; Yoshizato et al., 1985]. According to Maeno et al. [2005] the calcium dependency of the proliferation follows a Gaussian distribution (last two factors in equation (3.4)).

$$A_b = \frac{A_{b0}.m}{K_b^2 + m^2}.\frac{a_{cb}}{c_{cb}}.exp\left(-\frac{1}{2}.\left(\frac{Ca - b_{cb}}{c_{cb}}\right)^2\right) \tag{3.4}$$

Upon production of mineral matrix, osteoblasts gradually become entrapped by the matrix they are producing. When an osteoblast is completely surrounded by bone matrix, it will either mature and become an osteocyte or die (apoptosis). In both cases, this removes the osteoblast from the active matrix producing population. This removal is modelled by a constant decay term (d_b). Both apoptosis and differentiation of osteoblasts towards osteocytes are calcium dependent processes [Titorencu et al., 2007; Maeno et al., 2005]. This is included in the mathematical model by defining a threshold for the calcium concentration at which the value of the decay term increases.

Collagen matrix

The equation describing the evolution of the collagen matrix density was modelled according to Geris et al. [2008]. Extracellular matrix production was assumed proportional to the cell density of the matrix producing cells (the osteoblasts). The production rate decreases as the surrounding collagen matrix density increases.

Mineral matrix

The temporal variation of the mineral matrix is modelled in a similar way as the collagen matrix. The mineral matrix production is assumed proportional to the cell density of the matrix producing cells (the osteoblasts). The production rate decreases as the surrounding mineral matrix density increases. However, a sixth order polynomial was used to model the production of mineral matrix, in contrast with a linear decrease of the production rate of collagen matrix.

The mineralisation of the last fraction of (unmineralised) collagen takes place after a very long time. This period is not considered in the timeframe of the mathematical model but is taken into account by introducing an offset of 5%.

There are two conditions that need to be satisfied in order to have production of mineral matrix. Hydroxyapatite deposition occurs following the maturation of the collagen matrix during bone formation [Maeno et al., 2005; Barrère et al., 2006]. The first condition (equation (3.5)) implies that the collagenous matrix needs to be mature before mineralisation can take place:

$$m \; > \; 85\% \; . \; m_{max} \tag{3.5}$$

where m_{max} represents the maximal collagen density. Calcium is used by osteoblasts for the production of hydroxyapatite and for other general metabolic activities. The second condition (equation (3.6)) demands that at least an equivalent amount of calcium deposited

as hydroxyapatite should be taken up by the mineral matrix producing cells (the osteoblasts). Parameter Q in equation (3.6) represents a proportionality constant.

$$P_{bb}.(0,95 - \kappa_{bb}.b)^6.c_b.Q \ < \ J_{Leaky}.c_b.\frac{Ca}{H_{Ca4} + Ca} \tag{3.6}$$

Calcium

In most of the aforementioned processes, the calcium concentration plays an important role. The kinetics of the dissolution of the calcium phoshate granules is modelled by a general empirical equation:

$$\frac{dc}{dt} = k.s.(c_\infty - c)^n \tag{3.7}$$

where $\frac{dc}{dt}$ is the rate of dissolution, k is the rate constant for dissolution, s represents the specific area, c_∞ stands for the equilibrium concentration and c for the concentration of the solution and n is the effective order of the reaction [Zhang et al., 2003]. For the specific case that is modelled here, the equilibrium concentration is taken to be the maximal concentration at which artificial precipitation does not yet occur. The effective order of the reaction is considered to be 1. In this study, the parameters k and s are combined in the model parameter σ.

Biological mineralisation is a complex process resulting in the deposition of hydroxyapatite on the mature collagen matrix. The formation of intracellular vessicles containing bioapatite is a metabolic process involving protein and RNA synthesis and requiring the uptake of calcium [Stanford et al., 1995]. The calcium flux from the extracellular space towards the cytosol is modelled as a leakage flux [Maurya and Subramaniam, 2007].

$$J_{leaky}.\frac{Ca}{H_{Ca4} + Ca} \tag{3.8}$$

Sun et al. [2007] suggest a critical role for Ca^{2+} influx. The calcium uptake for the metabolic activities of both osteoblasts and MSCs is included in the mathematical model by a constant decay function (d_{Ca}).

Generic growth factor

Besides calcium, growth factors also play a key role in a lot of the modelled processes. The generic osteogenic growth factors are produced by osteoblasts, up to a certain saturation concentration, after which the production rate levels off. The production rate (E_{gb}) is not limited by the matrix density.

$$E_{gb} = \frac{G_{gb}.g_b}{H_{gb} + g_b} \tag{3.9}$$

The removal of growth factors is modelled by a decay function (d_{gb}) representing denaturation and irreversible binding to matrix proteins [Bailón-Plaza and van der Meulen, 2001]. The binding of a growth factor to a specific cell surface receptor initiates a signal transduction cascade. The growth factor-receptor complexes are subsequently removed from the cell surface via endocytosis. A significant amount of growth factors are, however, not recycled to the cell surface and will be internally degradated [Sorkin and Waters, 1993]. The removal of the growth factors from the osteogenic environment is modelled by:

$$(c_{m,t} - c_{m,t-0.0001}) \cdot \frac{G_{con}.g_b}{H_{con} + g_b} \tag{3.10}$$

where $c_{m,t}$ represents the MSC density at time t and $c_{m,t-0.0001}$ the MSC density at time $t - 0.0001$. The difference between these two densities indicates the amount of cells that differentiated or proliferated during that time interval and, consequently, the amount of growth factors that were removed from the osteogenic environment.

Set of equations

Briefly stated, this leads to the following set of equations:

$$\frac{\partial m}{\partial t} = P_{bs}.(1 - \kappa_b.m).c_b \tag{3.11}$$

$$\frac{\partial c_m}{\partial t} = A_m.c_m.(1 - \alpha_m.c_m) - F_1.c_m - d_{cm}.b.c_m \tag{3.12}$$

$$\frac{\partial g_b}{\partial t} = E_{gb}.c_b - d_{gb}.g_b - (c_{m,t} - c_{m,t-0.0001}) \cdot \frac{G_{con}.g_b}{H_{con} + g_b} \tag{3.13}$$

$$\frac{\partial c_b}{\partial t} = A_b.c_b.(1 - \alpha_b.c_b) + F_1.c_m - d_b.c_b \tag{3.14}$$

$$\frac{\partial b}{\partial t} = P_{bb}.(0.95 - \kappa_{bb}.b)^6.c_b \tag{3.15}$$

$$\frac{\partial Ca}{\partial t} = \sigma.(Ca_\infty - Ca) - J_{leaky}.c_b.\frac{Ca}{H_{Ca4} + Ca} - d_{Ca}.Ca.(c_b + c_m) \tag{3.16}$$

The scaling factors that were chosen for non-dimensionalisation, as well as the non-dimensionalised model parameter values can be found in section 3.3.2.

3.3 Parameters

3.3.1 Parameter values

The parameter values were determined using three different methods. First, a stability analysis was performed in order to determine the stability of different stationary states and to gain more understanding of the mathematical model. The parameter values were further derived from unpublished experimental data provided by Yoke Chin Chai [Lab for Skeletal Development and Joint Disorders, K.U. Leuven, Belgium] and from literature where possible.

Proliferation

Bailón-Plaza and van der Meulen [2001] derived for their model the values of the parameters A_{m0}, K_m, A_{b0} and K_b of the proliferation functions for MSCs and osteoblasts (equations (3.1) and (3.4)). A slightly smaller value for A_{m0} was adopted here. The parameters a_{cm}, b_{cm}, c_{cm}, a_{cb}, b_{cb} and c_{cb} that characterise the Gaussian dependency on the calcium concentration, were derived from unpublished experimental data provided by Yoke Chin Chai [Lab for Skeletal Development and Joint Disorders, K.U. Leuven, Belgium]. Appendix A describes in more detail the determination of these parameter values.

Differentiation

Bailón-Plaza and van der Meulen [2001] examined, in the absence of quantified cell differentiation rates, different values for the parameters describing MSC differentiation in a

sensitivity analysis. The same parameter values are adopted here. The differentiation of MSCs towards osteoblasts is a calcium dependent process. Studies on osteogenic differentiation of MSCs *in vitro* show a Gaussian distribution with an optimal differentiation in a narrow range of calcium concentrations (1.2 mM - 1.8 mM) [Dvorak et al., 2004; Liu et al., 2009]. Dvorak et al. [2004] report an eightfold increase of differentiated cells at the optimal calcium concentration.

Cell decay

The rate of osteoblast removal is not available from literature or experimental data and has been estimated by Bailón-Plaza and van der Meulen [2001] in a linear stability analysis. Their estimates are adopted in the presented mathematical model. The rate of MSC apoptosis is not available from literature or experimental data and has been estimated.

Matrix synthesis and degradation

Matrix synthesis rate decreases proportionally with the increase of the corresponding matrix density. The production will stop when the matrix density reaches its maximum value. The parameters κ_b and κ_{bb} are inversely proportional to the limiting matrix density. As such, they represent the balance between synthesis and degradation of extracellular collagen matrix and bone matrix respectively. The values of Bailón-Plaza and van der Meulen [2001] are adopted here. The initial production rates (P_{bs} and P_{bb}) were investigated numerically. Yuan et al. [2006] report the initiation of ectopic bone formation at 20 days post implantation, P_{bs} was varied in order to fit this time scale. The amount of bone formation after 90 days is approximately 31 % according to Yuan et al. [2006]. The parameter P_{bb} was chosen to fit the reported amount of bone formation.

Growth factor production

Experimental data on the production rates of growth factors are not available. However, Geris et al. [2008] explored a range of parameter values numerically. The magnitude of the production rate (G_{gb}) is determined numerically and the value of the parameter H_{gb} is chosen in such a way that the saturation level for the production occurs around typical growth factor concentration levels. The mathematical model adopts the numerical estimates of Geris et al. [2008].

Growth factor decay and consumption

The parameter value for the decay term of growth factors (d_{gb}) is adopted from Geris et al. [2008] who used typical values for the half life of growth factors involved in fracture healing (typically below and around 30 minutes). A half-life of 13 minutes corresponds to a decay constant of 75 day^{-1}. The parameter H_{con} was chosen in such a way that the term $\frac{G_{con}.g_b}{H_{con}+g_b}$ becomes equal to 1 for growth factor concentrations higher than 1000 $\frac{ng}{ml}$. In the absence of data G_{con} was assumed to have a dedimensionalised value of 1.

CaP dissolution

Experimental data on the dissolution rate and specific surface area of CaP scaffolds are not available. The dedimensionalised parameter $\tilde{\sigma}$ was estimated to be 10. Since osteoblasts do

not survive when the calcium concentration exceeds 50 mM [Maeno et al., 2005], this value was adopted for Ca_∞.

Ca^{2+} consumption

The formation of intracellular vessicles containing bioapatite is a metabolic process requiring the uptake of calcium [Stanford et al., 1995]. The calcium flux from the extracellular space towards the cytosol (J_{Leaky}) is estimated to have a dedimensionalised value of 750. The parameter H_{Ca4} was chosen in such a way that the term $\frac{Ca}{H_{Ca4}+Ca}$ becomes equal to 1 for calcium concentrations higher than 10 mM. The parameter d_{Ca}, which models the calcium uptake for the metabolic activities of both osteoblasts and MSCs, has a dedimensionalised value of 100.

3.3.2 Scaling and non-dimensionalisation

The following scaling factors were chosen for the non-dimensionalisation of the model variables:

$$\tilde{t} = \frac{t}{T}, \quad \tilde{c_m} = \frac{c_m}{c_0}, \quad \tilde{c_b} = \frac{c_b}{c_0}, \quad \tilde{m} = \frac{m}{m_0}, \quad \tilde{b} = \frac{b}{m_0}, \quad \tilde{g_b} = \frac{g_b}{g_0}, \quad \tilde{Ca} = \frac{Ca}{Ca_0}$$

The time scale of $T = 1$ day was taken from Geris et al. [2008], based on studies of Harrison et al. [2003]. Representative concentrations for the collagen content ($m_0 = 0.1$ g/ml) and growth factors ($g_0 = 100$ ng/ml) are adopted from Geris et al. [2008]. A typical value for the cell density ($c_0 = 10^6$ cells/ml) is derived from Bailón-Plaza and van der Meulen [2001]. The scaling factor for the calcium concentration was assumed to be equal to the extracellular calcium concentration (1 mM).

The model parameters were non-dimensionalised as follows (the tildes represent the non-dimensional parameters):

$$\begin{aligned}
\tilde{P_{bs}} &= \frac{P_{bs}.c_0.T}{m_0}, \quad \tilde{\kappa_b} = \kappa_b.m_0, \quad \tilde{A_{m0}} = \frac{A_{m0}.T}{m_0}, \quad \tilde{K_m} = \frac{K_m}{m_0}, \quad \tilde{a_{cm}} = \frac{a_{cm}}{Ca_0}, \\
\tilde{b_{cm}} &= \frac{b_{cm}}{Ca_0}, \quad \tilde{c_{cm}} = \frac{c_{cm}}{Ca_0}, \quad \tilde{\alpha_m} = \alpha_m.c_0, \quad \tilde{H_{11}} = \frac{H_{11}}{g_0}, \quad \tilde{Y_{11}} = Y_{11}.T, \\
\tilde{G_{gb}} &= \frac{G_{gb}.T.c_0}{g_0}, \quad \tilde{H_{gb}} = \frac{H_{gb}}{g_0}, \quad \tilde{d_{gb}} = d_{gb}.T, \quad \tilde{A_{b0}} = \frac{A_{b0}.T}{m_0}, \quad \tilde{K_b} = \frac{K_b}{m_0}, \\
\tilde{a_{cb}} &= \frac{a_{cb}}{Ca_0}, \quad \tilde{b_{cb}} = \frac{b_{cb}}{Ca_0}, \quad \tilde{c_{cb}} = \frac{c_{cb}}{Ca_0}, \quad \tilde{\alpha_b} = \alpha_b.c_0, \quad \tilde{d_b} = d_b.T, \quad \tilde{P_{bb}} = \frac{P_{bb}.c_0.T}{m_0}, \\
\tilde{\kappa_{bb}} &= \kappa_{bb}.m_0, \quad \tilde{\sigma} = \sigma.T, \quad \tilde{Ca_\infty} = \frac{Ca_\infty}{Ca_0}, \quad \tilde{J_{leaky}} = \frac{J_{leaky}.T.c_0}{Ca_0}, \quad \tilde{H_{Ca4}} = \frac{H_{Ca4}}{Ca_0}, \\
\tilde{d_{Ca}} &= d_{Ca}.T.c_0, \quad \tilde{F_{11}} = F_{11}, \quad \tilde{F_{12}} = F_{12}, \quad \tilde{G_{con}} = G_{con}.c_0, \quad \tilde{H_{con}} = \frac{H_{con}}{g_0}, \quad \tilde{d_{cm}} = d_{cm}.m_0.T
\end{aligned}$$

This results in the following set of non-dimensionalised parameter values:

$$\begin{aligned}
\tilde{P_{bs}} &= 0.18, \quad \tilde{\kappa_b} = 1, \quad \tilde{A_{m0}} = 0.85, \quad \tilde{K_m} = 0.1, \quad \tilde{a_{cm}} = 5.98, \\
\tilde{b_{cm}} &= 3.33, \quad \tilde{c_{cm}} = 1.67, \quad \tilde{\alpha_m} = 1, \quad \tilde{H_{11}} = 14, \quad \tilde{Y_{11}} = 10, \quad \tilde{G_{gb}} = 350, \quad \tilde{H_{gb}} = 1,
\end{aligned}$$

$$\begin{aligned}
\tilde{d_{gb}} &= 75, \quad \tilde{A_{b0}} = 0.202, \quad \tilde{K_b} = 0.1, \quad \tilde{a_{cb}} = 41.82, \quad \tilde{b_{cb}} = 5.06, \quad \tilde{c_{cb}} = 1.9, \\
\tilde{\alpha_b} &= 1, \quad \tilde{d_b} = 0.1, \quad \tilde{P_{bb}} = 0.0398, \quad \tilde{\kappa_{bb}} = 1, \quad \tilde{\sigma} = 10, \quad \tilde{Ca_\infty} = 50, \quad \tilde{J_{leaky}} = 750, \\
\tilde{H_{Ca4}} &= 0.01, \quad \tilde{d_{Ca}} = 100, \quad \tilde{F_{11}} = 8, \quad \tilde{F_{12}} = 1.5, \quad \tilde{d_{cm}} = 1.5, \quad \tilde{G_{con}} = 1, \quad \tilde{H_{con}} = 0.001
\end{aligned}$$

3.4 Simulation details

The set of non-linear differential equations was implemented in Matlab (The MathWorks, Inc.). In order to solve the aforementioned differential equations, a time delay and initial conditions need to be specified.

Time delay

The proposed mathematical model does not include the whole lineage of osteoprogenitor cells. Only two cell types, the undifferentiated MSCs and fully differentiated osteoblasts, are modelled. To minimise the error due to this simplification, a time delay is adopted. Malaval et al. [1999] report eight to ten population doublings in cultures of osteoprogenitors before the appearance of differentiated osteoblasts. This results in a time delay of 11 days. The mature osteoblasts start producing collagen after three days. The dde routines of Matlab (The MathWorks, Inc.) were used to implement the time delays and solve the set of differential equations.

Initial conditions

At the start of the simulation there are MSCs ($\tilde{c}_{m,ini} = 1$) and growth factors ($\tilde{g}_{b,ini} = 15$) present. The calcium concentration is assumed equal to the normal extracellular concentration ($\tilde{Ca}_{ini} = 1$). Only a very small amount of collagen matrix ($\tilde{m}_{ini} = 0.01$) is present at the beginning of the simulation. All other variables are assumed to be zero initially.

Discontinuities

To model specific events, like a bolus injection of growth factors or the gradual decrease of calcium release, Matlab (The MathWorks, Inc.) provides specific options like “Jumps” and “InitialY”. The interested reader can find more documentation on these topics on the Matlab help-file.

3.5 Results

3.5.1 Normal bone formation

Using the parameters as described in section 3.3, the model predicts 31 % bone formation at 90 days post implantation. Figure 3.2 shows the temporal evolution of the extracellular matrix density, MSCs, growth factor concentration, osteoblasts, bone matrix density and calcium concentration.

The calcium concentration initially increases, due to the dissolution of the calcium phosphates. This increase, as well as the presence of osteogenic growth factors, triggers the differentiation of the MSCs towards osteoblasts. The remaining stem cells proliferate

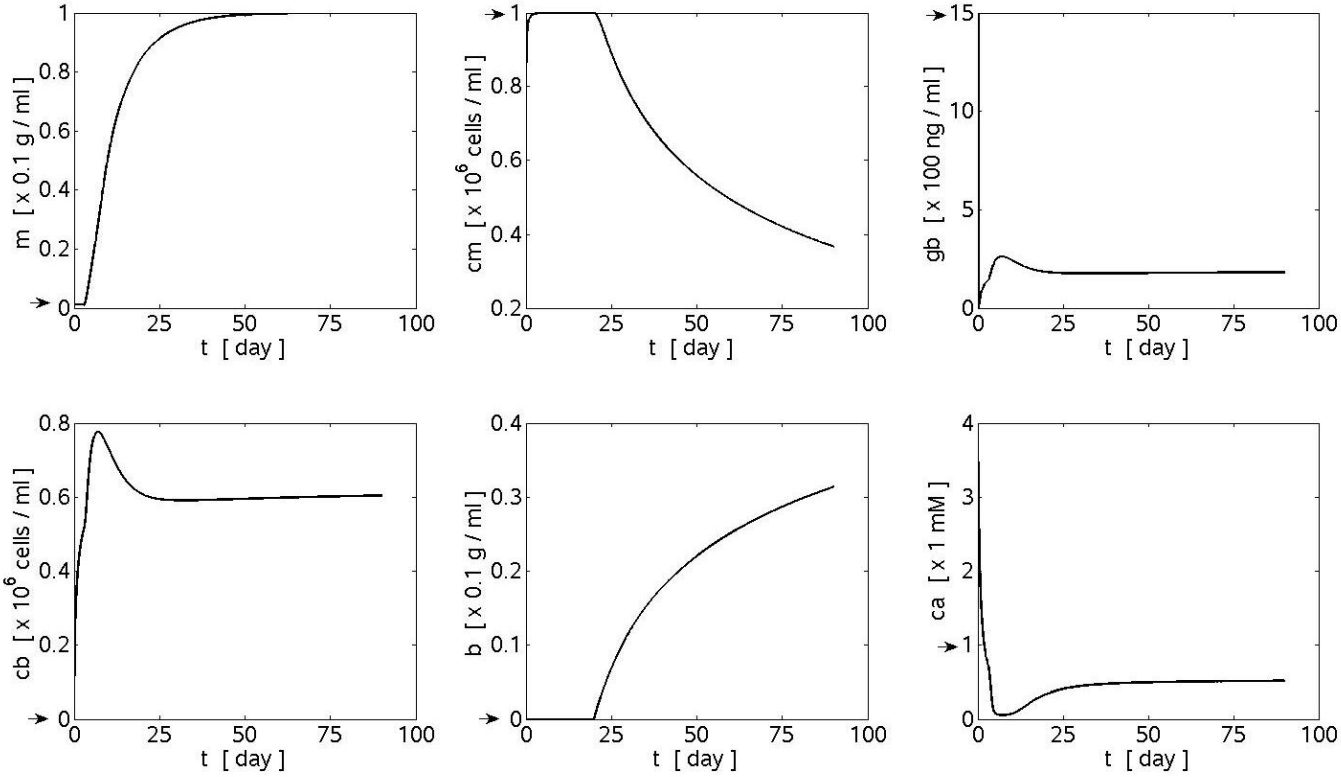

Figure 3.2: Temporal evolution (days post implantation) of collagen matrix density (m), mesenchymal stem cell density (c_m), growth factor concentration (g_b), osteoblast cell density (c_b), bone matrix density (b) and calcium concentration (Ca) during normal bone formation. The arrows indicate the initial conditions.

until they reach the maximal cell density. As the total cell density (MSCs + osteoblasts) increases, the metabolic need for calcium rises and the calcium concentration decreases. After three days the differentiated osteoblasts start to produce collagen matrix. This process continues and at a collagen matrix density of 85 % it triggers the mineralisation of the osteoid. Gradually the scaffold gets filled with bone, and the MSCs that are trapped in the bone matrix die.

3.5.2 Impaired bone formation

Decalcified scaffold

Eyckmans et al. [2010] suggest that CaP granules need to be present in sufficient quantities to induce ectopic ossification. Experimental evidence of this hypothesis is given by the observations that the bone spicules were only present on the CaP granules, and that no bone or fibrous tissue was found 8 weeks after implantation of cellularised decalcified scaffolds [Eyckmans et al., 2010]. This impaired form of bone formation was simulated by reducing the dissolution rate of the calcium phosphate scaffold (σ) from 10 to 0.

Figure 3.3 shows the temporal evolution of the different cells and tissues in the decalcified scaffold. The initial concentration of growth factors allows some differentiation of MSCs.

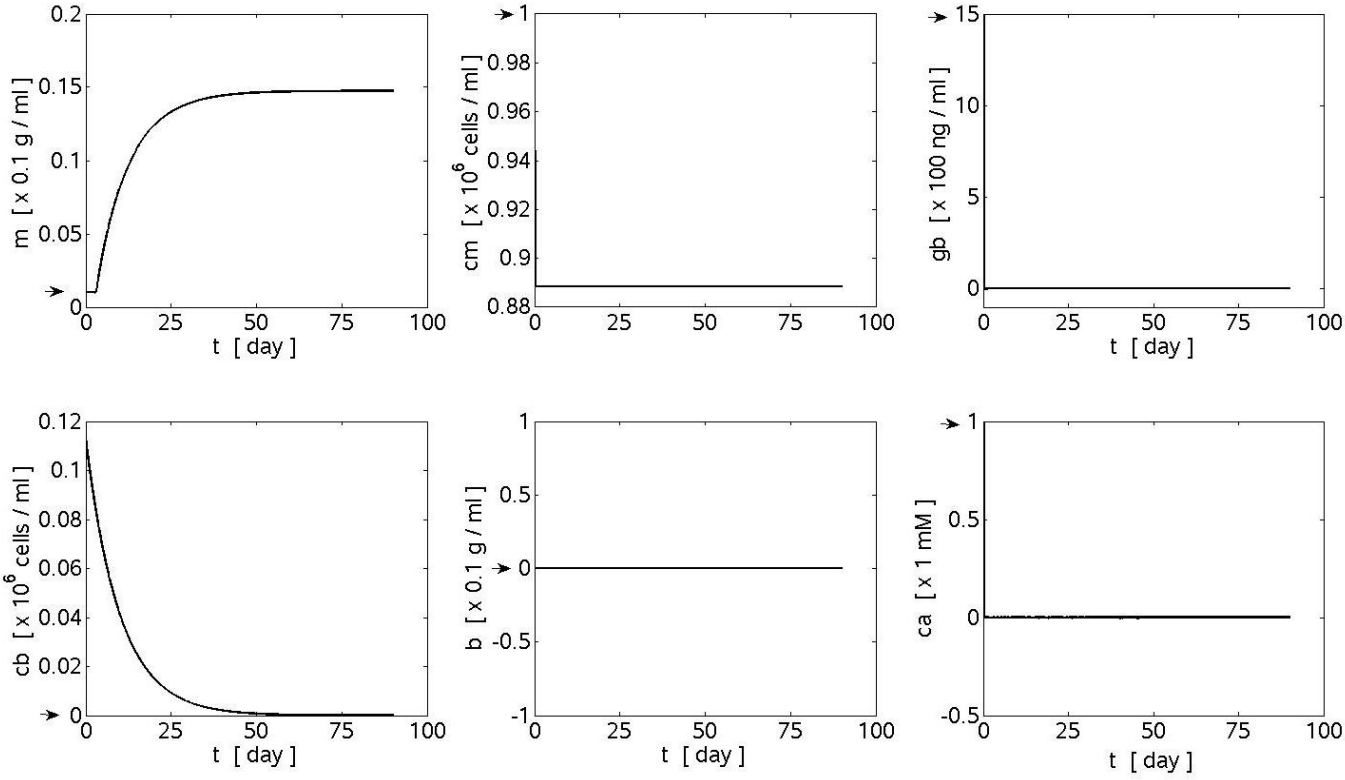

Figure 3.3: Temporal evolution (days post implantation) of collagen matrix density (m), mesenchymal stem cell density (c_m), growth factor concentration (g_b), osteoblast cell density (c_b), bone matrix density (b) and calcium concentration (Ca) during bone formation in a decalcified scaffold ($\sigma = 0$). The arrows indicate the initial conditions.

Due to the metabolic needs of both osteoblasts and MSCs, the calcium concentration drops quickly. Since, from that time point on, the derivatives of equations (3.12), (3.13) and (3.16) become equal to zero, the simulation predicts constant profiles for the variables c_m, g_b and Ca. This is, however, not physiologically possible. In reality, the lack of calcium ions will induce the apoptosis of the MSCs. Although the concentration of osteoblasts is low, there is some production of collagen matrix. The production rate gradually decreases due to the apoptosis of the osteoblasts. Remark the absence of bone formation in the decalcified scaffold.

Insufficient cell seeding

Eyckmans et al. [2010] report that a minimal amount of 10^6 cells is needed to induce ectopic bone formation. This finding is supported by the experimental results of Kruyt et al. [2008]. They determined a minimal bone marrow stromal cell density (BMSC density) of 8.10^4 $\frac{BMSCs}{cm^3}$ for bone formation in a BCP scaffold. The discrepancy between the reported minimal amount might be explained by the different experimental set-up (mice vs goats) and cell source (hPDCs vs hBMSCs). The calcium model can simulate the effect of insufficient cell seeding by reducing the initial seeding density of MSCs ($\tilde{c}_{m0}$) from 1 to 0.3.

The temporal evolution of the different cells and tissues for a low seeding condition is

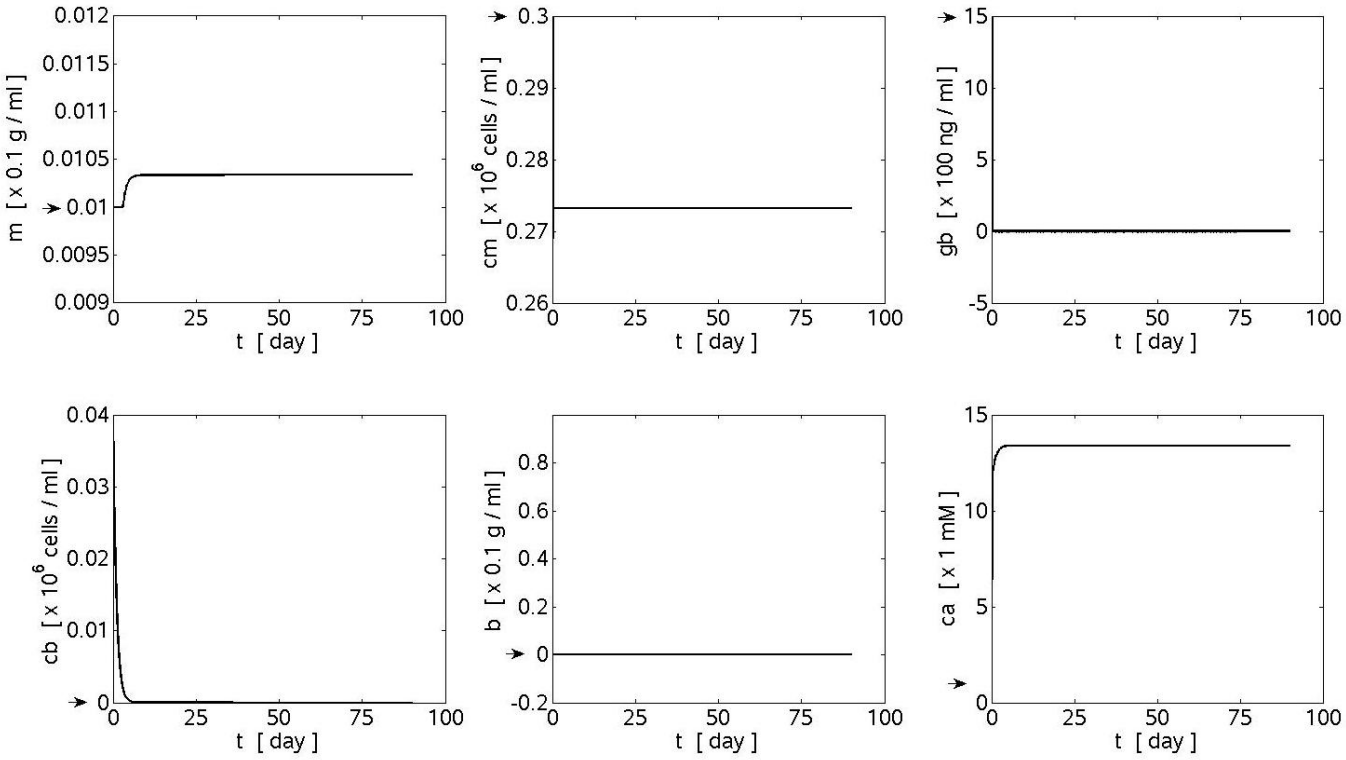

Figure 3.4: Temporal evolution (days post implantation) of collagen matrix density (m), mesenchymal stem cell density (c_m), growth factor concentration (g_b), osteoblast cell density (c_b), bone matrix density (b) and calcium concentration (Ca) in a scaffold with low initial seeding density ($\tilde{c}_{m0} = 0.3$). The arrows indicate the initial conditions.

illustrated by figure 3.4. As is suggested by Eyckmans et al. [2010], no bone formation is found at 8 weeks post implantation. Since the concentration of growth factors is too low to induce differentiation, the osteoblasts gradually die. Consequently, no collagen or bone matrix is found in the scaffold. The calcium concentration remains high enough to satisfy the consumption by the MSCs, with the result that the stem cells are maintained at a slightly lower density than the initial seeding density.

3.6 Discussion

3.6.1 Simulation results

Normal bone formation

In the experiments reported by Hartman et al. [2005], the percentage of bone formation was determined at day 7, 21 and 42 post implantation. The percentage of bone formation was calculated as the ratio of the surface area of newly formed bone to the surface area of the CaP-implant. These values are represented by the bars in figure 3.5. Since the amount of modelled bone formation cannot exceed 1, figure 3.5 shows the temporal evolution of the predicted bone tissue fraction (continuous line).

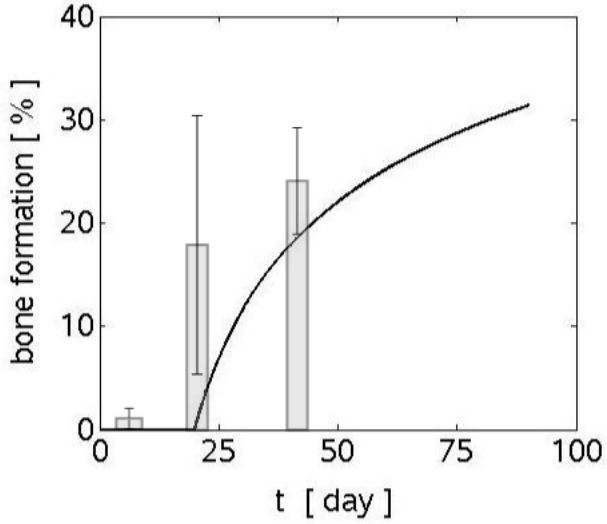

Figure 3.5: Predicted (continuous line) and experimentally measured (bars, average + standard deviation) bone tissue fraction. The bars represent the bone formation as determined by histomorphometry at week 1, 3 and 5 by Hartman et al. [2005].

The results of the simulation and experiment correspond qualitatively. However, the bone formation is observed to start at a later time point in the simulation. If smaller time delays would be adopted, the bone formation would also start earlier in the simulation. The amount of bone measured at day 21 is much larger than the predicted amount. It is worth noting, however, that this time point has a large standard deviation. Remark as well that Hartman et al. [2005] measures the amount of bone formation in scaffolds that were subcutaneously implanted in rats. The parameters of the calcium model were, however, fitted according to the data for dogs [Yuan et al., 2006]. The predicted amount of bone at 42 days corresponds to the experimental observations.

Roldan et al. [2010] report the amount of bone formation in a highly porous biphasic calcium phosphate scaffold. They measured a median of 45 % at 84 days post implantation, where the bone formation was calculated as the ratio of newly mineralised bone area to ceramic area. The difference between this experimental (mice) and predicted result could be attributed to the fact that the computational model fitted the canine experimental data of Yuan et al. [2006]. Roldan et al. [2010] also use highly porous scaffolds ($\pm$ 93%) whereas the samples used by Yuan et al. [2007] have a macroporosity of 40%.

Bone apposition inside an ectopically implanted disc was investigated by Kruyt et al. [2007]. They report a bone formation percentage of $19.8 \pm 6.9\%$ at 63 days post implantation. The contact percentage was calculated as the ratio of bone-scaffold contact length to scaffold perimeter length. The difference between this experimental (goats) and predicted result could be explained by the fact that the computational model fitted the canine experimental data of Yuan et al. [2006]. Kruyt et al. [2007] also use scaffolds with an 80/20 weight percent ratio of HA to tricalcium phosphate whereas Yuan et al. [2007] implants scaffolds with an 60/40 weight percent ratio.

From the previous discussions it seems that the animal model is a crucial parameter. This is also suggested by Ripamonti [1996], who showed a dramatic difference in the amount

of bone formation between different animal species. In order to gain more understanding of the interactions between biomaterials and animal species, further research should be conducted in this field. This will further advance the design of porous bone substitutes for therapeutic purposes.

Impaired bone formation

Eyckmans et al. [2010] found no bone formation in decalcified scaffolds. The present model assumes that the deprivation of Ca^{2+} is the underlying reason for this observation. However, the CaP spicules also form an anchorage for the osteogenic cells. The removal of this support in the decalcified scaffold may thus impair the survival of the seeded cells and limit the amount of bone formation.

Eyckmans et al. [2010] report that a minimal amount of 1.10^6 cells is needed to induce ectopic bone formation. It is, however, interesting to investigate whether a certain therapy might induce bone formation, even with less cell seeding. A possible strategy could include the use of growth factors, since bone morphogenetic proteins (BMPs) have specific biologic activities, like the induction of bone formation at ectopic sites *in vivo*. This was experimentally investigated by Kim et al. [2005] and Liang et al. [2005]. They both report ectopic bone formation in scaffolds loaded with BMP-2, although no cells were seeded. A major difference with the 1D-model is, however, the fact that these decellularised scaffolds are ectopically implanted thereby causing the migration of MSCs in the nearby tissue towards the scaffold. The calcium model does not have this spatial dependency as a result of which it needs a certain initial MSC concentration to start the biological process.

A possible therapy for a scaffold loaded with 1/3 of the standard seeding cell density is illustrated in figure 3.6. When the scaffold is ectopically implanted, the calcium concentration will increase rapidly due to the dissolution of the calcium phosphates. However, since the initial cell seeding is lower, the need for calcium is reduced. A possible therapy might thus concentrate on removing the excessive amount of Ca^{2+}. This is simulated by exponentially reducing the parameter σ from eight to four. The reduction in calcium release creates a more viable environment for the osteogenic cells. As can be seen in figure 3.6, the MSCs and osteoblasts start to proliferate. Collagen matrix is produced by the osteoblasts and bone formation starts at 40 days post implantation. The amount of bone formation can be further increased by injecting a bolus of growth factors. This was done at 50 days post implantation and causes the differentiation of MSCs and, consequently, a rapid increase in the osteoblast concentration. Remark that the amount of bone formation at 90 days is almost 25%, which would be zero without the reduction in calcium release due to insufficient cell seeding (see figure 3.4).

3.6.2 Simplifications

The current model assumes that the dissolution of calcium phosphate granules is the key mechanism by which the granules influence cellular activity. The dissolution of the calcium phosphate granules frees up calcium ions that can subsequently alter the cellular metabolism. Calcium can only influence bone cells when it is an ion, not when it is bound to other atoms. There are, however, other mechanisms of influence proposed in literature. Barrère et al. [2006], for example, cite the effect of topography and exposed surface area for protein bonding. More information on this particular subject can be found in section 2.3. The

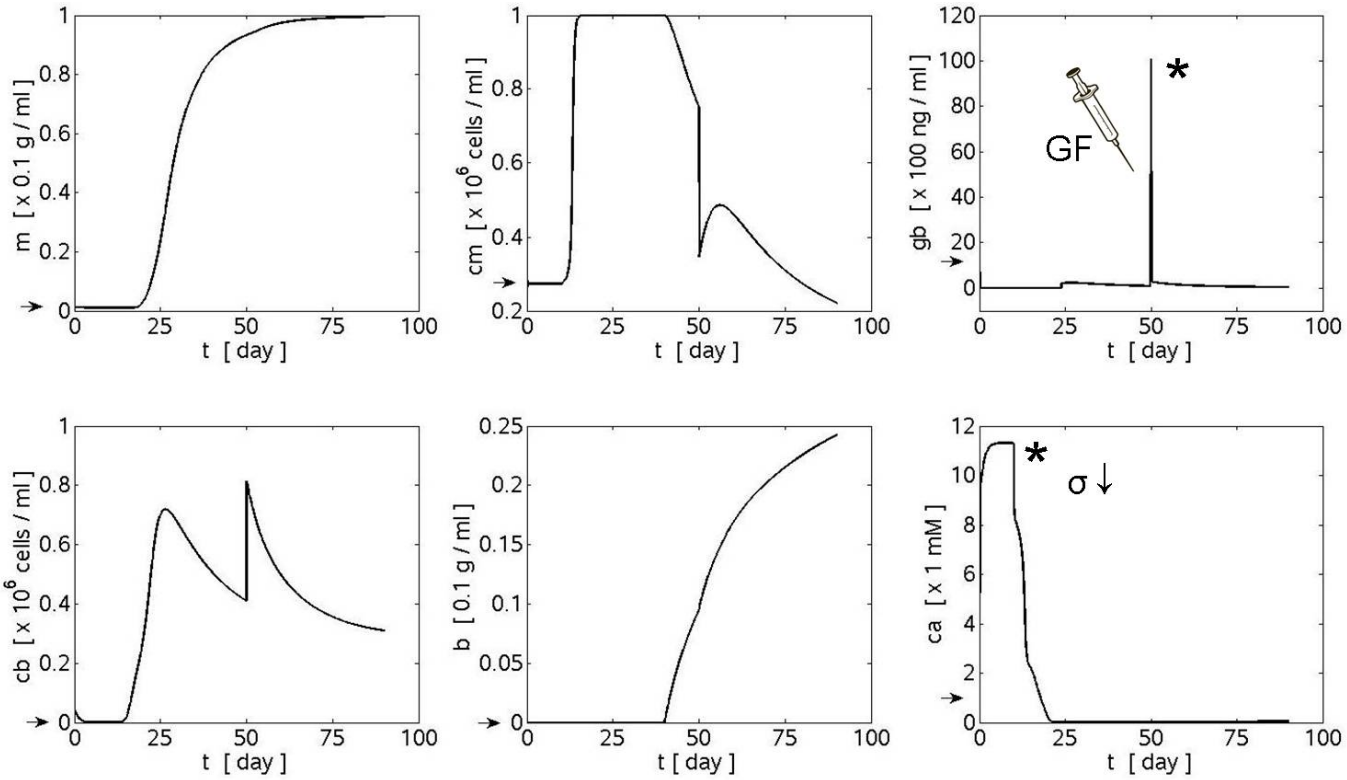

Figure 3.6: Temporal evolution (days post implantation) of collagen matrix density (m), mesenchymal stem cell density (c_m), growth factor concentration (g_b), osteoblast cell density (c_b), bone matrix density (b) and calcium concentration (Ca) in a scaffold with an initial cell density of $\tilde{c}_{m0} = 0.3$. After ten days the calcium release is exponentially reduced ($\sigma = 8 \rightarrow \sigma = 4$). A bolus of growth factors is injected at day 50 post implantation. The arrows indicate the initial conditions.

incorporation of some of these mechanisms may further refine the proposed mathematical model.

Due to the lack of experimental data, the parameter σ was estimated. However, if this parameter could be determined more accurately, the model could be used to test different biomaterials *in silico*. Namely, for every calcium phosphate the optimal seeding density could be determined, since this depends on the dissolution rate and specific surface area of the bioapatite. Also, the expected amount of bone formation could be calculated *in silico*, allowing for an *in silico* triage of new biomaterials and thereby reducing *in vitro* experimentation on poorly performing biomaterials. The specific surface area of a scaffold can be derived from gas adsorption or μCT measurements. The dissolution rate can be derived from calcium concentration measurements at consecutive timepoints, as was done by Zhang et al. [2001] and Zhang et al. [2003]. Recently, a number of characterisation measurements and calcium dissolution tests were preformed on clinical CaP scaffolds within Prometheus. These data will be used in the future to derive biomaterial specific values of σ.

When the CaP scaffold is ectopically implanted, proteins will adsorb on the surface of the biomaterial. This adsorbed protein layer will influence the dissolution behaviour of the

implanted scaffold. Therefore, not only the initial dissolution rate but also the decrease in calcium release should be fully investigated and quantified.

The parameter σ is not the only parameter that was estimated due to a lack of experimental data. The uptake of calcium by osteoblasts (J_{leaky}), the apoptosis rate of MSCs in the bone matrix (d_{cm}), the consumption of growth factors during differentiation and proliferation (G_{con}) and the amount of calcium uptake for metabolic activities (d_{ca}) are also parameters that should be investigated and quantified in future experiments.

In the proposed mathematical model there is no artificial deposition of hydroxyapatite on the collagen matrix. This assumption is supported by the findings of Chang et al. [2000] for *in vitro* experiments. The validity of this assumption for *in vivo* conditions is, however, questionable.

The key role of calcium in several intra- and extracellular processes is long established. The complex calcium dynamics that underlie these different phenomena are simplified by the proposed mathematical model. The uptake of calcium by osteoblasts for hydroxyapatite production is characterised by a leakage flux (J_{leaky}) from the extracellular space to the cytosol. Osteogenic cells also store Ca^{2+} in the endoplasmic reticulum (ER). However, the presented calcium model does not include the contribution of Ca^{2+} stored in the ER or other organelles to the hydroxyapatite production.

There is no calcium flux going from the intracellular towards the extracellular space. This assumption is supported by the fact that the cells need calcium for the hydroxyapatite production. Both MSCs and osteoblasts take up calcium for their metabolic activities (d_{ca}).

However, calcium ions might influence these metabolic activities by activating G-coupled proteins that initiate intracellular signalling cascades. In this transduction mechanism there is no uptake of calcium ions by the cell. Moreover, one calcium ion can activate more than one G-coupled protein. The current model, however, uses a black box approach. This means that a certain input (the calcium concentration) has a certain output (proliferation and differentiation), but how this input is transduced into the output (the underlying intracellular mechanisms) is not modelled. This approach is intrinsically a simplification, but can be justified by the limited knowledge that is available on the specific transduction mechanisms. At a later stage the intracellular and cellular models might be combined to give a more accurate description.

The current model does not include chondrocytes. This means that only intramembranous ossification is being modelled. A further extension of the proposed mathematical model might include adding other cell types like chondrocytes, fibroblasts and osteoprogenitor cells in additional stages of differentiation. Moreover, also osteoclasts could be included since Ca^{2+} can be considered as a coupling factor between osteoclasts and osteoblasts, as was mentioned in section 2.4. This extension could be inspired by the mathematical framework of Lemaire et al. [2004] who modelled the interactions between osteoblast and osteoclast activities during bone remodelling. The coupling factor Ca^{2+} is, however, not a variable in their model. A more refined mathematical model is proposed by Peterson and Riggs [2010]. They model the integral calcium homeostasis and bone remodelling using 28 coupled differential equations including not only different cell types and biochemical signals, but also some key hormones (e.g. PTH) and intracellular variables (e.g. Runx2 and CREB). The effect of calcium on the differentiation and proliferation of osteogenic cells, as described in this chapter, is not included in the framework of Peterson and Riggs [2010].

Furthermore, their focus lies on bone remodelling, whereas the presented Master's thesis concentrates on bone formation. At a later stage the presented calcium model might be combined with the mathematical framework of Peterson and Riggs [2010] to give a more accurate description of the integral calcium homeostasis during bone formation.

Another important aspect that is not included in the mathematical model is angiogenesis. The invasion of blood vessels will present an additional source of calcium ions and growth factors. Thus, even in the absence of calcium phosphate granules, there might be bone formation. This was observed by Hartman et al. [2005]. They implanted seeded titanium scaffolds subcutaneously in the back of rats. Although, the amount of bone formation was much less when compared with the CaP scaffolds, it was not zero. This is in contrast with the observations of Eyckmans et al. [2010], who saw no bone formation when there were no CaP granules present. This discrepancy could be explained by the use of different animal models (rat vs mice), cells (bone marrow cells vs hPDC's) and biomaterial construct (a complete titanium scaffold versus a collagen scaffold seeded with CaP granules). However, further research is necessary to identify whether some critical parameters, that could explain this discrepancy, are still undiscovered.

The proposed mathematical model focusses on calcium only. However, Stanford et al. [1995] report the influence of organophosphates on mineralisation. According to their data P_i triggers the mineral formation and Ca^{2+} regulates the amount of mineral deposition after the initation by phosphate. In the future, it would be interesting to investigate a mathematical model that focusses on phosphate ions. The mathematical framework would be similar to the calcium model proposed here, only the parameter values would change. In a later stage both models could be combined to give a more complete description of the mineralisation process.

A last simplification lies in the fact that the model only looks at 1D variations. A further extension, including spatial variations will be discussed in chapter 5.

3.7 Conclusion

This chapter presented a 1D mathematical model that describes the effect of calcium on the activity of osteogenic cells. It incorporates some key features such as proliferation, differentiation and apoptosis and its results have been successfully corroborated by comparison with experimental data from literature. Application of the calcium model to the set-up of bone formation, allowed to simulate decalcified scaffold and insufficient cell seeding conditions. Simulations of these adverse biological situations predicted the formation of little or no bone, as was shown experimentally. A therapy was designed for the condition of insufficient cell seeding.

To the author's knowledge, the model presented here, is the first to establish a mathematical description of the effect of calcium on the activity of osteogenic cells at the tissue level. Sandino et al. [2010] also simulate cell differentiation in a CaP scaffold, however, they focus on the mechanical stimuli instead of the biochemical stimuli like Ca^{2+} and growth factors. Future research should focus on the coupling of mechanical and biological influences on the bone formation process. The study presented in this chapter is an illustration of the potential of mathematical models to help solve the biological puzzle of bone formation.

Chapter 4

Sensitivity analysis by design of experiments

4.1 Introduction

The computational calcium model describes the effect of calcium on the cellular activity of osteogenic cells. However, the current model does not account for the uncertainty in input parameters and some assumptions. Moreover, some assumptions about parameter values are not yet fully established. Identifying these parameters could lead towards designing specific experiments to measure unknown parameters of significance. Firstly, a sensitivity analysis can be used to determine main effects as well as important interactions between factors. Secondly, a sensitivity analysis could also be used to simplify the model by determining and eliminating insignificant model parameters. Finally, a sensitivity analysis not only allows to optimise the response, but also to assess the stability and global optimality of the optimum in the parameter space.

Section 4.2 highlights the major differences between physical and computer experiments. Section 4.3 describes the different methods that can be used to determine the parameters of significance. Details on the specific method that is used in this study are given in section 4.4. The results are discussed and interpreted in sections 4.5 and 4.6. The last section recapitulates the most important findings of this chapter.

4.2 Physical experiments versus computer experiments

To answer a particular research question at hand, proper experimentation is paramount. An important aspect of proper experimentation is the design of the experiment. An efficient experimental design can greatly improve the reliability of the gained knowledge while reducing the cost of the experiment. This is especially important for physical experiments, which can be tedious and expensive, but, with a proper design, can provide reliable results in the presence of unavoidable experimental and measurement errors [Montgomery, 2009; Myers and Montgomery, 1995]. Although computer experiments are deterministic, experimental design can also be useful to ensure a reliable outcome with a minimum of computational time when the phenomena under study are complex and highly non-linear. Computer experiments require, however, the use of hardware and are only an approximation of the complex physical process under study. In spite of these disadvantages,

computer experimentation may provide an interesting alternative when the number of input parameters is too large for the physical experiment to be run or some economical or ethical reasons prohibit the physical experiment [Santner et al., 2003].

Once the experimentation has been executed, there are appropriate statistical methods to analyse the resulting data. This is true whether the data are generated by a physical process or by a computational model, like the calcium model that is considered here. However, there are some significant differences between the data generated by a physical experiment and the data generated by a computer code.

In contrast to physical experiments, a computer experiment uses a deterministic simulation model. This implies that running the computer code with the same input parameters will yield identical observations. Computer experiments thus lack random error (noise), unlike physical experiments, which have substantial error due to the variability in the input parameters and the environment. As a consequence, the traditional principles developed to deal with this variability, such as blocking, randomisation and replication, cannot be used for the design and analysis of computer experiments [Montgomery, 2009]. The p-values from fitted statistical models lose their usual meanings. They have become indications, since no valid confidence intervals can be determined from these deterministic data.

In addition to being deterministic, computer experiments can be time-consuming. Moreover, the number of factors in a computer simulation can be quite large, ranging from 15 to 20 or more. The range of variation for each of these factors can also be much larger in computer experiments than in physical experiments. Although a lot of methods were initially created for physical experiments, they can be extended to the context of numerical simulation [Saltelli et al., 2000]. The remaining part of this chapter will focus on the design and analysis of computer experiments.

4.3 Design and analysis of computer experiments

A variety of methods exists to conduct a sensitivity analysis by design of experiments. This section provides a short introduction to different techniques that are most commonly found in the biomedical literature. A more detailed discussion can be found in Montgomery [2009], Myers and Montgomery [1995] and Saltelli et al. [2000].

4.3.1 OAT-design

The simplest class of designs is that of the one-at-a-time (OAT) experiments, where the effect of one factor is assessed by varying the value of only that factor and keeping all other factors fixed. This approach is often referred to as ceteris paribus [Saltelli et al., 2000]. The standard OAT-design uses a “nominal” or “standard” value per factor. The combination of nominal values for all the factors is called the reference or base-line condition. Next, two extreme values are proposed to represent the range of each factor. Usually the “standard” value will be in the middle of the two other levels. The magnitudes of the differences between the outputs for the extreme values and the “standard” values are then compared to find the factors that influence the model output the most [Saltelli et al., 2000]. The OAT-method was used by Lacroix [2001] and Geris et al. [2006].

The main advantage of this method is its simplicity. However, OAT experiments can only study one factor at the time and cannot, because of this restriction, capture interactions

between factors. Another disadvantage is the necessary selection of a reference (base-line condition) [Isaksson et al., 2008].

4.3.2 Factorial designs

Full factorial design

In a full factorial design all possible combinations of the levels of each factors are investigated. For example, if there are a levels of factor A and b levels of factor B then the total experiment will consist of ab runs. In order to explain the basic principles, consider the experiment in figure 4.1.

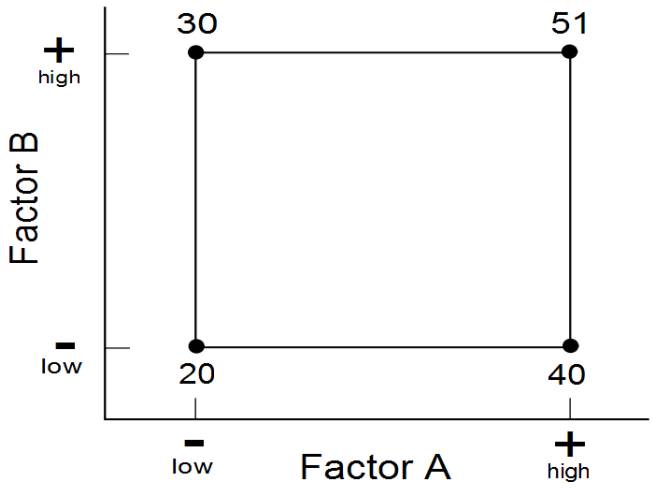

Figure 4.1: A two-factor factorial experiment with the response of the 4 runs shown at the corners. Remark that in this experiment $a = 2$ and $b = 2$ which results in $ab = 4$ runs.

This is a two-factor (A and B) experiment with both factors at two levels (+, high and -, low). The main effect of factor A in this design can be calculated as the difference between the average response at the low level of A and the average response at the high level of A. In this example this is equal to:

$$A = \frac{40 + 51}{2} - \frac{20 + 30}{2} \tag{4.1}$$

In general one can define the effect of a factor as the change in response produced by a change in the level of the factor [Montgomery, 2009]. A full factorial design can also estimate interactions between factors, as is illustrated in figure 4.2. At the low level of B, the effect of A is:

$$A = 50 - 20 = 30 \tag{4.2}$$

At the high level of B, the effect of A is:

$$A = 12 - 40 = -28 \tag{4.3}$$

These results show that the effect of A depends on the level chosen for factor B, which indicates that there is interaction between the factors A and B. Moreover, the magnitude

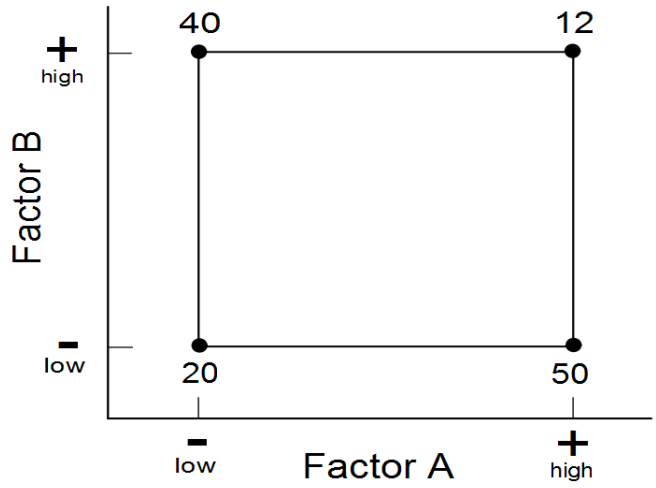

Figure 4.2: A two-factor factorial experiment with interaction between the factors A and B.

of the interaction effect is the average difference between these two effects of A, namely [Montgomery, 2009]:

$$AB = \frac{-28 - 30}{2} = -29 \tag{4.4}$$

These two simple examples illustrate the basic principles of full factorial design. The above principles can obviously be extended to more factors and levels. Using other, more complex techniques a full statistical analysis of the model can thus be obtained.

Full factorial designs have several advantages. They are more efficient than OAT-experiments and provide information on the interactions between factors. These designs do not require a base-line condition, which is necessary for an OAT-design. Furthermore, they can study the effects of a factor at several levels of the other factors, yielding conclusions that are valid over a range of experimental conditions. However, when the computational model contains a lot of parameters and the number of levels is large, the experimental cost can become very high [Montgomery, 2009; Saltelli et al., 2000].

Fractional factorial design

As the number of factors grows, the computational cost can increase rapidly. For example, a 2^6 full factorial design requires 64 runs, of which only six are used to estimate the main effects and 15 to estimate the two-factor interactions. The remaining runs are used to calculate the three-factor and higher-order interactions [Myers and Montgomery, 1995]. Fractional factorial designs are based on the idea that at some point higher-order interactions tend to become negligible, so that the information on the main effects and lower-order interactions can be obtained by running only a fraction of the complete factorial experiment [Saltelli et al., 2000; Myers and Montgomery, 1995].

In order to explain the basic principles of fractional factorial design, consider a situation in which three factors (A, B and C), each at two levels, are of interest but the experimenter

Table 4.1: Plus and minus signs for the 2^3 factorial design [Montgomery, 2009].

Treatment Combination	**Factorial Effect**							
	I	A	B	C	AB	AC	BC	ABC
a	+	+	-	-	-	-	+	+
b	+	-	+	-	-	+	-	+
c	+	-	-	+	+	-	-	+
abc	+	+	+	+	+	+	+	+
ab	+	+	+	-	+	-	-	-
ac	+	+	-	+	-	+	-	-
bc	+	-	+	+	-	-	+	-
(1)	+	-	-	-	+	+	+	-

cannot run all $2^3 = 8$ experiments. The experimenter would like to obtain some information from only four runs, one-half fraction of a 2^3 design. Table 4.1 shows the 2^3 design.

Suppose that the first four runs are selected from table 4.1. This allows us to estimate the main effects (similar to full factorial design):

$$A = \frac{1}{2}.(a - b - c + abc) \tag{4.5}$$

$$B = \frac{1}{2}.(-a + b - c + abc) \tag{4.6}$$

$$C = \frac{1}{2}.(-a - b + c + abc) \tag{4.7}$$

and the two-factor interactions are then given by:

$$BC = \frac{1}{2}.(a - b - c + abc) \tag{4.8}$$

$$AC = \frac{1}{2}.(-a + b - c + abc) \tag{4.9}$$

$$AB = \frac{1}{2}.(-a - b + c + abc) \tag{4.10}$$

If one compares these results, one notices that $A = BC$, $B = AC$ and $C = AB$. Consequently, it is impossible to differentiate between A and BC, B and AC and C and AB. This phenomenon is called aliasing or confounding [Montgomery, 2009]. Since the design in table 4.1 confounds the main effects with two-factor interactions, this design is called a resolution III design. However, the main effects are not confounded with other main effects. In a resolution IV design no main effects are confounded with other main effects or with any two-factor interactions, but two-factor interactions are confounded with each other. The designs in which no main effect or two-factor interaction is confounded with any other main effect or two-factor interaction, but in which two-factor interactions are confounded with three-factor interactions, is called a resolution V design [Montgomery, 2009; Myers and Montgomery, 1995; Saltelli et al., 2000].

From this discussion it is clear that a higher resolution is less restrictive in the assumptions regarding which interactions are negligible in order to obtain a unique interpretation of the data [Montgomery, 2009]. Obviously, in practice, there is a trade-off between resolution and computational cost. The above principles can obviously be extended to more factors

and levels. Using other, more complex techniques a statistical analysis of the model can thus be obtained.

Fractional factorial designs thus provide information on the (lower-order) interactions between factors, can study different factors simultaneously and do not require a reference (base-line condition). Furthermore, they can study the effects of a factor at several levels of the other factors, yielding conclusions that are valid over a range of experimental conditions. They require less time and cost than a full factorial analysis, but, if the focus is on interactions, then a full factorial or a higher resolution design is suggested. The main disadvantage of fractional factorial designs is the fact that the results are only valid within the chosen parameter space for the sensitivity analysis. This limitation applies, however, also to other methods like OAT and Taguchi [Isaksson et al., 2008]. Another shortcoming is the fact that interactions are confounded, i.e. the effects of certain interactions cannot be separated from each other.

Fractional factorial designs are often used in screening experiments to identify efficiently the subset of factors that are important and to provide some information on interactions [Myers and Montgomery, 1995]. Isaksson et al. [2008] determined, for example, the most important cellular characteristics for fracture healing using a resolution IV fractional factorial design and a three-level Taguchi orthogonal array. A resolution IV fractional factorial design was also used by Malandrino et al. [2009] to analyse the influence of six material properties on the displacement, fluid pore pressure and velocity fields in the L3-L4 lumbar intervertebral disc.

4.3.3 Taguchi's Method

Professor Taguchi recommends the use of statistical experimental design methods to assist in quality improvement during the development of a product or process. In a manufacturing process, for example, there are controllable factors (control factors) and uncontrollable factors (noise factors) that cause the variability in the final products. The goal of robust parameter design is essentially to find the levels of the control factors that are least influenced by the noise factors [Montgomery, 2009].

In the Taguchi parameter design methodology one orthogonal design is chosen for the control factors (inner array) and one orthogonal design is selected for the noise factors (outer array). Then, the inner and outer arrays are crossed to give the complete parameter design lay-out. After the experiment is run, the resulting data may be summarised and interpreted. For this purpose, Taguchi recommends the use of signal-to-noise ratios [Myers and Montgomery, 1995].

Taguchi's methodology has received a lot of attention in statistical literature. His philosophy was very original, but the implementation and technical nature of data analysis has received some criticism. Firstly, it does not allow the estimation of interaction terms. Secondly, some of the designs are empirically determined ("they work") but are suboptimal in comparison to rigorous alternatives such as fractional factorial designs [Montgomery, 2009]. Moreover, the signal-to-noise ratio does not always distinguish between processes that are characterised by different mean and variance properties [Myers and Montgomery, 1995]. Finally, if the Taguchi approach works and yields good results, one may still not know what caused the result because of the aliasing of critical interactions. In other words, the problem may be solved (short-term success) but one does not know *why* it works so

that no process knowledge (long-term success) has been gained. A more detailed discussion on Taguchi's method is given by Montgomery [2009] (chapter 12, supplementary material) and Myers and Montgomery [1995] (chapter 10, pages 462-480).

Despite of the criticism, Taguchi's approach is often used in biomedical literature, because of its simplicity. It is, for example, used by Yang et al. [2007] to optimise a cervical ring cage, and by Lin et al. [2007] to determine the relative contribution of different parameters on the biomechanical response of a single tooth implant placed in the maxilla. The application of Taguchi's robust parameter design is also demonstrated in the context of finite elements by Dar et al. [2002].

4.3.4 Space-filling designs

Isaksson et al. [2008] identify the most important cellular characteristics of their mechanoregulatory bone-healing model by means of a two-level screening experiment. However, with only two, discrete levels for every input (parameter value) one cannot capture the behaviour of the response (output of the model) for values between these levels (see figure 4.3). To avoid the risk of disregarding any complex behaviour, which is likely for sophisticated non-linear models, one would intuitively like to assess more levels by spreading the experimental points in space [Santner et al., 2003]. This is not problematic, since one is dealing with a computer experiment in which all the factors can easily adopt different values. Various methods to achieve an effective spreading of points, commonly referred to as space-filling designs, have been suggested in literature as appropriate experimental designs for computer experiments. Two well-established space-filling designs are latin hypercube sampling (LHS) and uniform sampling, into which this section will give a short introduction. The interested reader can find more information on these and other space-filling designs in Santner et al. [2003] and Fang et al. [2006].

Latin hypercube sampling

The building principle of a latin hypercube design (LHD) can be illustrated by the following, simple example. Consider a square-shaped, 2D experimental region which is divided into n equally spaced rows and columns (n corresponds to the number of points in the design). This results in n^2 cells that, in the next step, are filled with integers as to form a Latin square, an arrangement in which each integer appears exactly once in every row and column. Then, one integer is selected at random and in each of the n cells that contain this integer a random point is selected. The resulting design is a latin hypercube sample of size n [Santner et al., 2003]. An example of a space-filling LHD is given in figures 4.3 (III) and 4.4 (left). The design shown on the right-hand side of figure 4.4 is also a LHD but it is not space-filling. More elaborate algorithms, which aim at ensuring the space-filling property of latin hypercube designs, are described by Fang et al. [2006].

The LHD has many strengths: it is computationally cheap to generate, it can deal with large number of runs and input variables and has an excellent performance in computer experiments [Santner et al., 2003; Fang et al., 2006]. A disadvantage of LHD is that it is not flexible with regard to adding additional points. The fact a LHD is well-suited for monotonic response functions, but may not be adequate for non-monotonic response functions is also a major disadvantage [Fang et al., 2006].

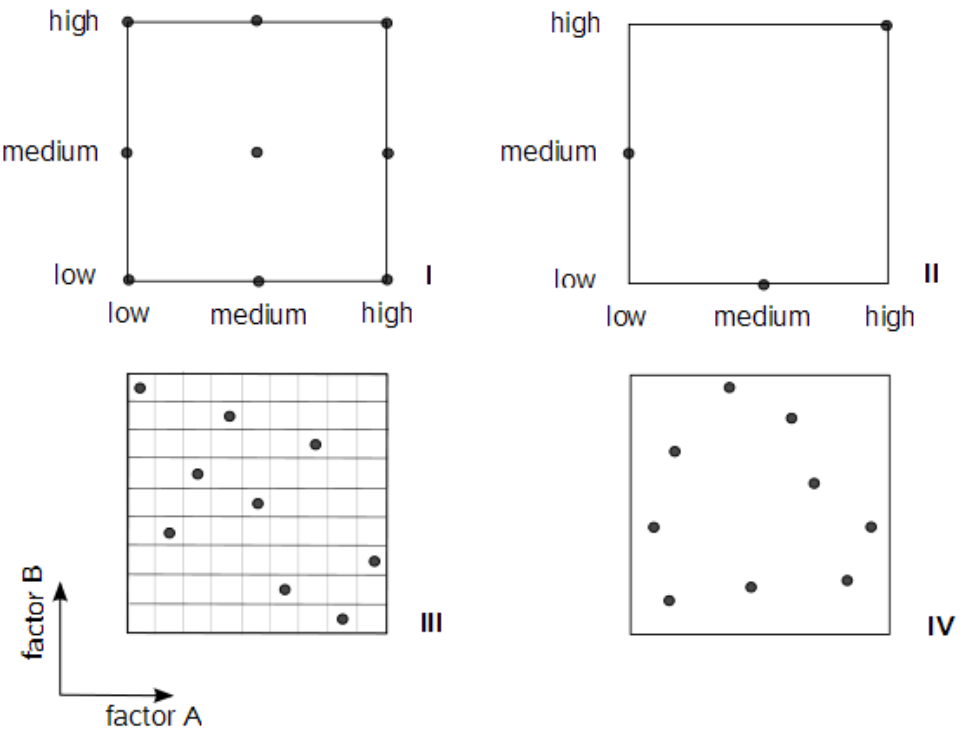

Figure 4.3: Schematical overview of different designs for two factors A and B. I: 3 level full factorial design, II: 3 level fractional factorial design, III: LHD, IV: uniform design. Remark that the factorial designs only use discrete levels, whereas the space-filling designs spread the points in space.

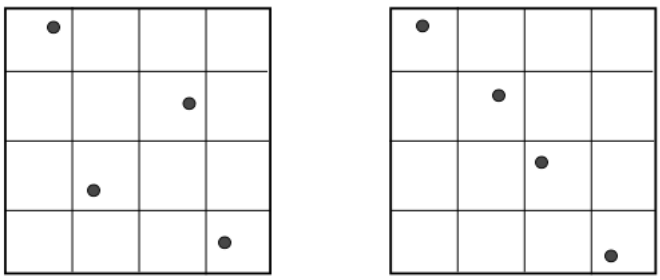

Figure 4.4: Two latin hypercube designs (n=4). There is one point in every row and column. Remark that the right design is not space-filling.

Uniform design

The uniform design was proposed by Fang et al. [2006]; Fang [1980]; Wang and Fang [1981] as a way of experiment to find as much information as possible, using relatively few experimental points. The goal was to find the best estimator of the overall mean (overall

mean model). This can be achieved by an uniform spreading of points, since, if all the points were clustered at one corner of the experimental space, the sample mean would represent the population mean rather poorly [Fang et al., 2006]. Other than the fact that it seems intuitively reasonable to use designs that spread the points evenly across space, it was noted that the points in orthogonal designs are typically uniformly spread. Thus, there might be a possibility that these uniform designs are often orthogonal [Santner et al., 2003].

It was found that uniform designs limit the effects of aliasing, are efficient and robust and have have an excellent performance in computer experiments. Aliasing or confounding means that the design cannot differentiate between main effects and interactions or lower-order interactions and higher-order interactions. This phenomenon is more thoroughly discussed in section 4.3. Users have reported that the uniform design is easy to understand and convenient, in that designs with small size have been tabulated for general use. However, the construction of a uniform design is computationally very demanding [Fang et al., 2006].

4.4 Materials and methods

This section describes in detail the different aspects of the design of experiment approach that was used to study the calcium model. In order to identify the input parameters that have the largest influence on the outcome variables, three different designs were explored: a resolution IV fractional factorial design, as was used by Isaksson et al. [2008], and two space-filling designs. This approach was chosen to allow a thorough interpretation and a comparison between the different design methods.

Section 4.4.1 describes the parameters that were included in the analysis. The criteria that characterise the performance of the system are defined in section 4.4.2. The different designs and methods of data analysis are discussed in sections 4.4.3 and 4.4.4 respectively.

4.4.1 Factors and levels

Table 4.2 lists the 33 parameters that were examined in the parametric study. The investigated properties include all the parameters of the calcium model except α_m, α_b, κ_b and κ_{bb}. These factors were excluded from the analysis, since their ranges would not have any physiological meaning. Namely, the maximal viable cell density and matrix density do not vary, due to different experimental conditions. Moreover, Isaksson et al. [2008] also exclude m_{max} (the maximal amount of matrix in an element) and c_{max} (the maximal cell concentration in an element), which are clearly similar to the parameters omitted here. In order to study the effect of the initial conditions, m_0, c_{m0}, g_{b0}, c_{b0}, b_0 and Ca_0 were included in the investigated set of parameters.

Within the study, each of the investigated parameters is referred to as a factor. The ranges of the factors that are adopted in the different designs, as well as the standard values, are listed in table 4.2. The chosen parameter space for each of the investigated factors was obtained from a literature study and experimental data. In the following tildes on non-dimensional values are omitted for simplicity.

- Bailón-Plaza and van der Meulen [2001] explored a range of values for P_{bs} numerically. The same range was adopted here.

Table 4.2: Ranges and standard values of the model parameters.

Parameter	Range	Standard value
P_{bs}	0.1 - 2	0.18
κ_b	/	1
A_{m0}	0.1 - 1.01	0.85
K_m	0.01 - 0.1	0.1
α_m	/	1
Y_{11}	10 - 100	10
H_{11}	10 - 20	14
a_{cm}	4.72 - 6.97	5.98
b_{cm}	3.05 - 3.73	3.33
c_{cm}	1.55 - 1.70	1.67
d_{cm}	0.001 - 3.5	1.5
G_{gb}	200 - 1000	350
H_{gb}	0.1 - 2	1
d_{gb}	33 - 1000	75
H_{con}	0.0001 - 0.1	0.001
G_{con}	1 - 75	1
A_{b0}	0.2 - 2.02	0.202
K_b	0.01 - 0.1	0.1
α_b	/	1
d_b	0.05 - 0.2	0.1
a_{cb}	35.2 - 46.94	41.82
b_{cb}	3.32 - 5.41	5.06
c_{cb}	1.9 - 2.28	1.9
P_{bb}	0.0298 - 0.0731	0.0398
κ_{bb}	/	1
J_{leaky}	400 - 800	750
H_{Ca4}	0.01 - 0.1	0.01
d_{ca}	10 - 500	100
σ	0 - 22	10
F_{11}	6.5 - 10	8
F_{12}	1.2 - 1.8	1.5
m_0	0.01 - 0.1	0.01
c_{m0}	0 - 1	1
g_{b0}	10 - 100	15
b_0	0 - 1	0
Ca_0	1 - 50	1

- The parameter κ_b is inversely proportional to the limiting matrix density. As such, it represents the balance between synthesis and degradation of extracellular collagen matrix. As mentioned above, this parameter is excluded from the sensitivity analysis since a range would not have a physiological meaning.
- Assuming that the maximal cell proliferation occurs at the initial matrix density, Bailón-Plaza and van der Meulen [2001] calculate a value for the parameter A_{m0}. Consequently, the range of initial matrix densities determines the range of parametric study values of A_{m0}.
- Bailón-Plaza and van der Meulen [2001] assume that $K_m = m_0$. This permits the calculation of the range for the parameter K_m, based on the range for m_0.
- The parameter α_m is inversely proportional to the limiting MSC density. As mentioned above, this parameter is excluded from the sensitivity analysis, since a range would not have a physiological meaning.
- Bailón-Plaza and van der Meulen [2001] estimated a range of the cell conversion constant Y_{11}. The same range is adopted here.
- It was stated by Bailón-Plaza and van der Meulen [2001] that a range of initial growth factor concentrations induced the transformation of MSCs to osteoblasts *in vitro*. The same range was adopted here for g_{b0}. Moreover, this range sets a threshold value for the growth factor concentration necessary to induce differentiation. The range of parameter H_{11} was determined by varying the respective parameter to such an extent that the threshold value was met.
- The ranges of a_{cm}, b_{cm}, c_{cm}, a_{cb}, b_{cb} and c_{cb} were derived from unpublished experimental data provided by Yoke Chin Chai [Lab for Skeletal Development and Joint Disorders, K.U. Leuven, Belgium].
- In the absence of data, the range for d_{cm} was estimated to be $0.001 - 3.5$.
- A range of values for G_{gb} was explored numerically by Bailón-Plaza and van der Meulen [2001]. The same range was adopted here.
- The range of values for H_{gb} was chosen so that the saturation level for the production of growth factors occurs at typical growth factor concentrations.
- Growth factors have short *in vivo* half-lives, usually less than 30 minutes [Bailón-Plaza and van der Meulen, 2001; Coffey et al., 1990; Dasch et al., 1989; Edelman et al., 1993]. Assuming a range of $1 - 30$ min in half-lives, the corresponding range of the decay constant d_{gb} can be calculated.
- The parameter H_{con} was chosen in such a way that the term $\frac{G_{con} \cdot g_b}{H_{con} + g_b}$ becomes equal to 1 for growth factor concentrations higher than 10.
- In the absence of data, the range of G_{con} was assumed to be $1 - 75$.
- The range of A_{b0} was assumed to be twice the range of A_{m0}.
- Bailón-Plaza and van der Meulen [2001] assume that $K_b = m_0$. This permits the calculation of the range for the parameter K_b, based on the range for m_0.
- The parameter α_b is inversely proportional to the limiting osteoblast cell density. As mentioned above, this parameter is excluded from the sensitivity analysis, since a range would not have a physiological meaning.
- During the screening experiment (L_{64}), Isaksson et al. [2008] use $0.05 - 0.2$ as range to describe the apoptosis of osteoblasts (d_b) in normalised cell variables. The same range was adopted here.
- The parameter P_{bb} was numerically varied in order to match the variation in bone

formation experimentally found by Yuan et al. [2006].

- The parameter κ_{bb} is inversely proportional to the limiting bone matrix density. As such, it represents the balance between synthesis and degradation of bone matrix. As mentioned above, this parameter is excluded from the sensitivity analysis, since a range would not have a physiological meaning.
- In the absence of data, the range of J_{leaky} was estimated to be $400 - 800$.
- The parameter H_{Ca4} was chosen in such a way that the term $\frac{Ca}{H_{Ca4}+Ca}$ becomes equal to 1 for calcium concentrations higher than 10.
- In the absence of data, the range of d_{ca} was chosen to be $10 - 500$.
- In the absence of data, the range of σ was chosen to be $0 - 22$.
- Dvorak et al. [2004] report a tenfold increase of differentiated cells at the optimal calcium concentration. Taking into account the range of optimal calcium concentrations, a range for F_{11} can be established from their experimental values.
- Studies on osteogenic differentiation of MSCs *in vitro* show an Gaussian distribution with an optimal differentiation in a narrow range of calcium concentrations (1.2 mM - 1.8 mM) [Dvorak et al., 2004; Liu et al., 2009]. This range was adopted for F_{12}.
- The initial extracellular matrix density is estimated to be between $0.01 - 0.1$.
- The initial concentration of MSCs and osteoblasts was allowed to vary between a conservative range of $0 - 1$, thereby taking into account all possible values.
- The initial bone matrix density was estimated to vary between a conservative range of $0 - 1$, thereby taking in account all possible values.
- The initial calcium concentration was chosen to vary between a conservative range of $1 - 50$, where the lower limit represents the physiological concentration and the upper limit the maximal possible value.

4.4.2 Responses

In order to assess the results obtained from the parametric study, criteria that characterise the outcome of the system were determined. In this study, 9 different outcome analyses were performed (see table 4.3). Firstly, to evaluate the effect of time, the amount of bone formation was measured at different time points (7, 21 and 42 days post implantation). Secondly, to assess the effect of response definition, three different response goals were tested for every time point: “match target”, “maximise” and “none”. The experimental data of Hartman et al. [2005] determined the lower and upper limits of the target to be matched. For the second response goal, i.e. “maximise”, the amount of bone formation was allowed to vary across the entire range. The last response goal, i.e. “none”, did not require any limits.

4.4.3 Design of the matrix

Isaksson et al. [2008] use a resolution IV fractional factorial design to identify the most important factors of their cell/tissue model. As mentioned in section 4.3, a major disadvantage of this method is the fact that interactions are confounded, i.e. the effects of certain interactions cannot be separated from each other. Expecting that interactions could play an essential role in the calcium model proposed here, some space-filling designs were used as well. These space-filling designs provide information about all portions of the experimental region, instead of only two, discrete levels.

Table 4.3: Definition of the responses for the parametric study.

Response name	Lower limit	Upper limit	Response goal
bone formation after 7 days	0.0001	0.0141	match target
21 days	0.071	0.3	match target
42 days	0.161	0.3	match target
bone formation after 7 days	0	1	maximise
21 days	0	1	maximise
42 days	0	1	maximise
bone formation after 7 days	/	/	none
21 days	/	/	none
42 days	/	/	none

In total three designs were tested: a resolution IV fractional factorial with 128 runs, a LHD with 80 runs and a uniform design with 80 runs. The low and high levels of the resolution IV orthogonal array were taken to be respectively the lower and upper limit of the ranges specified in table 4.2. The arrays were generated and analysed with the statistical analysis software JMP (8.0.1 SAS Institute Inc.).

4.4.4 Data analysis

The data of all three designs were analysed using a screening analysis and a stepwise regression. The two-space filling designs were also modelled as a Gaussian process. The following sections describe the statistics that are computed by JMP.

Screening analysis

The aim of a screening analysis is to estimate the importance of each factor and rank them accordingly. The significance of the estimated effects is expressed using a p-value where p denotes the probability that the result is obtained by chance or, in other words, the probability of obtaining a false positive (type I error). Therefore, a low p-value (e.g. less than 0.01) indicates a high significance level. JMP generates the p-values based on the method of Lenth. The idea behind this method is to estimate the standard error from the median value of the parameter estimates.

Stepwise regression

The goal of a stepwise regression is to automatically obtain a model that includes a minimal amount of significant factors. At each step the significance of the residual factors (the factors that are not included in the current model) is determined. The factors with a significance probability of $p < 0.25$ are entered into the model. Then the software determines if the other factors that are included in the model, are still significant. If the significance of the factors is greater than 0.25, the corresponding factors are removed from the model. Consequently, a factor can be added to the model at one step and removed at the following step. The previous description corresponds to the "mixed mode", i.e. the method alternates between the forward and backward steps. The direction could also be specified otherwise: forward (only extra factors are included in the model) and backward (there is only a removal of factors).

The stepwise regression was conducted on the main effects only. The direction was set to "mixed". The sum of squares (SS), which represents the reduction in the error SS, if the term is entered into the model, or the increase in the error SS, if the term is removed from the model, was considered as a measure of importance for each factor. The error sum of squares (SSE) is calculated as the sum of the squared distances of each point from the mean.

Gaussian process

This platform is used to model the relationship between a continuous response and one or more continuous variables. A Gaussian process is, in fact, a natural generalisation of a Gaussian distribution to infinitely many variables. As is commonly known, a multivariate *Gaussian distribution* is characterised by a mean *vector* and covariance matrix. If one extends this definition to infinite dimensions, the vectors become functions and thus a *Gaussian process* is characterised by a mean and covariance *function*. So intuitively, since the Gaussian distribution is used as a probability distribution to fit data and make predictions, a Gaussian process can also be used to fit models with an infinite number of parameters. Gaussian processes are easy to use and give very good results. A major disadvantage, however, is the computational complexity of $O(n^3)$, which limits the size of the datasets. Some very clear lectures on the topic of Gaussian processes by MacKay D. [`http://videolectures.net/gpip06_mackay_gpb/`] and Rasmussen C. [`http://videolectures.net/epsrcws08_rasmussen_lgp/`] are available on the internet.

JMP calculates a functional ANOVA table (see appendix B), in which the variation is computed using a function-driven method. The functional main effect of parameter X is the integrated total variation due to X alone. The ratio of functional X effect to the total variation is listed as the main effect (ME). The functional interaction effects are computed in a similar way. The total sensitivity (TS) is the sum of the main effect and all the interaction terms. Due to this addition the sum of the TS of the different factors does not add to 1. By this definition, the TS represents the amount of influence of a factor and all its two-way interactions.

Prediction profiler

To further interpret the data a prediction profiler was used. The profiler is an interactive tool that separately plots the predicted response function and 95 % confidence interval as function of all main factors. It allows the value of one main factor to be changed while the others are held constant at the current values. When a value is changed, the profiler traces the predicted response, updating all plots simultaneously. Example prediction profiler plots are shown in figure 4.5 on page 44.

To some extent, the importance of a factor can be assessed by the slope of the prediction trace. The profiler also allows the detection of interaction effects, since the slope and curvature in the plots of other factors will shift by modifying one factor. If the profiler only changes in height, not in slope or shape, then there are no interaction effects present.

4.5 Results

An overview of the most important factors as function of time point and design is given in table 4.4. More detailed information can be found in appendix B where the most important factors are set in bold.

4.5.1 Resolution IV fractional factorial design

According to the screening analysis, the amount of bone formation during the early stage (day 7 post implantation) was most influenced by the initial amount of bone (b_0), the optimal calcium concentration for differentiation (F_{12}) and the threshold growth factor concentration for differentiation (H_{11}). The mid stage (day 21 post implantation) was sensitive to the same factors, whereas the late stage (42 days post implantation) was only influenced by the initial amount of bone (b_0). For all the time points H_{11}, F_{12} and b_0 are characterised by the highest sum of squares in a stepwise regression analysis, thereby confirming the previous result. The three different response goals (i.e. "match target", "maximise" and "none") do not yield different results.

4.5.2 Latin hypercube design

A scatterplot matrix confirmed that the levels of each factor are evenly spaced across the entire range. At all time points the amount of bone formation was most influenced by the initial amount of bone (b_0) and the amount of calcium taken up by osteoblasts for hydroxyapatite production (J_{Leaky}). According to the stepwise regression, J_{Leaky} (45%), b_0 (25%) and H_{gb} (20%) contribute the most to the early stage, J_{Leaky} (33%), H_{gb} (25%) and a_{cm} (17 %) to the mid stage and J_{Leaky} (39%), b_0 (18%) and H_{gb} (16%) to the late stage. These results are similar to the performed screening experiment. The results were also modelled as a Gaussian process. As can be seen in tables B.2, B.3 and B.4 there is a large difference between the total sensitivity and the main effect. This means that factor interactions have an essential contribution to the overall importance of the factor. If the total sensitivity is taken as a measure of importance, a_{cm}, P_{bb} and J_{Leaky} are the most important factors for the early stage, J_{Leaky}, b_{cb} and c_{m0} for the mid stage and J_{Leaky}, c_{cb} and b_{cb} for the late stage of bone formation. Similar results are obtained, if the main effect is taken as a measure of importance. However, there are two exceptions: H_{11} is more important than c_{m0} at day 21 and b_0 is more important than c_{cb} at day 42. The three different response goals (i.e. "match target", "maximise" and "none") do not yield different results.

4.5.3 Uniform design

A scatterplot matrix confirmed that the levels of each factor are evenly spaced across the entire range. At all time points the amount of bone formation was most influenced by K_m, F_{11} and c_{b0}. Y_{11} was also statistically significant for the amount of bone formation at day 7 post implantation. These screening results were at all time points confirmed by the stepwise regression. The results were also modelled as a Gaussian process. Tables B.5, B.6 and B.7 show that there is a large difference between the total sensitivity and the main effect. This means that the interactions between factors are very important in the calcium model. If the total sensitivity is taken as a measure of importance, F_{11}, c_{b0} and Ca_0 are the most important factors at all stages. Similar results are obtained, if the main effect is taken

as a measure of importance. However, there is one exception: K_m is more important than Ca_0 for the amount of bone formation at day 42 post implantation. The three different response goals (i.e. "match target", "maximise" and "none") do not yield different results.

4.6 Discussion

Both the screening analysis and the stepwise regression gave similar results for the fractional factorial design at all the time points. This conclusion is also valid for the LH and uniform design. The Gaussian process does not, however, yield similar results as the screening analysis or the stepwise regression (table 4.4). Some factors do reoccur, but their relative importance has shifted (e.g. J_{Leaky} is the most important factor according to a regression analysis on the data of the LHD for day 7 (SS=0.44), whereas it is second in the Gaussian process (TS=0.17)). Moreover, some factors that were not important in the regression or screening analysis have a large influence in the Gaussian model, e.g. Ca_0 has a total sensitivity of 55% in the Gaussian model of the data of the uniform design at day 21, but this factor does not appear in the results of the other analyses.

The fractional factorial design indicates b_0, F_{12} and H_{11} as the most influential factors. These results vary little over the different time points, and are the same for both the screening and regression analysis. It is logical that the initial amount of bone formation (b_0) has an effect on the total amount of bone formation. H_{11} represents the threshold concentration of growth factors that is necessary for the differentiation of MSCs towards osteoblasts. F_{12} is the optimal calcium concentration for differentiation. Both factors are parameters in the same term, i.e. F_1, and can thus be considered important for differentiation.

According to the LHD, other factors than b_0, F_{12} and H_{11} are important, although b_0 remains an important parameter. Since these factors shift from time point to time point, the different stages will be discussed separately. Taking together the three different methods of analysis, b_0, J_{Leaky}, H_{gb}, a_{cm} and P_{bb} are the most influential factors for the amount of bone formation at day 7 post implantation. These parameters appear in different terms in the set of equations (equations (3.11) - (3.16)). The amount of bone formation at 21 days is mostly determined by J_{Leaky}, b_0, a_{cm}, H_{gb}, c_{cm}, b_{cb} and c_{m0}. The first four of these parameters are also important for the bone formation at day 7. b_0, J_{Leaky}, H_{gb}, c_{cb} and b_{cb} are the most important factors for the amount of bone formation at day 42. Again, some of these factors are also important for the bone formation at the other time points. Both a_{cm} and c_{cm}, as well as b_{cb} and c_{cb}, represent the calcium dependency of the proliferation of MSCs and osteoblasts respectively. c_{m0} is also important for proliferation, since it determines the starting point on the logistic growth function. These factors can thus be considered important for proliferation.

The uniform design yields other results than the fractional factorial or LH design. The factors do not shift from time point to time point. Taking together the three different methods of analysis, K_m, F_{11}, c_{b0} and Ca_0 are the most influential factors. These parameters are present across the set of equations.

It is clear that the three designs yield different results, although some similarities exist. Firstly, the initial conditions appear in all the results, clearly indicating their importance.

Table 4.4: Overview of the most important factors as function of time point and design.

	bone formation at day 7					**bone formation at day 21**					**bone formation at day 42**				
	fractional factorial	LHS		uniform		fractional factorial	LHS		uniform		fractional factorial	LHS		uniform	
screening analysis	b_0	J_{Leaky}		K_m		b_0	J_{Leaky}		K_m		b_0	J_{Leaky}		K_m	
	F_{12}	b_0		F_{11}		F_{12}	b_0		F_{11}		/	b_0		F_{11}	
	H_{11}	/		c_{b0}		H_{11}	/		c_{b0}		/	/		c_{b0}	
stepwise regression	b_0	H_{gb}		K_m		b_0	J_{Leaky}		K_m		b_0	J_{Leaky}		K_m	
	F_{12}	J_{Leaky}		F_{11}		F_{12}	H_{gb}		F_{11}		H_{11}	b_0		F_{11}	
	H_{11}	b_0		c_{b0}		H_{11}	c_{cm}		c_{b0}		F_{12}	H_{gb}		c_{b0}	
Gaussian model		TS	ME	TS	ME		TS	ME	TS	ME		TS	ME	TS	ME
	/	a_{cm}	a_{cm}	Ca_0	Ca_0	/	J_{Leaky}	J_{Leaky}	Ca_0	Ca_0	/	J_{Leaky}	J_{Leaky}	Ca_0	K_m
	/	P_{bb}	P_{bb}	c_{b0}	c_{b0}	/	b_{cb}	b_{cb}	c_{b0}	c_{b0}	/	c_{cb}	b_0	c_{b0}	c_{b0}
	/	J_{Leaky}	J_{Leaky}	F_{11}	F_{11}	/	P_{bb}	H_{11}	F_{11}	F_{11}	/	b_{cb}	b_{cb}	F_{11}	F_{11}

Secondly, the influential factors are usually present across the entire set of equations, suggesting that interactions are potentially important. Although the factors are scattered, the fractional factorial design indicates more differentiation-related terms, whereas the proliferation-related factors are considered to be influential by the LHD. Notice, however, that different factors in one term can possibly work in other directions, thus effectively cancelling out the combined effect. This, again, implies the importance of investigating the interactions present in the calcium model.

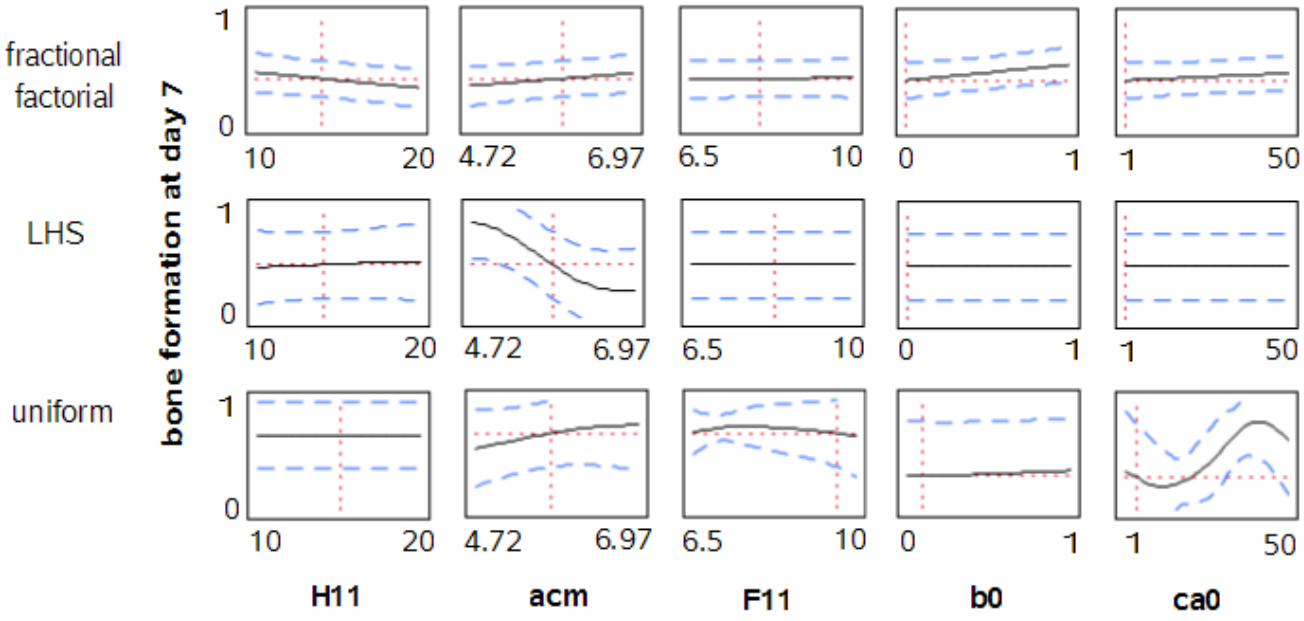

Figure 4.5: Prediction profiler plots for the amount of bone formation at day 7 for different designs and factors. The y-axis displays the amount of bone formation, the x-axis the range of the corresponding factor. The dashed blue line represents the 95% confidence interval.

Figure 4.5 shows some profiles for the amount of bone formation at day 7. There are some striking differences between the three designs and between the factors displayed here. The fractional factorial design only used two levels. The intermediate values are represented by a linear relationship between the lower and upper limit. This is a serious disadvantage of the technique, since it does not allow modelling of non-linearity, which is clearly present in the calcium model (observe e.g. the profile of bone formation as function of Ca_0 in the uniform design)!

As mentioned in section 4.4.4, the importance of a factor can be assessed by the slope of the profile plot. For the fractional factorial design this means that H_{11} and b_0 are more important than F_{11}, which is indeed the case, if one looks at table 4.4. A similar conclusion can be drawn for the other two designs. Remark as well, that the amount of bone formation can be maximised by lowering a factor (e.g. a_{cm} in LHD) or by increasing a factor (e.g. Ca_0 in uniform design). It is important to realise, however, that the slope and shape of the curves can change when the value of another factor is altered. This is illustrated in figure 4.6.

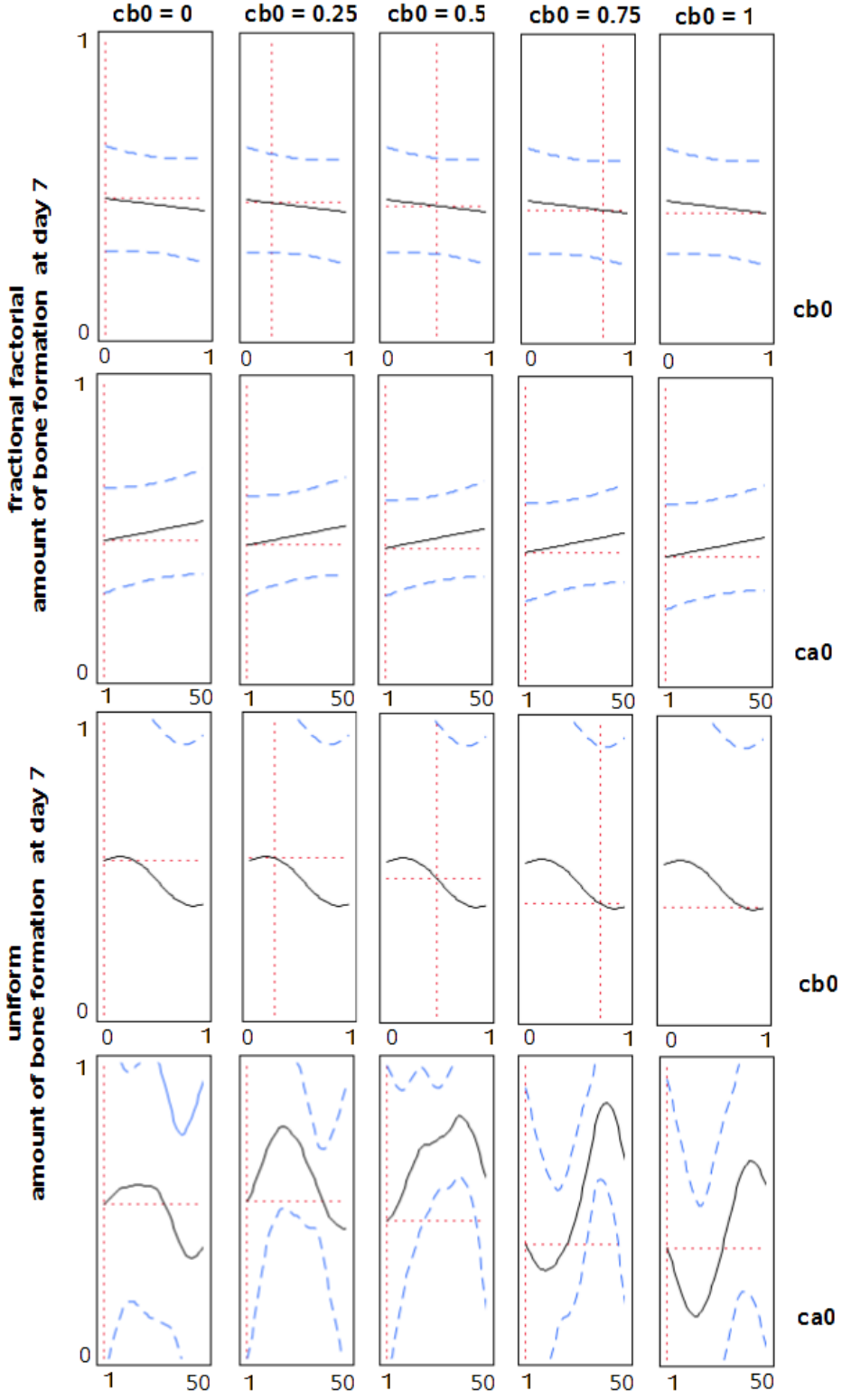

Figure 4.6: Prediction profiler plots for the amount of bone formation at day 7 for the fractional factorial and uniform design. The y-axis displays the amount of bone formation, the x-axis the range of the corresponding factor. The dashed blue line represents the 95% confidence interval. Note that the profiles of Ca_0 change as the value of c_{b0} is altered.

For the fractional factorial design, the profile of the amount of bone formation as function of Ca_0 decreases in height for increasing values of c_{b0}, but not in slope or shape. This is clearest, if one compares the left and right most pictures in figure 4.6 ($c_{b0} = 0$ and $c_{b0} = 1$). According to section 4.4.4, this suggests that there are no interactions present between these two factors. This also holds for the other factors included in the analysis.

The parameter interactions cannot be grasped with the fractional factorial design, since it has only two levels and the resolution is too low. As explained in section 4.3, in a resolution IV design no main effects are confounded with other main effects or with any two-factor interactions, but two-factor interactions are confounded with each other. This means practically that only conclusions on the main effects can be drawn, since the interactions are confounded with each other. The use of only two levels implies a linear profile, which will obviously not capture the nonlinearities that are present. In conclusion, the low spatial and design resolution limit the accuracy of the fractional factorial method.

Looking at the results of the uniform design in figure 4.6, the profiles change drastically in shape when the value of c_{b0} is altered, which means there is a high interaction between c_{b0} and Ca_0. In table B.5 one can also remark an interaction value of 0.16, which confirms the previous observation. These interactions can be founded by a more biological point of view. As the initial amount of osteoblasts (c_{b0}) increases, the optimal calcium concentration increases as well (the peak in figure 4.6 shifts towards the right). This is logical since these osteoblasts need calcium to survive, proliferate and make hydroxyapatite nodules. A higher initial osteoblast concentration thus implies a higher need for calcium which is nicely reflected in the profiles. Interestingly, the amount of bone formation goes down with increasing initial concentration of osteoblasts (c_{b0}). This result is counterintuitive since the osteoblasts are the key to bone formation. These bone cells use, however, a lot of calcium that might be necessary for other (metabolic) processes. Moreover, it might be more optimal to go through all the different sequential events of bone formation (proliferation, differentiation and matrix production) in contrast with starting halfway through the biological process. Or, in other words, to try to mimic the biological processes as well as possible by starting with MSCs instead of osteoblasts. This concept is not new, and is commonly known in developmental biology as “path-dependence”. “Path-dependence” means that each developmental stage depends on the previous ones, and that these previous stages provide the optimal conditions for the next stages [Lenas et al., 2009]. From this point of view, the initial osteoblast concentration should indeed be low, as was predicted by the sensitivity analysis.

Another example is the interaction between K_b and Ca_0 (interaction value of 0.12 in table B.5). As can be seen in figure 4.7, the optimal initial calcium concentration decreases as K_b is increased (the calcium peak shifts to the left). This can be biologically explained in the following way. As K_b is increased, the peak in factor A_b decreases, meaning that the proliferation is less stimulated at low values of collagen matrix (m) (see figure 4.8). Since the initial proliferation of osteoblasts is less, less calcium is necessary to sustain their metabolic activity. Hence, the optimal calcium concentration decreases. Remarkably, the amount of bone formation increases with increasing value of K_b. This is again a counterintuitive result since A_b goes down with increasing K_b. Biologically this might be explained by the fact that bone formation is a slow process in which only some osteoblasts make the hydroxyapatite nodules instead of a lot of cells that would simply consume all the calcium in the environment. This suggestion of an optimal osteoblast cell density should be verified

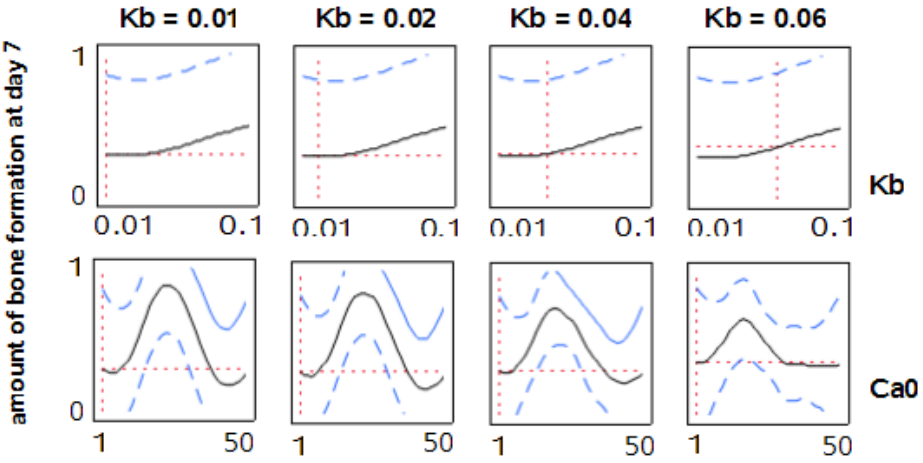

Figure 4.7: Prediction profiler plots for the amount of bone formation at day 7 for the uniform design. The y-axis displays the amount of bone formation, the x-axis the range of the corresponding factor. The dashed blue line represents the 95% confidence interval. Notice that the profile of Ca_0 changes as the value of K_b is altered.

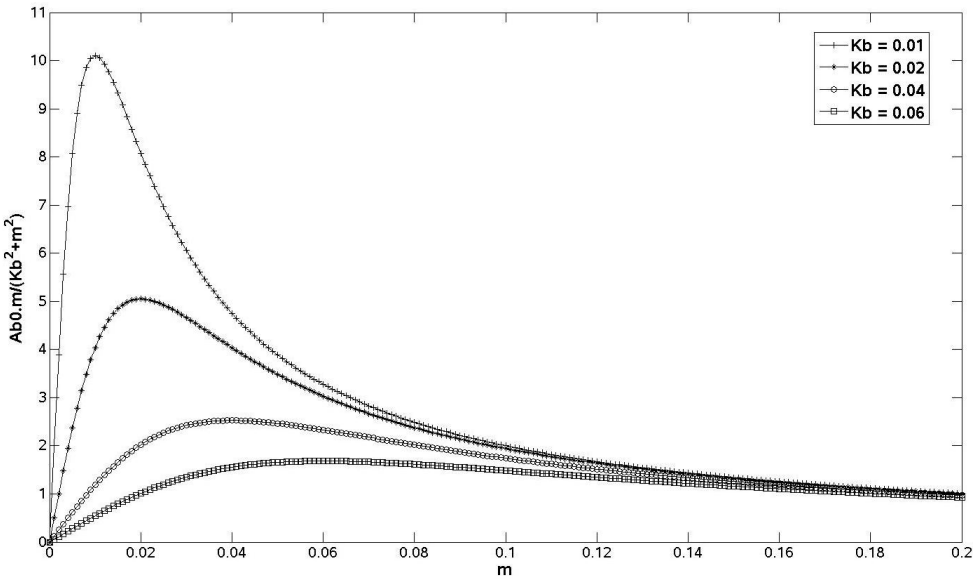

Figure 4.8: The proliferation factor $A_b = \frac{A_{b0}.m}{K_b^2+m^2}$ as function of m for different values of K_b.

experimentally. The previous interpretations were done for the amount of bone formation at 7 days. Similar conclusions can, however, be drawn for the other time points.

Like the uniform design, the LHD also shows some interesting features. Firstly, the interactions between factors are a lot smaller compared to the uniform design, the highest

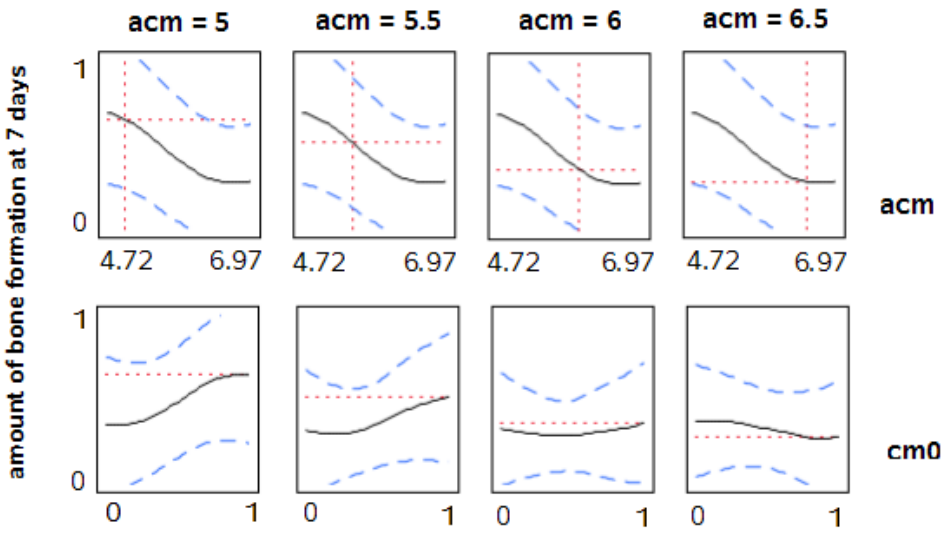

Figure 4.9: Prediction profiler plots for the amount of bone formation at day 7 for the LHD. The y-axis displays the amount of bone formation, the x-axis the range of the corresponding factor. The dashed blue line represents the 95% confidence interval. Notice that the profile of c_{m0} changes as the value of a_{cm} is altered.

interaction value is 0.0363 for P_{bb} and J_{Leaky} whereas c_{b0} and Ca_0 have an interaction value of 0.16 in the uniform design (see tables B.2 and B.5). Secondly, these results can also be interpreted from a biological point of view. As can be seen in figure 4.9, the optimal initial concentration of MSCs shifts from the right to the left when a_{cm} is increased. This implies that less MSCs are necessary for bone formation. This is a logical result since a_{cm} determines how much the proliferation of MSCs is stimulated at the optimal calcium concentration. At high values of stimulation, lower initial cell concentrations are more optimal. Too high initial concentrations are even unfavourable since these cells would consume all the calcium. Remark that the amount of bone formation goes down by increasing the value of a_{cm}. This again confirms that bone formation is a slow process in which only a small amount of cells participate. Like for the osteoblasts, there seems to be an optimal MSC density at which these cells "work" most efficiently. This hypothesis is supported by the experimental results of Kruyt et al. [2008]. They determined an optimal bone marrow stromal cell density (BMSC density) of 8.10^6 $\frac{BMSCs}{cm^3}$ for bone formation in a BCP scaffold. This suggestion should, however, be further investigated experimentally.

The results obtained from the LHD should be interpreted with caution. As mentioned in section 4.3, the LHD is well-suited for monotonic response functions, but may not be adequate for non-monotonic response functions. This does not necessarily imply that non-monotonic response functions, like the ones of the calcium model presented here, are incorrect. It means that their non-monotonicity may not be fully accounted for, in a similar - albeit much less pronounced - way as that non-monotonicity cannot be accounted for by the fractional factorial design. There are clearly a lot of differences between the uniform design and the LHD. They both assign different factors to be important, and the interaction values are much lower in the LHD. These differences might be caused by the fact that the

calcium model is clearly not monotonic. Hence, the results of the LHD might not be valid, even though some biological interpretation can be given to the results.

The prediction profiler also allows to determine the parameter set that would maximise the (predicted) amount of bone formation. This was tested for the uniform design at days 7, 21 and 42. Appendix C shows the sets of optimal parameter values corresponding to the different time points. The simulations in Matlab showed an increase in bone formation with respect to the standard value at all time points. The increase was, however, not the one predicted by the statistical model (35% versus 100% bone formation). This discrepancy could be explained by the fact that only 80 runs were included in the statistical model, whereas more data points might be necessary. It is also possible that the examined region was undersampled. This suggestion should be further investigated since the found discrepancy between the statistical predictions and simulation results questions the validity of the employed uniform design.

Given that the fractional factorial design is not satisfactory, due to the lack of non-linearities and interactions, and the LHD, due to the restricted applicability to monotonic response functions, the uniform design probably yields the best results. The results of the uniform design should, however, also be interpreted with caution, due to the found discrepancy between the statistical predictions and simulation results. Designs with more runs should be investigated for both the LHD and uniform design and this might even lead to a better correspondence between the results of both designs.

There are some conclusive remarks that need to be made. Firstly, the profiles were calculated for a certain set of parameter values (standard values). When the values of other parameters than the ones displayed in figures 4.6, 4.7 and 4.9 change, the profiles might change as well, due to the interactions. Secondly, the sensitivity analysis is able to identify the most important factors within the chosen parameter space. Likewise, the results of the parametric study depend on the outcome criteria that were defined. If the parameter ranges or the responses would be altered, a different result could be obtained [Saltelli et al., 2000]. Thirdly, the results of the study are based on a particular model, namely the calcium model, and should as such not be directly extrapolated to other similar computational models. Finally, some variables, which are suggested to have an important influence on the outcome, have not yet been adequately characterised and quantified. The uniform design indicates A_{b0}, c_{b0}, b_0 and Ca_0 as influential factors, but their range was estimated in a conservative way. More attention should be paid to these variables, and more experimental studies should investigate the influence of the initial conditions on the amount of bone formation. Moreover, the sensitivity analysis has led to some interesting biological hypotheses that need to be explored experimentally.

4.7 Conclusion

This chapter illustrates the potential of sensitivity analysis methods for evaluating computational model parameters. Firstly, the difference between computer and physical experiments was discussed. Secondly, an overview was presented of the different methods for computer experiments that are commonly used in biomedical literature. The overview discussed the strengths and shortcomings of each method. To compare the different methods, three different designs were used to determine the most influential parameters of the calcium

model. The resolution IV fractional factorial design was not satisfactory for the specific model under study, since it could not capture the non-linearities and higher-order parameter interactions. The latin hypercube design yielded some logical results, although these were different from the results of the uniform design. This discrepancy could be explained by the lack of support for non-monotonic response functions. The results of the uniform design should also be interpreted with caution due to the found discrepancy between the statistical predictions and simulation results. Some of the parameters that were indicated as influential, have not yet been fully characterised and quantified. The results of the uniform design also suggested some new insights in the biology of bone formation. Future experiments should preferentially focus on establishing the unknown parameter values and explore some of the suggested biological hypotheses that might further unravel the process of bone formation in CaP scaffolds.

Chapter 5

Extended calcium model

5.1 Introduction

In this chapter the development of an extended calcium model is elaborated. The main objective is to extend the calcium model proposed in chapter 3 with spatial coordinates (x and y). Section 5.2 describes the functional forms and equations of the extended model. The derivation of the parameters is explained in the following section (5.3). Section 5.4 provides information on the different simulation details. An overview of the simulations that were carried out using the extended calcium model is given in section 5.5. The results and simplifications of the mathematical model are thoroughly discussed in section 5.6. To conclude this chapter, the most important findings are recapitulated together with suggestions for further improvements of the extended calcium model.

5.2 Mathematical framework

The presented mathematical model is an extension of the calcium model. It is built on the model proposed by Geris et al. [2008]. The extended calcium model consists of six partial differential equations and describes the effect of calcium phosphates as a spatiotemporal variation of six variables: calcium concentration (Ca), MSC density (c_m), osteoblast density (c_b), mineral matrix density (b), collagen matrix density (m) and a generic, osteogenic growth factor concentration (g_b). The sum of the mineral matrix and the collagen matrix represents the total bone density. The following sections describe the individual terms.

Mesenchymal stem cells

The migration of MSCs is a combination of random (-kinesis) and directed (-taxis) motion, in response to gradients of soluble signals (chemo-) and gradients of cell-substrate adhesion (hapto-) [Pountos and Giannoudis, 2005; Thibault et al., 2007; Spaeth et al., 2008]. The random motion is modelled as a haptokinetic process. The form of the haptokinetic coefficient (D_m) was adopted from Olsen et al. [1997], based on experimental data of Dickinson and Tranquillo [1993]. The random motion is influenced by the matrix density (m) since cells cannot move in the absence of a substrate for attachment ($D_m = 0$ for $m = 0$) [Olsen et al., 1997]. Moreover, in the abundance of extracellular matrix, cell movement is restricted ($D_m \to 0$ as $m \to \infty$) [Olsen et al., 1997].

$$D_m = \frac{D_{hm}.m}{K_{hm}^2 + m^2} \tag{5.1}$$

The form of the chemotactic coefficients ($C_{m_{gbCT}}$ and $C_{m_{caCT}}$) was adopted from Geris et al. [2008]. Geris et al. [2008] model the chemotactic motion with a receptor-kinetic form that gives a maximal chemotactic response at a particular growth factor concentration. The chemotactic response of MSCs depends on osteogenic growth factors ($C_{m_{gbCT}}$) and extracellular calcium ($C_{m_{caCT}}$).

$$C_{m_{gbCT}} = \frac{C_{gbCTm}.g_b}{K_{gbCTm}^2 + g_b^2} \tag{5.2}$$

A similar functional form was used for the chemotactic response to Ca^{2+} since it is also receptor-mediated [Saidak et al., 2009; Aguirre et al., 2010; Olszak et al., 2000].

$$C_{m_{caCT}} = \frac{C_{caCTm}.Ca}{K_{caCTm}^2 + Ca^2} \tag{5.3}$$

Based on a kinetic analysis of a model mechanism for the cell-surface-receptor-extracellular-ligand binding dynamics [Sherratt, 1994], Olsen et al. [1997] derived a haptotactic coefficient ($C_{m_{HT}}$). The same functional form is adopted here.

$$C_{m_{HT}} = \frac{C_{kHTm}}{(K_{kHTm} + m)^2} \tag{5.4}$$

The functions that were used to model the proliferation and differentiation of MSCs in the calcium model are adopted here (see section 3.2).

Osteoblasts

The motion of osteoblasts is not included in the extended calcium model since differentiated cells are often considered to be less motile [Zahor et al., 2007]. The functions that were used to model the proliferation and differentiation of osteoblasts in the calcium model are adopted here (see section 3.2).

Collagen and mineral matrix

The spatiotemporal evolution of the collagen and mineral matrix were modelled as in the calcium model (see section 3.2).

Calcium

The local concentration of calcium plays an essential role in most of the aforementioned processes. Calcium ions are able to migrate inside the biomaterial, simulated here by a diffusion process with a constant diffusion rate (D_{ca}). Since Ca^{2+} can be bound to large molecules, thereby reducing the diffusion, an effective diffusion coefficient is used here [Keener and Sneyd, 2009].

Generic growth factor

Besides calcium, growth factors also play a key role in a lot of the modelled processes. Growth factors are able to migrate inside the porous biomaterial, modelled here by diffusion process with a constant diffusion rate (D_{gb}). The functions that were used to model the production and removal of growth factors in the calcium model are adopted here (see section 3.2).

Set of equations

This leads to the following set of non-dimensionalised equations, where the tildes are omitted for simplicity:

$$\frac{\partial m}{\partial t} = P_{bs}.(1-\kappa_b.m).c_b \tag{5.5}$$

$$\frac{\partial c_m}{\partial t} = \nabla\left(D_m\nabla c_m - C_{m_{caCT}}c_m\nabla Ca - C_{m_{gbCT}}c_m\nabla g_b - C_{mHT}c_m\nabla m\right) \tag{5.6}$$

$$+A_m.c_m.(1-\alpha_m.c_m) - F_1.c_m - d_{cm}.b.c_m \tag{5.7}$$

$$\frac{\partial g_b}{\partial t} = \nabla\left(D_{gb}\nabla g_b\right) + E_{gb}.c_b - d_{gb}.g_b \tag{5.8}$$

$$\frac{\partial c_b}{\partial t} = A_b.c_b.(1-\alpha_b.c_b) + F_1.c_m - d_b.c_b \tag{5.9}$$

$$\frac{\partial b}{\partial t} = P_{bb}.(0,95-\kappa_{bb}.b)^6.c_b \tag{5.10}$$

$$\frac{\partial Ca}{\partial t} = \nabla\left(D_{ca}\nabla Ca\right) + \sigma.(Ca_\infty - Ca) - J_{leaky}.c_b.\frac{Ca}{H_{Ca4}+Ca} \tag{5.11}$$

$$-d_{Ca}.Ca.(c_b+c_m) \tag{5.12}$$

The scaling factors that were chosen for non-dimensionalisation, as well as the non-dimensionalised model parameter values can be found in section 5.3.2.

5.3 Parameters

5.3.1 Parameter values

The parameter values were derived from experimental data and from literature where possible. Only the parameters that form an extension or adaptation of the calcium model in chapter 3 are discussed here.

Haptokinesis

Geris et al. [2008] report diffusion constants in the orders of magnitude of 10^{-8} to 10^{-6} cm^2/s, depending on the cell type under investigation and experimental conditions [Gruler and Bültmann, 1984; Friedl et al., 1998; Rupnick et al., 1988]. Geris et al. [2008] determined the haptokinetic coefficient (D_m) in the following way: the maximum rate of cell motility occurs at a matrix density of $m = K_{hm}$, yielding a value of $D_{hm} = 2.K_{hm}.D$. The parameter K_{hm} was chosen positive and higher than the initial matrix density. The same values are adopted here.

Chemotaxis

Geris et al. [2008] model the migratory response to increasing growth factor concentrations as a bell-shaped curve, based on experimental studies. They report a maximal chemotactic response for growth factor concentrations of 1 to 10 ng/ml. The values, as determined by Geris et al. [2008] from experimental evidence, are adopted here.

Many experimental studies have investigated the chemotactic response of monocytes [Olszak et al., 2000], osteoblasts [Godwin and Soltoff, 1997], breast cancer cells [Saidak et al., 2009] and bone marrow progenitor cells [Aguirre et al., 2010] to Ca^{2+}. They report a Gaussian distribution with a maximal effect achieved at concentrations of 3-10 mM Ca^{2+} [Aguirre et al., 2010]. Maximal chemotactic response is reported for calcium concentrations of 5 mM [Godwin and Soltoff, 1997] and 4.5 mM [Olszak et al., 2000]. The values of the parameters of the functional form (equation (5.3)) are determined from these experimental observations, since there are no reports on the chemotactic response of MSCs to Ca^{2+} available in literature.

Haptotaxis

For the haptotactic coefficient, Geris et al. [2008] assign values in the same order of magnitude as those of the chemotactic coefficients. This assumption was made due to a limited amount of available data. The same values are used here.

Diffusion

Geris et al. [2008] determined the value the diffusion coefficient of the osteogenic growth factor (D_{gb}) from its molecular weight. Using a relation developed by Vander et al. [1998], Geris et al. [2008] calculated orders of magnitudes of 10^{-8} cm^2/s.

The effective diffusion coefficient of Ca^{2+} was determined from Keener and Sneyd [2009].

5.3.2 Scaling and non-dimensionalisation

The following scaling factors were chosen for the non-dimensionalisation of the model variables:

$$\tilde{t} = \frac{t}{T}, \quad \tilde{c_m} = \frac{c_m}{c_0}, \quad \tilde{c_b} = \frac{c_b}{c_0}, \quad \tilde{x} = \frac{x}{L}, \quad \tilde{y} = \frac{y}{L}, \quad \tilde{m} = \frac{m}{m_0}, \quad \tilde{b} = \frac{b}{m_0}, \quad \tilde{g_b} = \frac{g_b}{g_0}, \quad \tilde{Ca} = \frac{Ca}{Ca_0}$$

The time scale and length scales of $T = 1$ day and $L = 3.5$ mm were taken from Geris et al. [2008], based on studies of Harrison et al. [2003]. Representative concentrations for the collagen content ($m_0 = 0.1$ g/ml) and growth factors ($g_0 = 100$ ng/ml) are adopted from Geris et al. [2008]. A typical value for the cell density ($c_0 = 10^6$ cells/ml) is derived from Bailón-Plaza and van der Meulen [2001]. The scaling factor for the calcium concentration was assumed to be equal to the extracellular calcium concentration (1 mM).

The model parameters were non-dimensionalised as follows (the tildes represent the non-dimensional parameters):

$$\tilde{P_{bs}} = \frac{P_{bs}.c_0.T}{m_0}, \quad \tilde{\kappa_b} = \kappa_b.m_0, \quad \tilde{A_{m0}} = \frac{A_{m0}.T}{m_0}, \quad \tilde{K_m} = \frac{K_m}{m_0}, \quad \tilde{a_{cm}} = \frac{a_{cm}}{Ca_0},$$

$$
\begin{aligned}
\tilde{b_{cm}} &= \frac{b_{cm}}{Ca_0},\quad \tilde{c_{cm}} = \frac{c_{cm}}{Ca_0},\quad \tilde{\alpha_m} = \alpha_m.c_0,\quad \tilde{H_{11}} = \frac{H_{11}}{g_0},\quad \tilde{Y_{11}} = Y_{11}.T,\\
\tilde{G_{gb}} &= \frac{G_{gb}.T.c_0}{g_0},\quad \tilde{H_{gb}} = \frac{H_{gb}}{g_0},\quad \tilde{d_{gb}} = d_{gb}.T,\quad \tilde{A_{b0}} = \frac{A_{b0}.T}{m_0},\quad \tilde{K_b} = \frac{K_b}{m_0},\\
\tilde{a_{cb}} &= \frac{a_{cb}}{Ca_0},\quad \tilde{b_{cb}} = \frac{b_{cb}}{Ca_0},\quad \tilde{c_{cb}} = \frac{c_{cb}}{Ca_0},\quad \tilde{\alpha_b} = \alpha_b.c_0,\quad \tilde{d_b} = d_b.T,\quad \tilde{P_{bb}} = \frac{P_{bb}.c_0.T}{m_0},\\
\tilde{\kappa_{bb}} &= \kappa_{bb}.m_0,\quad \tilde{\sigma} = \sigma.T,\quad \tilde{J_{leaky}} = \frac{J_{leaky}.T.c_0}{Ca_0},\quad \tilde{H_{Ca4}} = \frac{H_{Ca4}}{Ca_0},\quad \tilde{d_{Ca}} = d_{Ca}.T.c_0,\\
\tilde{F_{11}} &= F_{11},\quad \tilde{F_{12}} = F_{12},\quad \tilde{G_{con}} = G_{con}.c_0,\quad \tilde{H_{con}} = \frac{H_{con}}{g_0},\quad \tilde{d_{cm}} = d_{cm}.m_0.T,\\
\tilde{D_{hm}} &= \frac{D_{hm}.T}{L^2.m_0},\quad \tilde{K_{hm}} = \frac{K_{hm}}{m_0},\quad \tilde{C_{gbCTm}} = \frac{C_{gbCTm}.T}{L^2},\quad \tilde{K_{gbCTm}} = \frac{K_{gbCTm}}{g_0},\\
\tilde{C_{caCTm}} &= \frac{C_{caCTm}.T}{L^2},\quad \tilde{K_{caCTm}} = \frac{K_{caCTm}}{Ca_0},\quad \tilde{C_{kHTm}} = \frac{C_{kHTm}.T}{L^2.m_0},\\
\tilde{K_{kHTm}} &= \frac{K_{kHTm}}{m_0},\quad \tilde{D_{gb}} = \frac{D_{gb}.T}{L^2},\quad \tilde{D_{ca}} = \frac{D_{ca}.T}{L^2},\quad \tilde{Ca_\infty} = \frac{Ca_\infty}{Ca_0}
\end{aligned}
$$

This results in the following set of non-dimensionalised parameter values:

$$
\begin{aligned}
\tilde{P_{bs}} &= 0.1,\quad \tilde{\kappa_b} = 1,\quad \tilde{A_{m0}} = 0.85,\quad \tilde{K_m} = 0.1,\quad \tilde{a_{cm}} = 5.98, \tilde{b_{cm}} = 3.33,\\
\tilde{c_{cm}} &= 1.67,\quad \tilde{\alpha_m} = 1,\quad \tilde{H_{11}} = 14,\quad \tilde{Y_{11}} = 10,\quad \tilde{G_{gb}} = 350,\quad \tilde{H_{gb}} = 1,\\
\tilde{d_{gb}} &= 50,\quad \tilde{A_{b0}} = 0.202,\quad \tilde{K_b} = 0.1,\quad \tilde{a_{cb}} = 41.82,\quad \tilde{b_{cb}} = 5.06,\quad \tilde{c_{cb}} = 1.9,\\
\tilde{\alpha_b} &= 1,\quad \tilde{d_b} = 0.1,\quad \tilde{P_{bb}} = 0.0471,\quad \tilde{\kappa_{bb}} = 1,\quad \tilde{\sigma} = 0,\quad \tilde{Ca_\infty} = 50,\quad \tilde{J_{leaky}} = 750,\\
\tilde{H_{Ca4}} &= 0.01,\quad \tilde{d_{Ca}} = 100,\quad \tilde{F_{11}} = 8,\quad \tilde{F_{12}} = 1.5,\quad \tilde{d_{cm}} = 1.5,\quad \tilde{G_{con}} = 1,\quad \tilde{H_{con}} = 0.001\\
\tilde{D_{hm}} &= 0.014,\quad \tilde{K_{hm}} = 0.25,\quad \tilde{C_{gbCTm}} = 0.04,\quad \tilde{K_{gbCTm}} = 0.1,\quad \tilde{C_{caCTm}} = 1.6,\\
\tilde{K_{caCTm}} &= 8,\quad \tilde{C_{kHTm}} = 0.0034,\quad \tilde{K_{kHTm}} = 0.5,\quad \tilde{D_{gb}} = 0.005,\quad \tilde{D_{ca}} = 0.4973
\end{aligned}
$$

5.4 Simulation details

Geometrical domain

The numerical simulations are performed on a simplified representation of a pore in a CaP scaffold. Commercially available scaffolds (e.g. $NuOss^{TM}$) have typically macropores of 200-600 μm. The CaP spicule was assumed to have dimensions of $\pm$ 5 μm as can be seen in figure 2.2. Figure 5.1 shows a schematical representation of the geometrical domain.

Initial conditions

At the start of the simulation there are MSCs ($\tilde{c}_{m,ini} = 0.0001$) and growth factors ($\tilde{g}_{b,ini} = 15$) present. The calcium concentration is assumed equal to the normal extracellular concentration ($\tilde{Ca}_{ini} = 1$). Only a very small amount of collagen matrix ($\tilde{m}_{ini} = 0.01$) is present at the beginning of the simulation. All other variables are assumed to be zero initially.

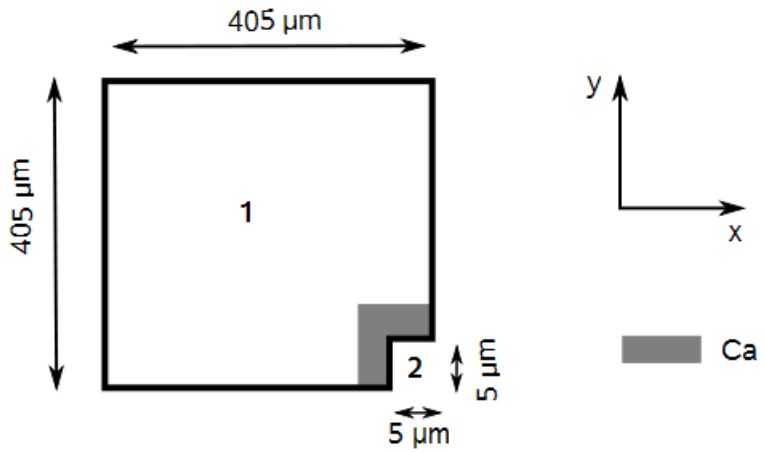

Figure 5.1: Geometrical domain of the extended calcium model. 1: pore, 2: CaP spicule. The Dirichlet boundary condition of Ca is also indicated.

Boundary conditions

The set of partial differential equations was completed by suitable boundary conditions. When the CaP scaffold is ectopically implanted, proteins will adsorb on the surface of the biomaterial. This adsorbed protein layer will influence the dissolution behaviour of the implanted scaffold. To take this decrease in calcium release into account, a time-dependent Dirichlet boundary condition was specified for Ca. It is assumed that after 15 days the calcium release decreases by 50 % ($\tilde{Ca}_{bc} = 20 \rightarrow \tilde{Ca}_{bc} = 10$).

Numerical implementation

The set of non-linear partial differential equations was implemented in Matlab (The MathWorks, Inc.). To solve the set of taxis-diffusion-reaction equations efficiently, a specific code created by Gerisch and Chaplain [2006] and adapted by [Gerisch and Geris, 2007], was used. This finite volume code was specifically developed for biological systems and can be used for 2D or 3D axi-symmetric geometries.

5.5 Results

The results of the simulation are shown in figure 5.2. The calcium concentration initially increases near the CaP spicule, causing the MSCs to proliferate (see figure 5.2, day 27). The conditions of the micro-environment are favourable so that the MSCs differentiate. The newly formed osteoblasts start to produce collagen matrix and growth factors. At 54 days, the collagen matrix is mature and the bone formation starts. The cell population gradually decreases and after 90 days the pore is filled with 25 % bone. Notice that the CaP spicule plays a key role in initiating the biological process.

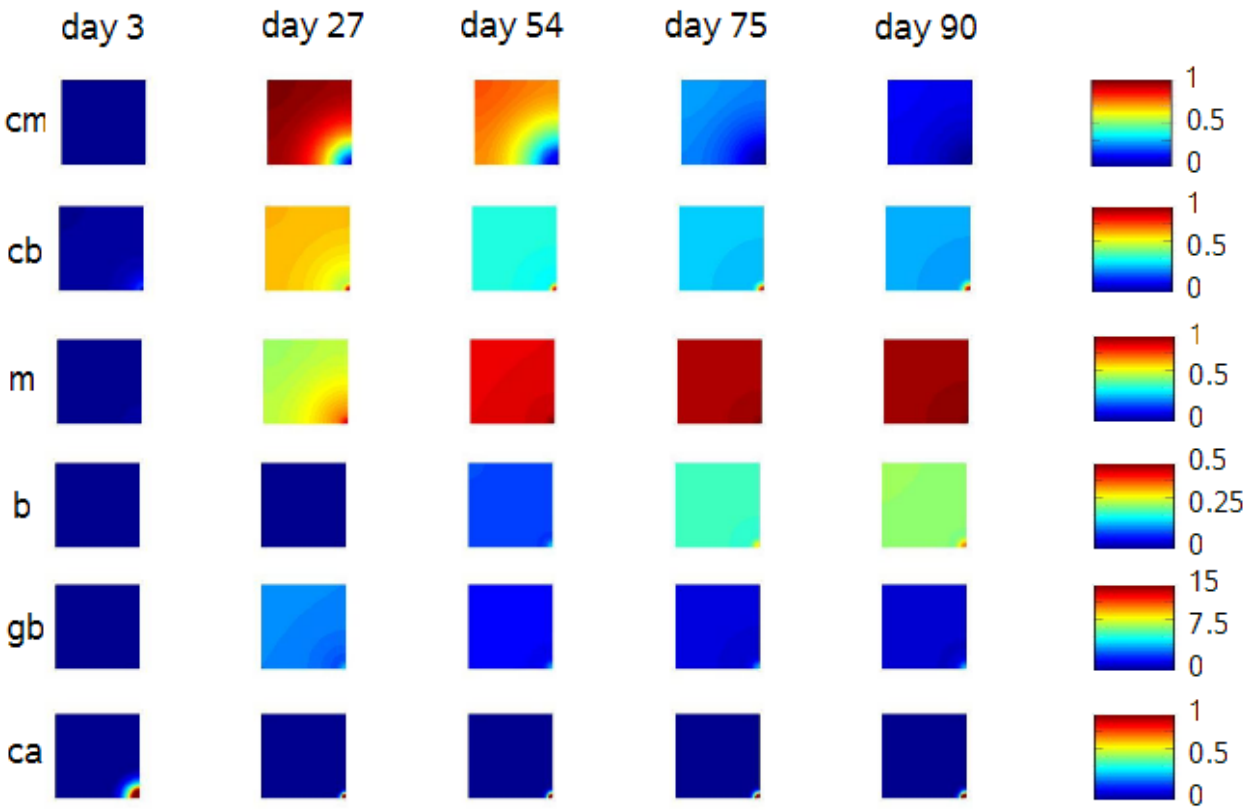

Figure 5.2: Spatiotemporal evolution (days post implantation) of MSC density (c_m), osteoblast density (c_b), collagen matrix density (m), mineralised matrix density (b), growth factor concentration (g_b) and calcium concentration (Ca).

5.6 Discussion

Unfortunately, there are no experimental data available to corroborate the predicted results. Some general remarks can, however, be made.

Firstly, as can be seen in figure 5.2, cells can proliferate and migrate anywhere in the geometrical domain. Biologically this is not possible, since osteogenic cells are anchorage-dependent, they need a substrate to grow on. The use of non-local terms in the set of equations is a possible solution for this simplification [Lee et al., 2001; Gerisch and Chaplain, 2008]. This mathematical tool allows to test whether a substrate is present in a small environment around the cell. If this is indeed the case, the cell will be able to migrate and proliferate.

Another interesting phenomena that could be incorporated in the mathematical description is the problem of moving boundaries. During the dissolution of the CaP spicules Ca^{2+} is released and consequently the CaP spicule decreases in size. This means that the boundary conditions for Ca shift in space. A more rigorous description of this simplification could further improve the accuracy of the simulations.

Furthermore, the current calcium model does not include angiogenesis. The invasion of

blood vessels will present an additional source of calcium ions and growth factors and will locally create a more favourable environment for proliferation, differentiation and finally bone formation. Further research should certainly focus on this aspect.

Finally, the simplifications of the 1D model are also applicable here.

5.7 Conclusion

In this chapter the extension of the calcium model with spatial coordinates was elaborated. It includes some key features such as proliferation, differentiation and migration. The current chapter focussed primarily on the correct modelling of migration, including the chemotactic response to Ca^{2+}. Numerical simulations were performed on a simplified representation of a pore in a CaP scaffold and interpreted with a biological point of view. Future research should focus on the incorporation of non-local terms and a correct description of moving boundaries. The extension of the mathematical model with angiogenesis could further improve the accuracy of the predicted results.

Chapter 6

Conclusion

The need for bone tissue regeneration is continuously increasing, due to the improvement of the quality of life and the improvement of life expectancy. Millions of fractures occur yearly worldwide, of which 5-10 % result in a delayed union or in a non-union. In order to find better solutions for the healing of large bone defects and non-unions, it is important to understand the complex process of bone formation, involving the participation of many different cell types and regulated by countless biochemical and mechanical factors. Mathematical models can help to explain and understand the underlying principles of this complex phenomenon and further unravel the interactions between the different influential factors.

It can be concluded from chapter 2 that calcium plays a key role in regulating the different subprocesses underlying osteogenesis. Hence, this Master's thesis focussed on the influence of calcium on the activity of osteogenic cells, resulting in the presented (extended) calcium model. The calcium model described in chapter 3, is inspired by the bioregulatory model of Geris et al. [2008]. However, some important simplifications and adaptations were made: some cell types and tissues were not included, the influence of calcium on proliferation, differentiation and migration has been modelled using literature and experimental data and some parameter values were altered to fit the current application of the model. The results of the calcium model have been successfully corroborated by comparison with experimental data from literature. Moreover, application of the calcium model to the set-up of bone formation, allowed to simulate a decalcified scaffold and insufficient cell seeding conditions. Simulations of these adverse biological situations predicted the formation of little or no bone, as was found experimentally. Moreover, the calcium model was used to design a therapeutic strategy for insufficient cell seeding *in silico*.

Chapter 4 provides an in depth discussion of the sensitivity analysis that was performed to determine the most influential parameters of the calcium model. This Master's thesis explored three different designs. The resolution IV fractional factorial design was not satisfactory for the specific model under study, since it could not capture the non-linearities and higher-order parameter interactions. The latin hypercube design yielded some logical results, although these were different from the results of the uniform design. This discrepancy could be explained by the lack of support for non-monotonic response functions. The results of the uniform design should also be treated with caution due to the difference between the statistical predictions and simulation results. Designs with more runs should be investigated for both the LH and uniform design.

Some of the parameters that were indicated as influential, have not yet been fully

characterised and quantified. More attention should be paid to these parameters in future experiments. The results of the uniform design also suggested some new insights in the biology of bone formation, i.e. the existence of an optimal osteoblast and MSC concentration during bone formation. The concept of "path-dependence" is also supported by the results of the sensitivity analysis.

The last chapter presented an extension of the calcium model with spatial coordinates thereby focussing primarily on the correct modelling of migration, including the chemotactic response to Ca^{2+}. Numerical simulations were performed on a simplified representation of a pore in a CaP scaffold and interpreted with a biological point of view. Although the extended calcium model could not be corroborated, it provides a proof of concept and first step towards a more complete spatiotemporal description of the influence of CaP biomaterials on ectopic bone formation.

Future experiments should preferentially focus at establishing the unknown parameter values related to the calcium release rate, the calcium uptake for hydroxyapatite production, the growth factor consumption, the apoptosis rate of MSCs and the calcium uptake for metabolic functions. Some of the suggested biological hypotheses should also be further explored. An accurate identification of the calcium release rate would allow *in silico* testing of specific biomaterials, as well as, the determination of optimal seeding densities for these different bioapatites. The importance and effect of the initial conditions should also be verified experimentally.

The performed sensitivity analysis successfully compared three different methods. However, some discrepancies that were found question the validity of the results. It is necessary to further explore the possibilities of these techniques by testing designs with more runs and focussing on the most important factors.

The mathematical model can be refined in several ways as well. Firstly, other cell types and tissues can be included to not only predict intramembranous ossification but also endochondral ossification. Secondly, the influence of organophosphates can be taken into account to provide a more complete description of mineralisation. Thirdly, the incorporation of non-local terms and a correct mathematical description of moving boundaries could further improve the calcium model. Finally, the extension of the calcium model with angiogenesis, which represents an additional source of growth factors and calcium, would further increase the accuracy of the mathematical framework in the spatial domain.

Currently, the (extended) calcium model can be used to predict the past, by simulating normal and adverse bone formation conditions. As was stated by van der Meulen and Huiskes [2002], the ultimate objective, however, should be to predict the future, by using the model to facilitate the screening of new biomaterials and to design novel therapeutic strategies *in silico*.

Appendices

Appendix A

Determination of the proliferation parameter values

Bailón-Plaza and van der Meulen [2001] derived for their model the values of the parameters A_{m0}, K_m, A_{b0} and K_b of the proliferation functions for MSCs and osteoblasts. Similar values were adopted in the calcium model. The parameters a_{cm}, b_{cm}, c_{cm}, a_{cb}, b_{cb} and c_{cb} that characterise the Gaussian dependency on the calcium concentration, were determined from unpublished experimental data provided by Yoke Chin Chai [Lab for Skeletal Development and Joint Disorders, K.U. Leuven, Belgium].

The total DNA content was measured at different time points (day 1, 3, 7, 14, 21 and 28) and calcium concentrations (0, 2, 4, 6, 8 and 10 mM). The data measured at 7 days were assumed to be representative of MSC proliferation, whereas the data measured at 28 days were assumed to be representative of osteoblast proliferation. The data were normalised with respect to the total DNA content measured at day 1. Since the 0 mM calcium concentration means that no exogenous calcium was added to the culture medium, which originally contained 1.8 mM of calcium, an offset was introduced to compensate for this effect. However, as can be seen in figure A.1, the proliferation is not zero at 0 mM. Therefore, the values of A_m and A_b are set to zero in the simulation code when the calcium concentration decreases below a certain threshold. A least-square fitting through the experimental data determined the parameters a_{cm}, b_{cm}, c_{cm}, a_{cb}, b_{cb} and c_{cb} of the Gaussian distributions.

Figure A.1 illustrates the proliferation as function of calcium concentration. The fitted Gaussian distributions correspond well to the values found in literature. The Gaussian distribution predicts an optimal proliferation of MSCs in a range of 2-4 mM Ca^{2+}. This is similar to data found in literature, i.e. Liu et al. [2009] report an optimal concentration of 1.8 mM. Maeno et al. [2005] measured maximal proliferation of osteoblasts at 5 mM Ca^{2+}, this is again nicely predicted by the fitted Gaussian function. The data also suggest that osteoblasts are more sensitive to Ca^{2+} than MSCs (factor 25 versus 7 in figure A.1). This hypothesis should, however, be further investigated experimentally.

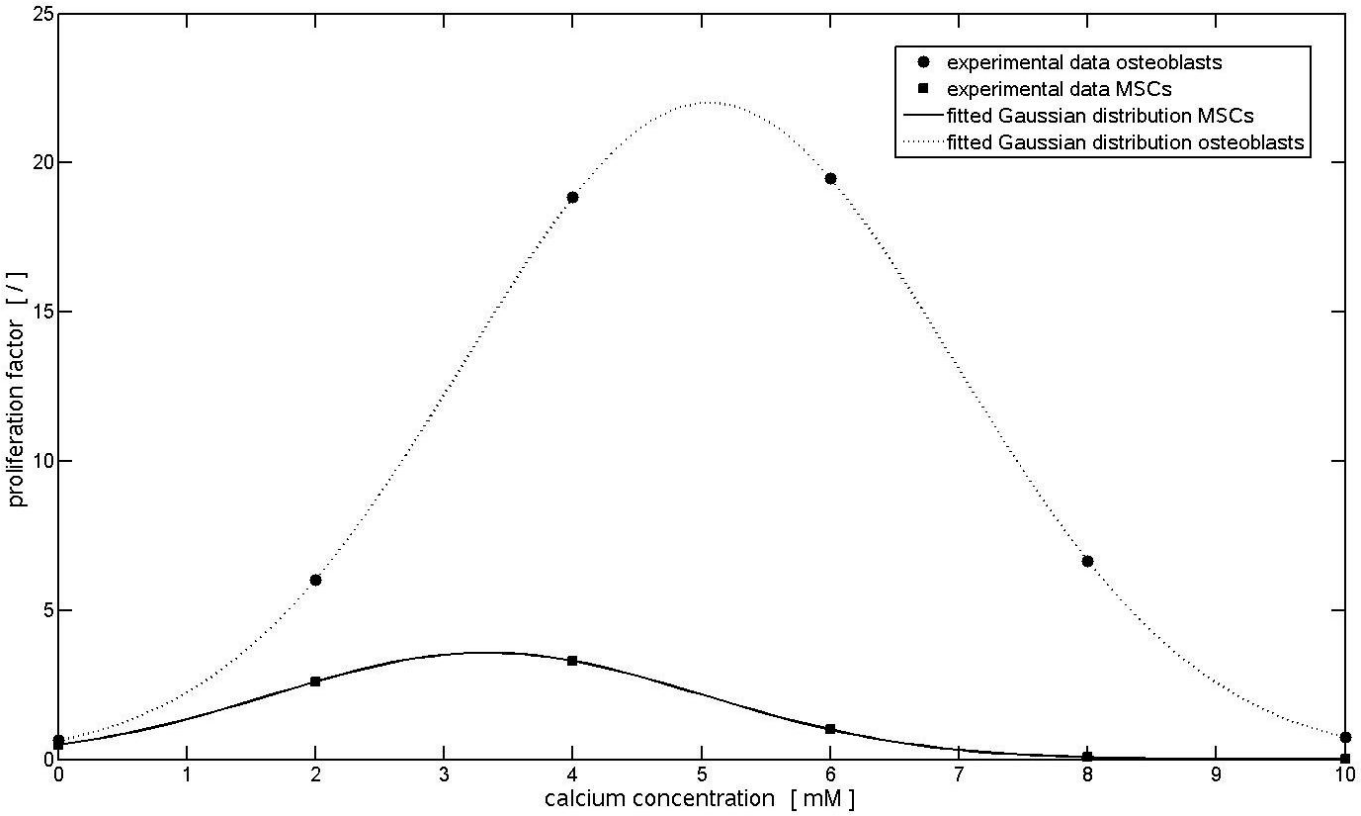

Figure A.1: Proliferation factor of MSCs and osteoblasts as function of calcium concentration.

Appendix B

Results of the sensitivity analysis by DOE

Table B.1: Overview of the results of the stepwise regression analysis as function of time point and design. The values in brackets represent the sum of squares (SS) and a high value indicates the importance of the factor.

bone formation at day 7			**bone formation at day 21**			**bone formation at day 42**		
fractional factorial	LHS	uniform	fractional factorial	LHS	uniform	fractional factorial	LHS	uniform
$\mathbf{H_{11}}$ (0.92)	H_{11} (0.11)	$\mathbf{K_m}$ (0.41)	$\mathbf{H_{11}}$ (0.85)	P_{bs} (0.087)	$\mathbf{K_m}$ (0.33)	$\mathbf{H_{11}}$ (0.77)	a_{cm} (0.087)	$\mathbf{K_m}$ (0.26)
a_{cm} (0.61)	a_{cm} (0.13)	Y_{11} (0.14)	a_{cm} (0.54)	$\mathbf{a_{cm}}$ (0.17)	Y_{11} (0.11)	a_{cm} (0.42)	c_{cm} (0.089)	Y_{11} (0.08)
b_{cm} (0.36)	c_{cm} (0.17)	b_{cm} (0.06)	b_{cm} (0.31)	b_{cm} (0.11)	b_{cm} (0.041)	d_{cm} (0.34)	$\mathbf{H_{gb}}$ (0.16)	b_{cm} (0.03)
d_{cm} (0.38)	$\mathbf{H_{gb}}$ (0.2)	c_{cm} (0.09)	d_{cm} (0.36)	c_{cm} (0.17)	c_{cm} (0.08)	A_{b0} (0.62)	d_{gb} (0.066)	c_{cm} (0.065)
A_{b0} (0.63)	K_b(0.15)	G_{con} (0.07)	A_{b0} (0.63)	$\mathbf{H_{gb}}$ (0.25)	H_{con} (0.031)	d_b(0.66)	K_b (0.042)	H_{con} (0.034)
d_b (0.63)	d_b (0.14)	A_{b0} (0.04)	d_b (0.63)	d_{gb} (0.16)	G_{con} (0.07)	c_{cb} (0.46)	d_b (0.1)	G_{con} (0.06)
c_{cb} (0.39)	P_{bb} (0.13)	a_{cb} (0.11)	c_{cb} (0.42)	d_b (0.16)	A_{b0} (0.033)	P_{bb} (0.31)	c_{cb} (0.066)	A_{b0} (0.027)
P_{bb} (0.38)	F_{12} (0.098)	b_{cb} (0.08)	P_{bb} (0.35)	a_{cb} (0.08)	a_{cb} (0.094)	d_{ca} (0.62)	$\mathbf{J_{Leaky}}$ (0.39)	a_{cb} (0.077)
d_{ca} (0.40)	$\mathbf{J_{Leaky}}$ (0.44)	P_{bb} (0.08)	d_{ca} (0.46)	c_{cb} (0.06)	b_{cb} (0.066)	σ (0.37)	H_{Ca4} (0.05)	b_{cb} (0.056)
$\mathbf{F_{12}}$ (0.92)	$\mathbf{b_0}$ (0.25)	σ (0.04)	$\mathbf{F_{12}}$(0.85)	$\mathbf{J_{Leaky}}$ (0.33)	P_{bb} (0.07)	$\mathbf{F_{12}}$ (0.74)	F_{11} (0.045)	P_{bb} (0.06)
$\mathbf{b_0}$ (0.95)	/	$\mathbf{F_{11}}$ (0.26)	$\mathbf{b_0}$ (0.95)	H_{Ca4} (0.07)	σ (0.035)	$\mathbf{b_0}$ (0.9)	F_{12} (0.063)	H_{Ca4} (0.024)
/	/	$\mathbf{c_{b0}}$ (0.19)	/	F_{12} (0.10)	$\mathbf{F_{11}}$ (0.22)	/	$\mathbf{b_0}$ (0.18)	σ (0.029)
/	/	b_0 (0.09)	/	b_0 (0.15)	$\mathbf{c_{b0}}$ (0.14)	/	/	$\mathbf{F_{11}}$ (0.18)
/	/	/	/	/	b_0 (0.08)	/	/	$\mathbf{c_{b0}}$ (0.1)
/	/	/	/	/	/	/	/	b_0 (0.062)

Table B.2: Overview of the results of the Gaussian model analysis for the LHS design of at 7 days. The main effect (range: $0-1$) is the total variation due to that factor alone. The interaction effect (range: $0-1$) is the total variation due to that interaction alone. The total sensitivity is the sum of the main effect and all the interaction terms.

name factor	total sensitivity	main effect	interactions								
			P_{bs}	H_{11}	a_{cm}	H_{gb}	A_{b0}	K_b	P_{bb}	J_{Leaky}	c_{m0}
P_{bs}	0.149	0.0152	/	0.0418	0.0379	0.00246	0.00164	0.000257	0.1	0.00566	0.0349
H_{11}	0.0930	0.0268	**0.0419**	/	0.00329	0.000239	0.00232	0.0007665	0.000862	0.01183	0.00515
a_{cm}	**0.262**	**0.155**	**0.0379**	0.00329	/	0.00125	0.00603	0.000438	0.0149	0.0127	0.0307
H_{gb}	0.05337	0.04483	0.00246	0.000239	0.00125	/	0.000315	0	0.000636	0.00276	0.0008
A_{b0}	0.0573	0.02418	0.00164	0.00232	0.00603	0.00032	/	0.000874	0.00387	0.00147	0.0165
K_b	0.0407	0.00932	0.000258	0.000767	0.000438	0	0.000874	/	0.000497	0.0176	0.011
P_{bb}	**0.17**	**0.0589**	0.01	0.000862	0.0149	0.000636	0.003866	0.000496	/	0.0636	0.0167
J_{Leaky}	**0.206**	**0.068**	0.00566	0.0183	0.0127	0.00277	0.00148	0.0176	**0.0636**	/	0.0233
c_{m0}	0.169	0.0295	0.0349	0.00516	0.0307	0.0008	0.0166	0.011	0.0167	0.0233	/

Table B.3: Overview of the results of the Gaussian model analysis for the LHS design of all factors at 21 days. The main effect (range: $0-1$) is the total variation due to that factor alone. The interaction effect (range: $0-1$) is the total variation due to that interaction alone. The total sensitivity is the sum of the main effect and all the interaction terms.

name factor	total sensitivity	main effect	interactions								
			P_{bs}	H_{11}	G_{gb}	A_{b0}	a_{cb}	b_{cb}	P_{bb}	J_{Leaky}	c_{m0}
P_{bs}	0.00819	0.003277	/	0.00146	0	0.000219	0	0.00113	0.000909	0.000756	0.000426
H_{11}	0.0559	**0.03406**	0.00146	/	0	0.00731	0.00103	0.00294	0.00447	0.00133	0.00325
a_{cm}	0.000938	0.000176	0	0	/	0.000255	0	0.000273	0	0.0000642	0
A_{b0}	0.0792	0.0253	0.000219	0.00731	0.000255	/	0.000326	0.00263	0.00589	0.0145	0.0228
a_{cb}	0.0484	0.0113	0	0.00103	0	0.000326	/	0.0209	0.000783	0.0137	0.000318
b_{cb}	**0.193**	**0.0702**	0.00113	0.00294	0.000273	0.00263	0.0209	/	0.0077	0.0734	0.0134
P_{bb}	0.156	0.0188	0.000909	0.00447	0	0.00589	0.000783	0.0077	/	0.0875	0.0294
J_{Leaky}	**0.383**	**0.127**	0.000756	0.00133	0.0000642	0.0145	0.0137	**0.0734**	**0.0875**	/	0.0643
c_{m0}	**0.155**	0.0211	0.000426	0.00325	0	0.0228	0.000312	0.0134	0.0294	**0.0644**	/

Table B.4: Overview of the results of the Gaussian model analysis for the LHS design at 42 days. The main effect (range: $0-1$) is the total variation due to that factor alone. The interaction effect (range: $0-1$) is the total variation due to that interaction alone. The total sensitivity is the sum of the main effect and all the interaction terms.

name factor	total sensitivity	main effect	interactions									
			P_{bs}	K_m	H_{11}	H_{gb}	d_{gb}	A_{b0}	b_{cb}	c_{cb}	J_{Leaky}	b_0
P_{bs}	0.136	0.0215	/	0	0.0180	0	0.00711	0.00421	0.0273	0.00537	0.0446	0.00646
K_m	0.0203	0.00856	0.000283	/	0.000074	0	0	0.0001521	0.00939	0.000206	0.00139	0.000162
H_{11}	0.0310	0.00741	0.0180	0	/	0	0.000108	0.000874	0.00131	0.00197	0.00107	0.000137
H_{gb}	0.00740	0.00421	0.000662	0	0	/	0	0.0000574	0.000280	0.0002	0.0017	0.000194
d_{gb}	0.0302	0.00353	0.00711	0	0.000108	0	/	0.000921	0.00235	0.00798	0.00763	0.000446
A_{b0}	0.0322	0.00601	0.00422	0.000152	0.000874	0.0000574	0.000921	/	0.00202	0.0108	0.00649	0.000684
b_{cb}	**0.173**	**0.0493**	0.0273	0.00939	0.00131	0.00028	0.00235	0.00202	/	0.0379	0.0387	0.00472
c_{cb}	**0.175**	0.0228	0.00537	0.000206	0.00197	0.0002	0.00798	0.0108	**0.0379**	/	0.082	0.00606
J_{Leaky}	**0.3079**	**0.1066**	**0.04465**	0.0014	0.00107	0.0017	0.00763	0.00649	0.0387	**0.0820**	/	0.0176
b_0	0.1125	**0.0760**	0.00646	0.000162	0.000137	0.000194	0.000446	0.000684	0.00472	0.00606	0.01764	/

Table B.5: Overview of the results of the Gaussian model analysis for the uniform design at 7 days. The main effect (range: $0-1$) is the total variation due to that factor alone. The interaction effect (range: $0-1$) is the total variation due to that interaction alone. The total sensitivity is the sum of the main effect and all the interaction terms.

name factor	total sensitivity	main effect	interactions								
			K_m	a_{cm}	A_{b0}	K_b	b_{cb}	F_{11}	c_{b0}	b_0	Ca_0
K_m	0.0637	0.0513	/	0.00032	0.000556	0	0	0.00298	0.000931	0	0.00725
a_{cm}	0.0798	0.0138	0.00032	/	0.000226	0.000304	0	0.000922	0.00990	0	0.0542
A_{b0}	0.0775	0.00963	0.000556	0.000226	/	0.000376	0.00211	0.0158	0.00272	0	0.0461
K_b	0.145	0.0181	0.000307	0	0.000376	/	0.00152	0.00219	0.00104	0	0.122
b_{cb}	0.0629	0.0283	0	0	0.00211	0.00152	/	0.00336	0.00448	0	0.02299
F_{11}	**0.1732**	**0.0868**	0.00298	0.000921	0.0158298	0.00219	0.003361	/	0.01268	0.000243	0.0482
c_{b0}	**0.2997**	**0.1043**	0.000931	0.0099	0.00272	0.00104	0.00448	0.01268	/	0.000181	0.16337
b_0	0.006258	0.003792	0	0	0	0	0	0.000243	0.000181	/	0.00188
Ca_0	**0.5499**	**0.08430**	0.00725	**0.05423**	0.04605	**0.1215**	0.0229	0.04821	**0.16337**	0.0018	/

Table B.6: Overview of the results of the Gaussian model analysis for the uniform design at 21 days. The main effect (range: $0-1$) is the total variation due to that factor alone. The interaction effect (range: $0-1$) is the total variation due to that interaction alone. The total sensitivity is the sum of the main effect and all the interaction terms.

name factor	total sensitivity	main effect	interactions								
			K_m	a_{cm}	A_{b0}	K_b	b_{cb}	F_{11}	c_{b0}	b_0	Ca_0
K_m	0.0548	0.0450	/	0.00025	0.000419	0.000308	0	0.00205	0.0009	0	0.00573
a_{cm}	0.1004	0.01503	0.00025	/	0.000631	0.000499	0	0.00109	0.0145	0.000025	0.06838
A_{b0}	0.0848	0.0124	0.000419	0.000631	/	0.000469	0.0113	0.0162	0.00312	0	0.0504
K_b	0.1569	0.0227	0.0003084	0.000499	0.000469	/	0.00241	0.00228	0.00132	0	0.127
b_{cb}	0.05798	0.02443	0	0	0.001128	0.00241	/	0.00202	0.00396	0	0.0239
F_{11}	**0.1572**	**0.0808**	0.00205	0.00109	0.0162	0.00228	0.00202	/	0.01382	0.000115	0.03885
c_{b0}	**0.3146**	**0.1103**	0.000903	0.0145	0.00312	0.00132	0.00396	0.01382	/	0.000142	0.1666
b_0	0.00465	0.002888	0	0	0	0	0	0.000115	0.000142	/	0.00142
Ca_0	**0.5514**	**0.06914**	0.00573	**0.0684**	0.0504	**0.1270**	0.02388	0.03885	**0.1666**	0.00142	/

Table B.7: Overview of the results of the Gaussian model analysis for the uniform design at 42 days. The main effect (range: $0-1$) is the total variation due to that factor alone. The interaction effect (range: $0-1$) is the total variation due to that interaction alone. The total sensitivity is the sum of the main effect and all the interaction terms.

name	total	main	interactions						
factor	sensitivity	effect	K_m	Y_{11}	A_{b0}	b_{cb}	F_{11}	c_{b0}	Ca_0
K_m	0.1498	**0.103**	/	0.000918	0.000525	0.000221	0.00272	0.01999	0.00945	0.013
Y_{11}	0.0103	0.00373	0.000918	/	0	0	0.000037	0.0002187	0.000367	0.004999
A_{b0}	0.01604	0.001634	0.000523	0	/	0	0	0.00442	0.00205	0.00737
b_{cb}	0.01596	0.00743	0.000221	0	0	/	0	0.00333	0.00085	0.00398
F_{11}	**0.29899**	**0.18704**	0.01999	0.000219	0.00442	0.00333	0.00261	/	0.02904	0.05233
c_{b0}	**0.3595**	**0.1019**	0.00945	0.000367	0.00205	0.00085	0.004026	**0.02904**	/	0.21183
Ca_0	**0.3691**	0.05442	0.012999	0.004999	0.00737	0.00398	0.0212	**0.0523**	**0.212**	/

Appendix C

Most beneficial parameter sets for the amount of bone formation

The prediction profiler plots were used to determine the parameter values that result in a maximal amount of bone formation at the different time points. The non-influential parameters were set at their standard value (see table 4.2). Table C.1 only includes the values of the influential factors. Remark that in table C.1 the optimal initial osteoblast concentration is quite high which does not correspond with the results displayed in figure 4.6 ($c_{b0} \cong 0.4$ in table C.1 versus $c_{b0} = 0$ in figure 4.6). It is important to realise, however, that a lot of interactions are present between the different factors. These interactions will influence the profile of the initial osteoblast density which might explain the observed difference in optimal initial osteoblast concentration.

Table C.1: Overview of the parameter values that result in a maximal amount of bone formation according to the uniform design.

name factor	**day 7**	**day 21**	**day 42**
K_m	0.04036	0.01	0.0565
a_{cm}	6.211	6.02	
d_{gb}	464.1		
A_{b0}	0.902		1.325
K_b		0.014	
b_{cb}	3.824	3.831	3.508
c_{cb}	2.0373		2.0921
F_{11}	8.4282	9.261	9.331
c_{b0}	0.349	0.478	0.427
Ca_0	10.45	23.87	23.02

Bibliography

Adams G., Chabner K., Alley I., Olson D., Szczepiorkowski Z., Poznansky M., Kos C., Pollak M., Brown E., and Scadden T. Stem cell engraftment at the endosteal niche is specified by the calcium-sensing receptor. *Nature*, 439:599–603, 2006.

Aguirre A., González A., Planell J.A., and Engel E. Extracellular calcium modulates in vitro bone marrow-derived flk-1^+ $cd34^2$ progenitor cell chemotaxis and differentiation through a calcium-sensing receptor. *Biochemical and Biophysical Research Communications*, 393: 156–161, 2010.

Alberts B., Johnson A., Lewis J., Raff M., Roberts K., and Walter P. *Molecular biology of the cell*. Garland Science, 5 edition, 2007. ISBN 978-0-8153-4105-5.

Bailón-Plaza A. and van der Meulen M. A mathematical framework to study the effects of growth factor influences on fracture healing. *Journal of Theoretical Biology*, 212:191–209, 2001.

Barrère F., van der Valk C., Dalmeijer R., Meijer G., van Blitterswijk C., de Groot K., and Layrolle P. Osteogenecity of octacalcium phosphate coatings applied on porous metal implants. *Journal of Biomedical Materials Research*, 66A:779–788, 2003.

Barrère F., van Blitterswijk C., and de Groot K. Bone regeneration: molecular and cellular interactions with calcium phosphate ceramics. *International Journal of Nanomedicine*, 1 (3):317–332, 2006.

Bhandari M. and Jain A. Bone stimulators: Beyond the black box. *Indian Journal of Orthopaedics*, 43(2):109–110, 2009.

Bootman M., Young K., Young J., Moreton R., and Berridge M. Extracellular calcium concentration controls the frequency of intracellular calcium spiking independently of inositol 1,4,5-triphosphate production in hela cells. *Biochemical Journal*, 314:347–354, 1996.

Breitwieser G. Extracellular calcium as an integrator of tissue function. *The International Journal of Biochemistry & Cell Biology*, 40:1467–1480, 2008.

Chang Y., Stanford C.M., and Keller J.C. Calcium and phosphate supplementation promotes bone cell mineralization: implications for hydroxyapatite-enhanced bone formation. *Journal of Biomedical Materials Research*, 52:270–278, 2000.

Coffey R.J., Russell W.E., and Barnard J.A. Pharmacokinetics of tgf beta with emphasis on effects in liver and gut. *Annals of the New York Academy of Sciences*, 593:285–291, 1990.

Dar F.H., Meakin J.R., and Aspden R.M. Statistical methods in finite element analysis. *Journal of Biomechanics*, 35:1155–1161, 2002.

Dasch J.R., Pace D.R., Waegell W., Inenaga D., and Ellingsworth L. Monoclonal antibodies recognizing transforming growth factor-beta. bioactivity neutralization and transforming growth factor beta 2 affinity purification. *The Journal of Immunology*, 142:1536–1541, 1989.

Dickinson R. and Tranquillo R. A stochastic model for adhesion-mediated cell random motility and haptokinesis. *Journal of Mathematical Biology*, 31:563–600, 1993.

Duncan R., Akanbi K., and Farach-Carsib M. Calcium signals and calcium channels in osteoblastic cells. *Seminars in nephrology*, 18:178–190, 1998.

Dvorak M. and Riccardi D. ca^{2+} as an extracellular signal in bone. *Cell Calcium*, 35: 249–255, 2004.

Dvorak M., Siddiqua A., Ward D., Carter D., Dallas S., Nemeth E., and Riccardi D. Physiological changes in extracellular calcium concentration directly control osteoblast function in the absence of calciotropic hormones. *Proceedings of the National Academy of Sciences*, 101(14):5140–5145, 2004.

Edelman E.R., Nugent M.A., and Karnovsky M.J. Perivascular and intravenous administration of basic fibroblast growth factor: vascular and solid organ deposition. *Proceedings of the National Academy of Sciences*, 90:1513–1517, 1993.

Eyckmans J., Roberts S.J., Schrooten J., and Luyten F.P. A clinically relevant model of osteoinduction: a process requiring calcium phosphate and bmp/wnt signalling. *Journal of Cellular and Molecular Medicine*, In press, 2010.

Fang K.-T., Li R., and Sudijanto A. *Design and modeling for computer experiments*. Chapman & Hall/CRC (Taylor & Francis Group), 2006.

Fang K.T. The uniform design: application of number-theoretic methods in experimental design. *Acta Mathematicae Applicatae Sinica*, 3:363–372, 1980.

Friedl P., Zänker K., and Bröker E. Cell migration strategies in 3-d extracellular matrix: differences in morphology, cell matrix interactions, and integrin function. *Microscopy Research and Technique*, 43:369–378, 1998.

Geris L., Gerisch A., Maes C., Carmeliet G., Weiner R., Vander Sloten J., and Van Oosterwyck H. Mathematical modeling of fracture healing in mice: comparison between experimental data and numerical simulation results. *Medical and Biological Engineering and Computing*, 44:280–289, 2006.

Geris L., Gerisch A., Vander Sloten J., Weiner R., and Van Oosterwyck H. Angiogenesis in bone fracture healing: A bioregulatory model. *Journal of Theoretical Biology*, 251:137 – 158, 2008.

Gerisch A. and Chaplain M.A.J. Robust numerical methods for taxis-diffusion-reaction systems: application to biomedical problems. *Mathematical and Computer Modelling*, 43: 49–75, 2006.

Gerisch A. and Chaplain M.A.J. Mathematical modelling of cancer cell invasion of tissue: local and non-local models and the effect of adhesion. *Journal of Theoretical Biology*, 250:684–704, 2008.

Gerisch A. and Geris L. *A finite volume spatial discretisation for taxis-diffusion-reaction systems with axi-symmetry: application to fracture healing*, chapter 27, pages 299–311. Birkhäuser Boston, 2007.

Godwin S. and Soltoff S. Extracellular calcium and platelet-derived growth factor promote receptor-mediated chemotaxis in osteoblasts through different signaling pathways. *The Journal of Biological Chemistry*, 272(17):11307–11312, 1997.

Gruler H. and Bültmann B. Analysis of cell movement. *Blood cells*, 10:61–77, 1984.

Habibovic P. and de Groot K. Osteoinductive biomaterials - properties and relevance in bone repair. *Journal of tissue engineering and regenerative medicine*, 1:25–32, 2007.

Hall B.K. *The osteoblast and osteocyte*, volume 1. Caldwell (N.J.): Telford, 1990. ISBN 0-93692-324-5.

Hall B.K. *Bone growth - A*, volume 6. LinkBoca Raton (Fla.): CRC, 1992. ISBN 0-8493-8826-0.

Hanawa T., Kamiura Y., Yamamoto S., Kohgo T., Amemiya A., Ukai H., Murakami K., and Asaoka K. Early bone formation around calcium-ion-implanted titanium inserted into rat tibia. *Journal of Biomedical Materials Research*, 36:131–135, 1997.

Harrison L.J., Cunningham J.L., Strömberg L., and Goodship A.E. Controlled induction of a pseudoarthrosis: a study using a rondent model. *Journal of Orthopaedic Trauma*, 17: 11–21, 2003.

Hartman E., Vehof J., Spauwen P., and Jansen J. Ectopic bone formation in rats: the importance of the carrier. *Biomaterials*, 26:1829–1835, 2005.

Isaksson H., van Donkelaar C., Huiskes R., Yao J., and Ito K. Determining the most important cellular characteristics for fracture healing using design of experiments methods. *Journal of Theoretical Biology*, 255:26–39, 2008.

Keener J. and Sneyd J. *Mathematical physiology I: cellular physiology*, volume 8 of *Interdisciplinary Applied Mathematics*. Springer Science + Business Media, second edition, 2009.

Kim C.-S., Kim J.-I., Kim J., Choi S.-H., Chai J.-K., Kim C.-K., and Cho K.-S. Ectopic bone formation associated with recombinant human bone morphogenetic proteins-2 using absorbable collagen sponge and β tricalcium phosphate as carriers. *Biomaterials*, 26: 2501–2507, 2005.

Kruyt M., De Bruijn J., Rouwkema J., Van Blitterswijk C., Oner C., Verbout A.B., and Dhert W. Analysis of the dynamics of bone formation, effect of cell seeding density, and potential of allogeneic cells in cell-based bone tissue engineering in goats. *Tissue Engineering: Part A*, 14(6):1081–1088, 2008.

Kruyt M.C., Dhert W.J., Oner F.C., van Blitterswijk C.A., Verbout A.J., and de Bruijn J.D. Analysis of ectopic and orthotopic bone formation in cell-based tissue-engineered constructs in goats. *Biomaterials*, 28:1798–1805, 2007.

Lacroix D. *Simulation of tissue differentiation during fracture healing*. PhD thesis, University of Dublin, 2001.

Langer R. and Vacanti J.P. Tissue engineering. *Science*, 260(5110):920–926, 1993.

Lee C.T., Hoopes M.F., Diehl J., Gilliland W., Huxel G., Leaver E.V., McCann K., Umbanhowar J., and Mogilner A. Non-local concepts and models in biology. *Journal of Theoretical Biology*, 210:201–219, 2001.

Lemaire V., Tobin F., Greller L., Cho C., and Suva L. Modeling the interactions between osteoblast and osteoclast activities in bone remodeling. *Journal of Theoretical Biology*, 229:293–309, 2004.

Lenas P., Moos M., and Luyten F. Developmental engineering: A new paradigm for the design and manufacturing of cell-based products. part i: from three-dimensional cell growth to biomimetics of in vivo development. *Tissue Engineering: Part B*, 15(00):1–14, 2009.

Liang G., Yang Y., Sunho O., Ong J.L., Zheng C., Ran J., Yiin G., and Zhou D. Ectopic osteoinduction and early degradation of recombinant human bone morphogenetic protein-2-loaded porous β-tricalcium phosphate in mice. *Biomaterials*, 26:4265–4271, 2005.

Lin C.L., Chang S.H., Chang W.J., and Kuo Y.C. Factorial analysis of variables influencing mechanical characteristics of a single tooth implant placed in the maxilla using finite element analysis and the statistics-based taguchi method. *European Journal of Oral Sciences*, 115:408–416, 2007.

Liu Y., Wang G., Cai Y., Ji H., Zhou G., Zhao W., Tang R., and Zhang M. In vitro effects of nanophase hydroxyapatite particles on proliferation and osteogenic differentiation of bone marrow-derived mesenchymal stem cells. *Journal of Biomedical Materials Research*, 90(4):1083–1091, 2008.

Liu Y.K., Lu Q.Z., Pei R., Ji H.J., Zhou G.S., Zhao X.L., Tang R.K., and Zhang M. The effect of extracellular calcium and inorganic phosphate on the growth and osteogenic differentiation of mesenchymal stem cells in vitro: implication for bone tissue engineering. *Biomedical Materials*, 4(2), 2009.

Lobovkina T., Gözen I., Erkan Y., Olofsson J., Weber S., and Orwar O. Protrusive growth and periodic contractile motion in surface-adhered vesicles induced by ca^{2+}-gradients. *Soft Matter*, 6:268–272, 2010.

Maeno S., Niki Y., Matsumoto H., Morioka H., Yatabe T., Funayama A., Toyama Y., Taguchi T., and Tanaka J. The effect of calcium ion concentration on osteoblast viability, proliferation and differentiation in monolayer and 3d culture. *Biomaterials*, 26:4847–4855, 2005.

Malandrino A., Planell J., and Lacroix D. Statistical factorial analysis on the poroelastic material properties sensitivity of the lumbar intervertebral disc under compression, flexion and axial rotation. *Journal of Biomechanics*, 42:2780–2788, 2009.

Malaval L., Liu F., Roche P., and Aubin J. Kinetics of osteoprogenitor proliferation and osteoblast differentiation in vitro. *Journal of Cellular Biochemistry*, 74:616–627, 1999.

Maurya M. and Subramaniam S. A kinetic model for calcium dynamics in raw 264.7 cells: 1. mechanisms, parameters and subpopulational variability. *Biophysical Journal*, 93: 709–728, 2007.

Montgomery D. *Design and analysis of experiments*. John Wiley and Sons, Inc., 7th edition, 2009.

Myers R. H. and Montgomery D.C. *Response surface methodology: process and product optimization using designed experiments*. John Wiley & sons, Inc., 1995. ISBN 0-471-58100-3.

Olsen L., Sheraratt J.A., Maini P.K., and Arnold F. A mathematical model for the capillary endothelial cell-extracellular matrix interactions in wound-healing angiogenesis. *Journal of Mathematics Applied in Medicine and Biology*, 14:261–281, 1997.

Olszak I., Poznansky M., Evans R., Olson D., Kos C., Pollak M., Brown E., and Scadden D. Extracellular calcium elicits a chemokinetic response from monocytes in vitro and in vivo. *The Journal of Clinical Investigation*, 105(9):1299–1305, 2000.

Peterson M. and Riggs M. A physiologically based mathematical model of integrated calcium homeostasis and bone remodeling. *Bone*, 46:49–63, 2010.

Pioletti D., Takei H., Lin T., Van Landuyt P., Ma Q., Kwon S., and Sung K.-L. The effects of calcium phosphate cement particles on osteoblast functions. *Biomaterials*, 21: 1103–1114, 2000.

Pountos I. and Giannoudis P. Biology of mesenchymal stem cells. *Injury, International Journal of the Care of the Injured*, 36:8–12, 2005.

Ripamonti U. Osteoinduction in porous hydroxyapatite implanted in heterotopic sites of different animal models. *Biomaterials*, 17(1):31–35, 1996.

Roldan J.C., Detsch R., Schaefer S., Chang E., Kelantan M., Waiss W., Reichert T.E., Gurtner G.C., and Deisinger U. Bone formation and degradation of a highly porous biphasic calcium phosphate ceramic in presence of bmp-7, vegf and mesenchymal stem cells in an ectopic mouse model. *Journal of Cranio-Maxillo-Facial Surgery*, In press, 2010.

Rupnick M., Stokes C., Williams S., and Lauffenburger D. Quantitative analysis of human microvessel endothelial cells using a linear under-agarose assay. *Laboratory Investigation*, 59:363–372, 1988.

Saidak Z., Boudot C., Abdoune R., Petit L., Brazier M., Mentaverri R., and Kamel S. Extracellular calcium promotes the migration of breast cancer cells through the activation of the calcium sensing receptor. *Experimental Cell Research*, 315:2072–2080, 2009.

Saltelli A., Chan K., and Scott E., editors. *Sensitivity analysis*. John Wiley & sons, Inc., 2000. ISBN 0-471-99892-3.

Sandino C., Checa S., Prendergast P., and Lacroix D. Simulation of angiogenesis and cell differentiation in a cap scaffold subjected to compressive strains using a lattice modeling approach. *Biomaterials*, 31:2446–2452, 2010.

Santner T.J., Williams B.J., and Notz W.I. *The design & analysis of computer experiments*. Springer-Verlag New York, Inc., 2003. ISBN 0-387-95420-1.

Shelton R.M., Rasmussen A.C., and Davies J.E. Protein adsorption at the interface between charged polymer substrata and migrating osteoblasts. *Biomaterials*, 9:24–29, 1988.

Sherratt J. Chemotaxis and chemokinesis in eukaryotic cells: the keller-segel equations as an approximation to a detailed model. *Bulletin of Mathematical Biology*, 56:129–146, 1994.

Sorkin A. and Waters C.M. Endocytosis of growth-factor receptors. *Bioessays*, 15:375–382, 1993.

Spaeth E., Klopp A., Dembinski J., Andreeff M., and Marini F. Inflammation and tumor microenvironments: defining the migratory itinerary of mesenchymal stem cells. *Gene Therapy*, 15:730–738, 2008.

Stanford C., Jacobson P., Eanes E., Lembke L., and Midura R. Rapidly forming apatitic mineral in an osteoblastic cell line (umr 106-01 bsp). *The Journal of Biological Chemistry*, 270(16):9420–9428, 1995.

Sun S., Liu Y., Lipsky S., and Cho M. Physical manipulation of calcium oscillations facilitates osteodifferentiation of human mesenchymal stem cells. *Journal of the Federation of American Societies for Experimental Biology*, 21:1472–1480, 2007.

Thibault M., Hoemann C., and Buschmann M. Fibronectin, vitronectin, and collagen i induce chemotaxis and haptotaxis of human and rabbit mesenchymal stem cells in a standardized transmembrane assay. *Stem Cells and Development*, 16:489–502, 2007.

Titorencu I., Jinga V., Constantinescu E., Gafencu A., Ciohodaru C., Manolescu I., Zaharia C., and Simionescu M. Proliferation, differentiation and characterization of osteoblasts from human bm mesenchymal stem cells. *Cytotherapy*, 9(7):682–696, 2007.

van der Meulen M. and Huiskes R. Why mechanobiology? a survey article. *Journal of Biomechanics*, 35:401–414, 2002.

Vander A., Sherman J., and Luciano D. *Human Physiology: the Mechanisms of the Body Function*. WCB McGraw-Hill, Bosten, MA, 1998.

Wang Y. and Fang K.T. A note on uniform distribution and experimental design. *KeXue TongBao*, 26:485–489, 1981.

Weinberg C.B. and Bell E. Regulation of proliferation of bovine aortic endothelial cells, smooth muscle cells and adventitial fibroblasts in collagen lattices. *Journal of Cellular Physiology*, 35:410–414, 1985.

Yang K., Teo E.C., and Fuss F.K. Application of taguchi method in optimization of cervical ring cage. *Journal of Biomechanics*, 40:3251–3256, 2007.

Yoshizato K., Taira T., and Yamamoto N. Growth inhibition of human fibroblasts by reconstituted collagen fibrils. *Biomedical Research*, 6:61–71, 1985.

Yuan H., van Blitterswijk C.A., de Groot K., and de Bruijn J.D. A comparison of bone formation in biphasic calcium phosphate and hydroxyapatite implanted in muscle and bone of dogs at different time periods. *Journal of Biomedical Materials Research*, 78A: 130–147, 2006.

Yuan J., Cui L., Zhang W.J., Liu W., and Cao Y. Repair of canine mandibular bone defects with bone marrow stromal cells and porous β-tricalcium phosphate. *Biomaterials*, 28: 1005–1013, 2007.

Zahor D., Radko A., Vago R., and Gheber L.A. Organization of mesenchymal stem cells is controlled by micropatterned silicon substrates. *Materials Science and Engineering C*, 27:117–121, 2007.

Zayzafoon M. Calcium/calmodulin signaling controls osteoblast growth and differentiation. *Journal of Cellular Biochemistry*, 97:56–70, 2006.

Zhang H., Li S., and Yan Y. Dissolution behavior of hydroxyapatite powder in hydrothermal solution. *Ceramics International*, 27:451–454, 2001.

Zhang Q., Chen J., Feng J., Cao Y., Deng C., and Zhang X. Dissolution and mineralization behaviors of ha coatings. *Biomaterials*, 24:4741–4748, 2003.

Zhou G.S., Su Z.Y., Cai Y.R., Liu Y.K., Dai L.C., Tang R.K., and Zhang M. Different effects of nanophase and conventional hydroxyapatite thin films on attachment, proliferation and osteogenic differentiation of bone marrow derived mesenchymal stem cells. *Biomedical Materials and Engineering*, 17:387–395, 2007.